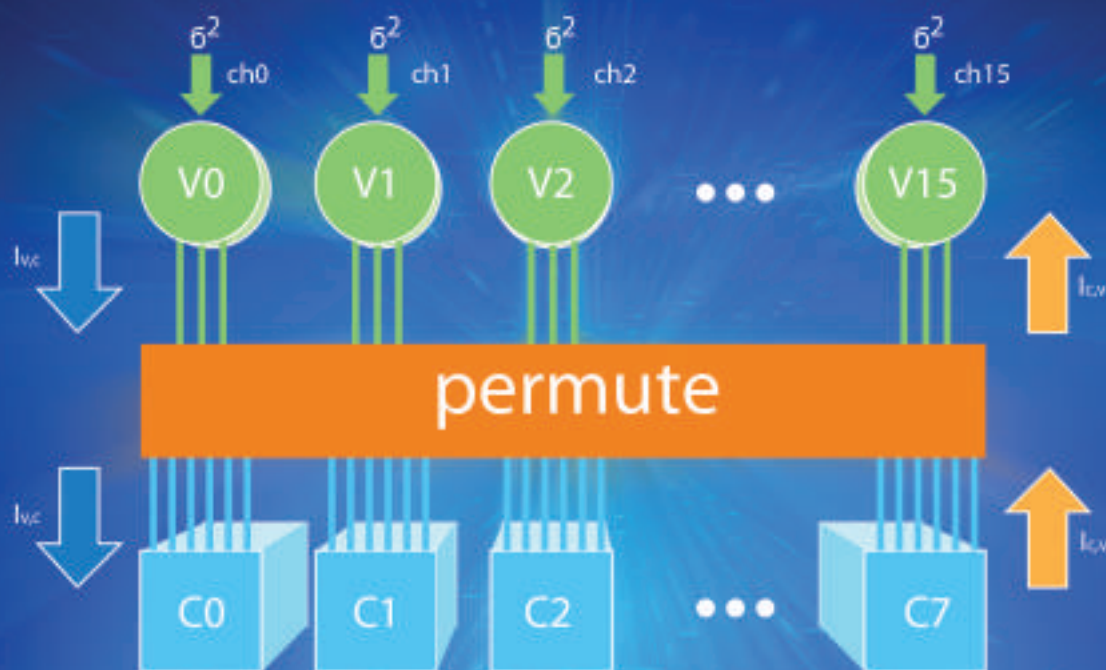


ZTE COMMUNICATIONS

An International ICT R&D Journal Sponsored by ZTE Corporation

April 2016, Vol. 14 No. 2

SPECIAL TOPIC: Optical Wireless Communications



ZTE Communications Editorial Board

Chairman

ZHAO Houlin: International Telecommunication Union (Switzerland)

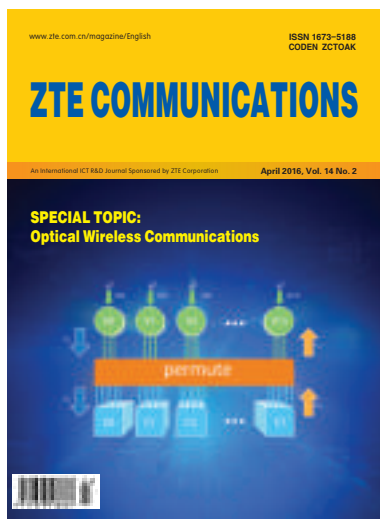
Vice Chairmen

SHI Lirong: ZTE Corporation (China) **XU Chengzhong:** Wayne State University (USA)

Members (in Alphabetical Order):

CAO Jiannong	Hong Kong Polytechnic University (Hong Kong, China)
CHEN Chang Wen	University at Buffalo, The State University of New York (USA)
CHEN Jie	ZTE Corporation (China)
CHEN Shigang	University of Florida (USA)
Connie Chang-Hasnain	University of California, Berkeley (USA)
CUI Shuguang	Texas A&M University (USA)
DONG Yingfei	University of Hawaii (USA)
GAO Wen	Peking University (China)
LI Guifang	University of Central Florida (USA)
LUO Falong	Element CXI (USA)
MA Jianhua	Hosei University (Japan)
PAN Yi	Georgia State University (USA)
REN Fuji	The University of Tokushima (Japan)
SHI Lirong	ZTE Corporation (China)
SUN Huifang	Mitsubishi Electric Research Laboratories (USA)
SUN Zhili	University of Surrey (UK)
Victor C. M. Leung	The University of British Columbia (Canada)
WANG Xiaodong	Columbia University (USA)
WU Keli	The Chinese University of Hong Kong (Hong Kong, China)
XU Chengzhong	Wayne State University (USA)
YANG Kun	University of Essex (UK)
YUAN Jinhong	University of New South Wales (Australia)
ZENG Wenjun	University of Missouri (USA)
ZHANG Honggang	Zhejiang University (China)
ZHANG Yueping	Nanyang Technological University (Singapore)
ZHAO Houlin	International Telecommunication Union (Switzerland)
ZHOU Wanlei	Deakin University (Australia)
ZHUANG Weihua	University of Waterloo (Canada)

► CONTENTS



Submission of a manuscript implies that the submitted work has not been published before (except as part of a thesis or lecture note or report or in the form of an abstract); that it is not under consideration for publication elsewhere; that its publication has been approved by all co-authors as well as by the authorities at the institute where the work has been carried out; that, if and when the manuscript is accepted for publication, the authors hand over the transferable copyrights of the accepted manuscript to *ZTE Communications*; and that the manuscript or parts thereof will not be published elsewhere in any language without the consent of the copyright holder. Copyrights include, without spatial or timely limitation, the mechanical, electronic and visual reproduction and distribution; electronic storage and retrieval; and all other forms of electronic publication or any other types of publication including all subsidiary rights.

Responsibility for content rests on authors of signed articles and not on the editorial board of *ZTE Communications* or its sponsors.

All rights reserved.

Special Topic: Optical Wireless Communications

Guest Editorial

01

GONG Chen, TANG Xuan, and WANG Xiaodong

Subcarrier Intensity Modulated Optical Wireless Communications: A Survey from Communication Theory Perspective

02

Md. Zoheb Hassan, Md. Jahangir Hossain, Julian Cheng, and Victor C. M. Leung

Short-Range Optical Wireless Communications for Indoor and Interconnects Applications

13

WANG Ke, Ampalavanapillai Nirmalathas, Christina Lim, SONG Tingting,
LIANG Tian, Kamal Alameh, and Efstratios Skafidas

Optimal Transmission Power in a Nonlinear VLC System

23

ZHAO Shuang, CAI Sunzeng, KANG Kai, and QIAN Hua

Modulation Techniques for Li-Fi

29

Mohamed Sufyan Islim and Harald Haas

► CONTENTS

ZTE COMMUNICATIONS

Vol. 14 No. 2 (Issue 50)

Quarterly

First English Issue Published in 2003

Supervised by:

Anhui Science and Technology Department

Sponsored by:

Anhui Science and Technology Information
Research Institute and ZTE Corporation

Staff Members:

Editor-in-Chief: CHEN Jie

Executive Associate

Editor-in-Chief: HUANG Xinming

Editor-in-Charge: ZHU Li

Editors: XU Ye, LU Dan, ZHAO Lu

Producer: YU Gang

Circulation Executive: WANG Pingping

Assistant: WANG Kun

Editorial Correspondence:

Add: 12F Kaixuan Building,

329 Jinzhai Road,

Hefei 230061, P. R. China

Tel: +86-551-65533356

Fax: +86-551-65850139

Email: magazine@zte.com.cn

Published and Circulated (Home and Abroad) by:

Editorial Office of

ZTE Communications

Printed by:

Hefei Tiancai Color Printing Company

Publication Date:

April 25, 2016

Publication Licenses:

ISSN 1673-5188

CN 34-1294/ TN

Advertising License:

皖合工商广字0058号

Annual Subscription:

RMB 80

LDPC Decoding for Signal Dependent Visible Light Communication Channels

41

YUAN Ming, SHA Xiaoshi, LIANG Xiao, JIANG Ming, WANG Jiaheng,
and ZHAO Chunming

Review

A Survey on Event Mining for ICT Network Infrastructure Management

47

LIU Zheng, LI Tao, and WANG Junchang

Research Papers

Review of AVS Audio Coding Standard

56

ZHANG Tao, ZHANG Caixia, and ZHAO Xin

Roundup

Introduction to *ZTE Communications*

22

Call for Papers: Special Issue on Multi-Gigabit Millimeter-Wave Wireless Communications

40

Optical Wireless Communications

► GONG Chen



GONG Chen received the MS degree in electrical engineering from Tsinghua University, China in 2008, and the PhD degree from the Columbia University, USA in 2012. He was a senior systems engineer with Qualcomm Research, Qualcomm Inc., USA from April 2012 to December 2013. He is currently with the Faculty at the University of Science and Technology of China, China. His research interests include wireless communications, optical wireless communications, and signal processing. He has been selected by the Young 1000 Talent Program of the China Government in 2014.

► TANG Xuan



TANG Xuan received the diploma (with honors) in electrical engineering from Nanyang Polytechnic, Singapore in 2007 and the BEng (first class honors) degree in electric and communication engineering from Northumbria University, UK in 2008. She was awarded her PhD degree in free-space optical communications in Optical Communications Research Lab (OCRG) at the same university in 2012. Her research interests include optical communication (outdoor wireless), digital communication and digital signal processing. Between 2012 and 2014, she holds a postdoc position in the Optical Wireless Information Systems Lab, Department of Electronic Engineering, Tsinghua University. Now she is an associate professor in the Quanzhou Institute of Equipment Manufacturing, Haixi Institutes, Chinese Academy of Science.

► WANG Xiaodong



WANG Xiaodong received the PhD degree in electrical engineering from Princeton University, USA. He is a professor of Electrical Engineering at Columbia University, USA. His research interests fall in the general areas of computing, signal processing and communications, and he has published extensively in these areas. Among his publications is a book *Wireless Communication Systems: Advanced Techniques for Signal Reception* (Prentice Hall, 2003). His current research interests include wireless communications, statistical signal processing, and genomic signal processing. He has served as an associate editor for the *IEEE Transactions on Communications*, the *IEEE Transactions on Wireless Communications*, the *IEEE Transactions on Signal Processing*, and the *IEEE Transactions on Information Theory*. He received the 1999 NSF CAREER Award, the 2001 IEEE Communications Society and Information Theory Society Joint Paper Award, and the 2011 IEEE Communication Society Award for Outstanding Paper on New Communication Topics. He is listed as an ISI highly-cited author.

The optical spectrum can serve as a good spectrum resource for wide-band wireless communications. The advantages of optical wireless communications (OWC) mainly lie in two aspects: the potential large transmission bandwidth due to the high-frequency carrier, and the communication security due to no radio-frequency radiation. Thus OWC can be applied in the scenarios where the radio silence is required or the radio frequency radiation may cause explosions, for example in the battle field or some special areas in the storehouses.

OWC can be performed in the infrared spectrum, the visible light spectrum, and the ultra-violet spectrum. Daily OWC applications typically cater for the visible light spectrum, which can be achieved using the lighting emitting diode (LED) as the transmitter and the photodiode (PD)/avalanche photodiode (APD) as the receiver. A typical application of the visible light communication (VLC) is the indoor VLC auto-cell network, where the LEDs are mounted on the ceilings, and the user equipments (UEs) include handheld terminals, robots, and intelligent furniture and appliances. Information and control messages are transmitted from the LEDs to the mobile UEs in an indoor VLC intelligent network. Moreover, the visible light spectrum can be adopted for equipment identification. This can be achieved via a camera. The camera emits the light to the optoelectronic tags, and then the tags can be charged and identified.

Against those application requirements, the indoor VLC has attracted significant research interests from both academia and industrial areas. Due to the non-coherent characteristic of the LED-based VLC signals, the intensity-modulation direct-detection (IM/DD) communication signal processing has been adopted. To increase the transmission rate, the orthogonal-frequency division-multiplexing protocols have been tailored for the indoor VLC. To mitigate the interference between the adjacent LEDs, various inter-cell interference cancellation protocols have been adopted, such as the beamforming, fractional-frequency reuse, and soft-frequency reuse. As the LEDs are lighting equipments, the communication should also yield the light constraints, which forms the catalogue of VLC under lighting constraints.

This special issue includes six papers. The first paper, "Subcarrier Intensity Modulated Optical Wireless Communications: A Survey from Communication Theory Perspective" by Julian Cheng et al., provides an overview on the communication theoretic aspects on the subcarrier intensity modulated optical wireless communications. The second paper, "Short-Range Optical Wireless Communications for Indoor and Interconnects Applications" by WANG Ke et al., introduces the short-range OWC for indoor and M2M communications. The third paper, "Optical Transmission Power in a Nonlinear VLC system" by QIAN Hua et al., optimizes the transmission power for the VLC system with nonlinearity. The fourth paper, "Modulation Techniques for Li-Fi" by Mohamed Sufyan Islim and Harald Haas, shows the modulation techniques for Li-Fi communications. The fifth paper, "LDPC Decoding for Signal Dependent Visible Light Communication Channels" by ZHAO Chunming et al., provides the decoding techniques for the indoor VLC with signal-dependent noise.

Subcarrier Intensity Modulated Optical Wireless Communications: A Survey from Communication Theory Perspective

Md. Zoheb Hassan¹, Md. Jahangir Hossain², Julian Cheng², and Victor C. M. Leung¹

(1. Department of Electrical and Computer Engineering, University of British Columbia, Vancouver, BC V6T 1Z4, Canada;

2. School of Engineering, University of British Columbia, Kelowna, BC V1V 1V7, Canada)

Abstract

Subcarrier intensity modulation with direct detection is a modulation/detection technique for optical wireless communication systems, where a pre-modulated and properly biased radio frequency signal is modulated on the intensity of the optical carrier. The most important benefits of subcarrier intensity modulation are as follows: 1) it does not provide irreducible error floor like the conventional on-off keying intensity modulation with a fixed detection threshold; 2) it provides improved spectral efficiency and supports higher order modulation schemes; and 3) it has much less implementation complexity compared to coherent optical wireless communications with heterodyne or homodyne detection. In this paper, we present an up-to-date review of subcarrier intensity modulated optical wireless communication systems. We survey the error rate and outage performance of subcarrier intensity modulations in the atmospheric turbulence channels considering different modulation and coding schemes. We also explore different contemporary atmospheric turbulence fading mitigation solutions that can be employed for subcarrier intensity modulation. These solutions include diversity combining, adaptive transmission, relay assisted transmission, multiple-subcarrier intensity modulations, and optical orthogonal frequency division multiplexing. Moreover, we review the performance of subcarrier intensity modulations due to the pointing error and synchronization error.

Keywords

Atmospheric turbulence fading; optical wireless communications; subcarrier intensity modulation

1 Introduction

In the last two decades, wireless communication systems have experienced a major evolution. Various smart wireless devices, such as smartphones, laptops and tablets, are equipped with various data-intensive multimedia applications such as wireless video surveillance, mobile TV, live streaming of high definition video, online gaming, social networking, and cloud storage. The direct implication of such evolution of wireless communications is an exponential surge of data traffic that the wireless communication channels need to transport with a small latency. Recent studies predict that there will be a several hundred-fold increase of data traffic volume in the next ten years along with a ten times increase of connected devices. The ability to support such an exponential growth of data traffic with diverse quality-of-service (QoS) requirements will be the key success factor for the future generation wireless networks [1]. Since there is a fundamental limit on the capacity of the existing radio-frequency (RF) wireless networks, and the existing RF spectrum is heavily li-

censed, the upper portion of the electromagnetic spectrum needs to be utilized for future generation wireless networks [2]. In recent years, optical wireless communication (OWC) has drawn a significant attention as a complementary technology to the conventional RF wireless communication systems. OWC is a broadband wireless communication system that uses optical carrier (visible, infrared or ultra-violet), which is propagated through the unguided transmission mediums (atmosphere or space), in order to transmit the information signal from one end to another. OWC systems have a significantly higher data rate than RF wireless communication systems. Cost effective rapid deployment, enhanced security and avoidance of interference (thanks to the narrow beam width of the optical carrier), protocol transparency, and freedom from spectrum licensing regulations are the additional benefits of the OWC systems [3], [4]. Besides theoretical investigations on the performance of OWC systems, several successful demonstrations of OWC systems supporting 10 Gbps or higher throughput are reported in recent years [5]. Moreover, the OWC system supporting 1.25 Gbps over a link distance of 500 m to 2 km is also available on the

Subcarrier Intensity Modulated Optical Wireless Communications: A Survey from Communication Theory Perspective

Md. Zoheb Hassan, Md. Jahangir Hossain, Julian Cheng, and Victor C. M. Leung

market. The anticipated benefits of the OWC systems from the theoretical investigations and the successful field trials strongly support the OWC systems technology for becoming an important candidate for future generation wireless networks.

In the last decade, due to the development of the optoelectronic devices, and due to increasing demand of the higher bandwidth, OWC has earned much research attentions. At present, OWC is used in various civilian applications. The most important application of OWC is as a cost-effective solution (because of its freedom from spectrum licensing regulations) to the so called “last-mile” problem by bridging end-users with the existing fiber-optic infrastructure. OWC can also be used to connect multiple campus buildings or enterprise buildings with the server building (connected to the backbone network), and can realize super high-speed local area networks (LAN) without installing expensive fiber cable among the buildings. Moreover, because of high data speed and flexible deployment feature, OWC can be used to facilitate high definition (HD) quality video transmission in wireless video surveillance networks, and broadcasting HD video signal to the temporary video studios (which are connected to the central studios via satellite uplink). One such example is the use of OWC technology by BBC to transport the HD video signals among the temporary studios located at Cape Town, South Africa during the 2010 FIFA World Cup event [2]. Moreover, because of the rapid deployment feature, OWC is an attractive solution for temporary communications during a disaster recovery period. For example, OWC was used in the post recovery period of the 9/11 terrorist attack on the world trade centers, New York, USA. It was reported in [6] that the OWC system can achieve at least 99.99% availability when the link range is below 300 m. In the future cloud-based small cell networks, the distance between nearby low power base stations (BTSs) will be on the order 100 m, and a wireless backhaul solution will be required in order to connect the BTSs with each other because these low power BTSs will be deployed randomly in a plug-and-play fashion. Since an OWC system is not licensed and can provide high data rate over a short distance (on the order of 100 m), it can be a potential candidate of wireless backhaul solution for cloud based mobile networks [7]. In addition, because of inexpensive and rapid deployment feature, OWC is also a potential solution for connecting different remote rural parts of the world to the internet in a cost-effective way. In fact, one of the most prominent applications of OWC in the coming years will be the use of OWC by the Facebook Inc. in its internet.org project that aims to provide internet connectivity to more than 4 billion people who are not yet online [8].

For an outdoor OWC system both intensity modulation with direct detection (IM/DD) and coherent modulation with homodyne/heterodyne detection were proposed in the literature. The coherent modulation with homodyne/heterodyne detection allows long-range transmission and improves background noise rejection. However, most of the practical OWC systems employ

IM/DD due to its low-complexity implementation. Recently, IM/DD-based subcarrier intensity modulation (SIM) was proposed in the literature as a suitable alternative to the conventional on-off keying (OOK) and pulse-position modulation (PPM) based intensity modulations. In a SIM OWC system, a pre-modulated and properly biased RF subcarrier is used to modulate the intensity of the optical carrier. Commercial RF technology is relative mature and inexpensive, and the use of SIM can benefit an OWC system in two ways. First, SIM OWC system uses multiple subcarriers to carry the information, which essentially increases the throughput. This transmission technique is known as multiple subcarrier intensity modulation (MSIM) which will be discussed in Section 4. Second, a SIM OWC system can be seamlessly integrated with a fiber optic network where subcarrier modulation is already in use in conjunction with wavelength division multiplexing. An experimental setup of the seamless integration of fiber optics and OWC is provided in [9]. In the last five years or so, a number of research works have been published towards analyzing performance of SIM OWC systems. Since SIM is an important modulation/detection technique for the future OWC systems, an up-to-date survey exclusively on SIM OWC systems will be beneficial to the OWC research community as well as a broad range of audience. In this paper, we focus on the SIM OWC systems from a communication theory point of view. We discuss the performance of the different modulation and channel coding techniques for a single channel SIM OWC system in the presence of atmospheric turbulence induced fading. Since atmospheric turbulence induced signal fading is the most deleterious source of channel impairments for the outdoor OWC systems, appropriate fading mitigation solutions are required to improve the performance of the OWC systems. Therefore, we also explore different approaches, namely, diversity combining, adaptive transmission, relay assisted transmission, multiple-subcarrier intensity modulation, and optical orthogonal frequency division multiplexing (O-OFDM) for improving the performance of a SIM OWC system impaired by fading. Performance of a SIM OWC system can also be impaired by other channel and system impairments such as the pointing error and carrier phase synchronization error. Therefore, we also provide a review of the performance of a typical SIM OWC system with these channel and system impairments. We discuss different approaches for modeling those impairments, performance of different SIM systems in those impairments, and potential solutions to mitigate such impairments. Finally, we provide some future research directions on the SIM OWC systems.

2 OWC Channel Impairments and SIM System Model

2.1 OWC Channel Impairments

A typical outdoor OWC system exhibits three different types

Subcarrier Intensity Modulated Optical Wireless Communications: A Survey from Communication Theory Perspective

Md. Zoheb Hassan, Md. Jahangir Hossain, Julian Cheng, and Victor C. M. Leung

of channel impairments, namely, geometrical and misalignment loss, background radiation, and atmospheric loss. The geometrical loss happens due to divergence of the transmitted optical beam, and it can be quantified as a function of transmitter and receiver lens diameters, beam divergence angle, and link distance. The misalignment, also known as the pointing error, occurs when the transmitted optical beam deviates from its desired direction at the receiver plane. Different models of the pointing error and the performance loss due to the pointing error will be discussed in Section 5.1. The performance degradation of OWC systems due to background radiation and geometrical loss can be found in [2] and [6], respectively.

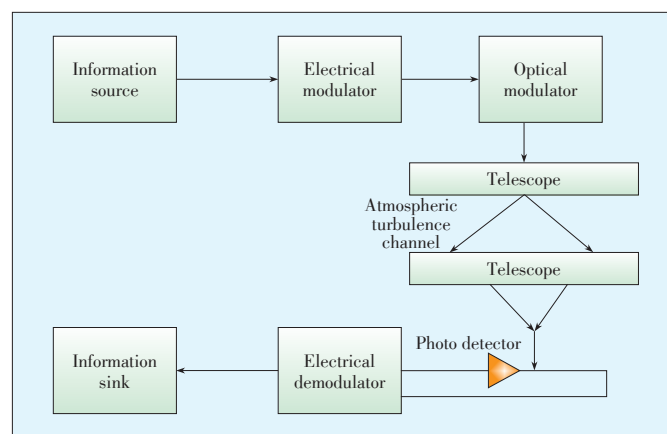
In a clear weather, the most detrimental atmospheric loss to the outdoor OWC system comes from the atmospheric turbulence induced fading or scintillation. Because of solar heating and wind, inhomogeneity in both temperature and wind takes place and results in the random atmospheric refractive index variation. Temperature changes in the air on the order of 1 K cause refractive index change on the order of several parts per million [4]. The resulting refractive index variations along the transmission path cause random fluctuations in both the amplitude and the phase of the received optical signal. Typically a deep fade may last up to 1–100 msec and result in loss of 10^9 consecutive information bits for a transmission rate of 10 Gbps. As fading severely degrades the performance of an outdoor OWC system, appropriate fading mitigation solutions must be employed, especially, for long-distance OWC systems. Since atmospheric turbulence fading is a random phenomenon, appropriate statistical models are necessary in order to theoretically analyze the impact of fading. Over the years, several statistical models have been proposed in order to describe the scintillation. The lognormal distribution is an important fading model for a weak turbulence condition. However, lognormal fading cannot describe the irradiance fluctuation caused by the moderate to strong turbulence fading. Different extensions of the lognormal distribution, such as log-exponential and log-Rice distributions, are proposed in order to describe atmospheric turbulence fading beyond the weak turbulence regimes. K -distribution is proposed to describe the strong atmospheric turbulence fading for an OWC system that has a link length more than 1 km. Negative exponential distribution is used to describe the atmospheric turbulence fading in the saturation regimes. Gamma-Gamma distribution is a widely accepted atmospheric turbulence fading model that describes a wide range of turbulence fading conditions from weak to strong [10]. Moreover, both K -distribution and negative exponential distributions can be obtained as the special cases of Gamma-Gamma distribution. Recently, a generalized distribution, namely, M -distribution has been proposed and it includes lognormal, Gamma-Gamma, shadowed-Rician, K -distribution, and negative exponential as the special cases [11]. Besides, two other statistical models of atmospheric turbulence fading, namely, double Gamma - Gamma distribution and exponential - Weibull (EW)

distribution, have also been proposed in [10] and [12], respectively. Double Gamma - Gamma distribution is more accurate than the Gamma-Gamma distribution for strong turbulence regimes considering spherical wave propagation, and for moderate turbulence regimes considering plane wave propagation. EW distribution is also more accurate compared to the conventional Gamma-Gamma distribution when aperture averaging is considered.

2.2 System Model of SIM OWC

Fig. 1 shows a block diagram of a conventional SIM OWC system where the information bit stream, obtained from the information source block, is first modulated on a RF subcarrier using a conventional electric modulator block. Both phase and/or amplitude modulators are used as the electrical modulator block. The pre-modulated RF subcarrier is then used to drive the intensity of an optical source. Usually for the outdoor OWC system, semiconductor laser diode is used as an optical source. Since the input of the semiconductor laser diode must be non-negative, the pre-modulated RF subcarrier is added with a DC bias before driving the laser diode. The output of the laser diode is transmitted to the atmosphere via a transmit telescope. At the receiver, a second telescope is used in order to collect the transmitted optical beam. The receiver telescope focuses the received optical signal to the photodetector which is placed at the focal point of the receiver telescope. The photodetector converts the received an optical signal into an electric one. After removing the DC bias from the electrical signal (through a bandpass filter), the electric signal is passed to the electric demodulator and detector, and the output of electrical demodulator/detector is collected at the information sink.

Typically in a SIM system, two types of photodetectors, positive-intrinsic-negative (PIN) and avalanche photodiode (APD), are used. The PIN photodetector works well with an OWC system operating over a few kilometers. APD photodetector is suitable for long range OWC systems because it provides an extra gain to the output current for the impact ionization effect. However, the impact ionization also increases the noise current gen-



▲ **Figure 1.** A typical SIM OWC system.

erated by the APD. As a result, for a given received optical power, the gain of an APD needs to be optimized in order to maximize the received signal-to-noise ratio (SNR) [13]. In addition, to facilitate the impact ionization, APD requires a higher reverse bias which eventually increases the circuit complexity and electrical power consumption. In a SIM OWC system, the noise generated from the receiver depends on the type of the photodetector used in the system. The noise current generated from the PIN photodetector is dominated by thermal noise. However, PIN also generates non-negligible shot noise when the background radiation is sufficiently high. On the other hand, the noise current generated from the APD photodetector is usually dominated by shot noise. In addition, depending on the load resistor, APD also adds some non-negligible thermal noise. Both thermal noise and shot noise can be modeled by zero mean additive white Gaussian noise (AWGN) processes

2.3 Advantages and Challenges of SIM OWC

Compared to the conventional modulation/detection schemes (e.g. OOK IM/DD, PPM, and coherent modulation) used in the OWC systems, SIM OWC improves error performance over the atmospheric turbulence fading and reduces implementation complexity. SIM OWC system does not suffer from the irreducible error floor like OOK IM/DD with fixed detection threshold as reported in [14]. Moreover, SIM does not suffer from poor bandwidth efficiency like PPM. Both PPM and coherent modulation with heterodyne and/or homodyne detection techniques require complex transceiver design compared to SIM¹. The reason is that PPM requires a tight symbol and slot synchronization, and coherent modulation requires synchronization of the local oscillator's phase, frequency, and polarization with the transmitted optical carrier's phase, frequency, and polarization. In addition, SIM allows multiple subcarriers to transmit the information signal, which improves the throughput. SIM OWC is also capable of coping with existing fiber optic cable networks employing sub-carrier multiplexing technique [2].

SIM OWC experiences mainly two challenges. The first challenge is the poor power efficiency due to addition of DC bias with the pre-modulated RF subcarrier signal. This effect becomes worse in the case of multiple subcarriers. However, the power efficiency of a SIM with multiple subcarriers can be improved, which will be discussed in Section 4.4. Moreover, when coherent RF modulation is used (i.e., coherent phase-shift keying (PSK)/coherent quadrature-amplitude modulation (QAM)) for pre-modulating the RF subcarrier, an accurate synchronization of carrier phases is required in order to obtain the optimal performance of a SIM system. The impact of imperfect

carrier phase synchronization on the performance of SIM will be discussed in Section 5.2.

3 Modulations and Channel Coding Techniques for SIM OWC

3.1 Modulation Schemes for SIM OWC

In this section, we present a brief literature review on the error rate performance of SIM OWC systems by using different modulation schemes over the atmospheric turbulence channels. SIM was first introduced in [15] where the bit-error rate (BER) performance of a SIM OWC system was investigated over a lognormal atmospheric turbulence fading channel employing differential PSK (DPSK), binary PSK (BPSK) and M -ary PSK (MSPK) modulations. A theoretical analysis of the superior error-rate performance of PSK SIM over OOK IM/DD with fixed detection threshold was presented in [14]. For an OOK IM/DD with fixed detection threshold, both information carrying signals and the response of the atmospheric turbulence fading to the non-zero DC bias (non-information signal) are the baseband random processes. Consequently, it is difficult for the receiver to differentiate between these two baseband random processes, and the demodulation of the information signal is always disturbed by the presence of non-information baseband random process. On the other hand, in a PSK SIM system, the information signal and the response of the atmospheric turbulence fading to the non-zero DC bias do not overlap in the frequency domain. As a result, the receiver can easily filter out the non-information signal which allows PSK SIM to have a superior demodulation performance. For this reason, in atmospheric turbulence condition, PSK SIM offers superior error rate performance compared to OOK IM/DD with fixed detection threshold. Following [14], the error rate performance of PSK SIM in different atmospheric turbulence conditions was extensively investigated in. In particular, the authors in [16] showed that the diversity order of the PSK SIM OWC over Gamma-Gamma turbulence channel depends only on the smaller channel parameter of the Gamma-Gamma turbulence fading. The authors in [17] showed that diversity orders of SIM OWC over both K -distributed and negative-exponential turbulence fading are 0.5. Moreover, the asymptotic analysis used in [17] also revealed the performance gap between the binary coherent and non-coherent modulated SIM in high signal-to-noise ratio (SNR) regimes. For example, the performance gaps between BPSK and DPSK SIMs over the K -distributed and negative-exponential turbulence channels are 3.92 dB in the high SNR regimes. This result is interesting because DPSK and BPSK have a 3 dB performance gap in the Rayleigh fading channels as reported in the RF literature. Different higher order PSK constellations were also used in the existing literature because of their improved spectral efficiency [18], [19]. In particular, both numerical and analytical results of [19] showed

¹The performance comparison of coherent and SIM for a typical outdoor OWC over the Gamma-Gamma atmospheric turbulence channels is performed in [27]. Because of improved error rate performance, achievable data rate, and background noise rejection capability, coherent OWC is preferred to SIM OWC for long haul communication. However, SIM OWC is a suitable candidate for a short range communication with a simple transceiver design requirement.

Subcarrier Intensity Modulated Optical Wireless Communications: A Survey from Communication Theory Perspective

Md. Zoheb Hassan, Md. Jahangir Hossain, Julian Cheng, and Victor C. M. Leung

that the performance gap between BPSK and binary DPSK (BDPSK) modulations is 0 dB over the lognormal turbulence channels. Since the lognormal fading applies for many short-range OWC systems, such a theoretical result supports the use of differential constellations in practical SIM systems.

Compared to the PSK modulation, the QAM modulation has a better error rate performance over the fading channels. Therefore, it has also gained attention for the SIM OWC systems. The average symbol error rate (ASER) performance of a generalized rectangular QAM (R-QAM) based SIM over the lognormal, Gamma-Gamma, K -distributed, and negative exponential turbulence channels fading channels was presented in [20], [21]. In these aforementioned works, PIN photodetector aided photo detection was considered. However, these works cannot be directly applied to the cases in which APD photodetectors are used because the expressions of the SNR are different in PIN and APD aided photo detection process. In particular, the instantaneous SNR in a PIN aided photo detection process is directly proportional to the square of the fading random variable, while the instantaneous SNR in an APD aided photo detection process is an algebraic function of the fading random variable. Since APD photodetectors are particularly useful for the long range OWC systems, it is also imperative to investigate BER performance of a SIM OWC employing APD photodetectors. The BER performance of a gray-coded generalized R-QAM based SIM over the lognormal and Gamma-Gamma turbulence channels and by using APD photodetectors was investigated in [22]. The results showed that the BER performance is sensitive to the gain of the APD photodetectors, and the optimal gain (for which minimum BER is obtained) of the APD photodetectors depends on the turbulence condition and link range. Moreover, when the gain of the APD photodetectors is carefully selected, the BER performance of an R-QAM SIM employing APD photodetectors outperforms the BER performance of an R-QAM SIM employing PIN photodetectors.

3.2 Channel Coding Techniques for SIM OWC

In order to improve the error rate performance of SIM over atmospheric turbulence channels, different forward error correction (FEC) channel coding techniques have been considered for the SIM OWC systems. A typical FEC channel coding technique adds redundant bits into the transmitted sequence so that the receiver can correct a limited number of errors in the received message. For OWC over atmospheric fading channel, channel coding is a useful fading mitigation solution for weak atmospheric turbulence condition. Channel coding can also be used to mitigate moderate to strong atmospheric turbulence fading when it is combined with other fading mitigation solutions [2], which will be discussed in Section 4. The FEC

code for the IM/DD system was introduced in [23]. The BER performance of a convolutional coded BPSK SIM was studied in [14]. These research works confirmed the performance improvement on the order of several dBs of the convolutional coded BPSK in atmospheric turbulence condition compared to the coded OOK IM/DD with fixed detection threshold. Using bit-by-bit interleaving, convolutional coded BPSK-SIM over the Gamma-Gamma was investigated in [24]. Since OWC channel experiences a quasi-static fading, and the data rate of a typical OWC system is on the order of Gbps; bit-by-bit interleaving requires the implementation of a large interleaver and it may not be suitable for the practical SIM OWC systems. Consequently, the authors in [24] also investigated the BER performance of a convolutional coded BPSK SIM when block interleaving is considered. Results of this work confirmed the superior error rate performance of the block interleaving compared to the case having no interleaving in the atmospheric turbulence condition². Recently, bit-interleaved coded modulation (BICM) was also considered for OWC systems because of the high spectral efficiency [25]. In a BICM system, the channel encoder is separated from the modulator by a bit interleaver, and it supports to choose code rate and modulation order independently. The results presented in this work show that significant gain in the error rate performance can be achieved by using interleaver/deinterleaver blocks in the system. The asymptotic analysis reveals that diversity order of a BICM SIM over the Gamma-Gamma turbulence channels depends on the smaller channel parameter of the Gamma-Gamma turbulence as well as the free distance of the convolutional code.

4 Fading Mitigation Solutions for SIM OWC Systems

In this section we discuss some common atmospheric turbulence fading mitigation schemes considered in the literature for SIM OWC systems. These schemes include diversity combining, adaptive transmission, relay assisted transmission, multiple-subcarrier intensity modulation, and O-OFDM.

4.1 Diversity Combining

Since atmospheric turbulence fading severely degrades both error rate performance and data rate performance of OWC systems, proper fading mitigation solutions are necessary for outdoor OWC systems. Maximum likelihood sequence detection (MLSD) is an earlier fading mitigation solution found in the literature. However, the optimal MLSD technique requires large computational complexity, and consequently, only suboptimal MLSD technique can be employed in practice. Aperture averaging is another fading mitigation solution where a lens of large aperture is used at the receiver end to average the received irradiance fluctuations. However, this approach has some limitations. First, the aperture of the receiver should be at least larger than the fading correlation length. This is some-

²It should be noted that interleaving introduces latency on the order of milliseconds or more; however, such latency can be reduced. The researchers at MIT Lincoln LAB have achieved the reduction of latency during the implementation of channel coding and interleaver for a 5.4 km long OWC link having data rates of 2.66 Gbps and 10 Gbps [26].

Subcarrier Intensity Modulated Optical Wireless Communications: A Survey from Communication Theory Perspective

Md. Zoheb Hassan, Md. Jahangir Hossain, Julian Cheng, and Victor C. M. Leung

times difficult, especially for long-range OWC systems (because the fading correlation length increases with the link distance). Second, a lens of a large aperture requires a photodetector of large area, which increases the parasitic capacitance of the photodetector and the device delay in the end. Diversity combining, which was originally proposed for fading mitigation in RF wireless communications, is a suitable alternative to the aforementioned fading mitigation solutions. In a diversity combining scheme, the information signal is transmitted through multiple laser transmitters, and/or received by multiple photodetectors where each photodetector has a small aperture area. The earlier work of diversity combining with multiple-input and multiple-output (MIMO) configuration in OWC systems can be found in [26]. The performance of the considered OWC systems was evaluated for three different diversity combining schemes, namely, maximal ratio combining (MRC), equal gain combining (EGC), and selection gain combining. It was reported that the performance gain of EGC is almost equal to that of MRC over the lognormal turbulence channels. This result is interesting because EGC usually has much less implementation complexity compared to MRC. Following this result, diversity transmission and/or reception techniques are extensively considered for improving the performance of SIM OWC systems. BER performance and outage probability were studied of a MIMO SIM (with repetition coding) over the Gamma-Gamma turbulence channels by considering all three diversity combining schemes, namely, MRC, EGC, and selection gain combining [27], [28]. The asymptotic analyses of these works revealed that the diversity order of a MIMO SIM is $MN\beta/2$ where M is the number of the transmit apertures, N is the number of the receive apertures, and β is the smaller channel parameter of the Gamma-Gamma turbulence. In addition to repetition coding (by which same information is repeatedly transmitted from all the transmitters in a given transmission slot), orthogonal STBC (OSTBC) is considered for MIMO OWC systems. Different from OSTBC for RF communications, the OSTBC for OWC systems uses non-negative real signal instead of complex conjugates. Therefore, an optimized OSTBC for the IM/DD OWC was proposed. The error rate performance comparison was performed for a MIMO SIM OWC employing repetition coding and OSTBC across laser terminals with BPSK and MPSK modulations [28]. The asymptotic high SNR analysis shows both OSTBC and repetition coding achieve full diversity order in atmospheric turbulence; however, repetition coding outperforms the OSTBC.

The aforementioned works on spatial diversity assume that each diversity branch exhibits an independent channel fading. However, such an assumption is only valid when a sufficient spacing (larger than the fading correlation length) exists between the two neighboring transceivers. The fading correlation length increases with the increase of link distance as well as that in fading severity. For example, the fading correlation lengths for a 500 m link in a moderated turbulence environ-

ment and a 1500 m link in a strong turbulence environment were reported as 6.4 cm and 37 cm, respectively [2]. Therefore, it is not always possible to ensure sufficient spacing between the transceivers, especially for the OWC systems that have transmitter and/or receiver of compact sizes. As a result, in practical condition, OWC systems experience spatially correlated fading that degrades the diversity and coding gain. The BER performance of a single-input multiple-output (SIMO) BPSK SIM with spatial correlation over lognormal turbulence fading channels was reported in [29]. With three photodetectors, the correlation coefficients of 0.3 and 0.6 result in 2.7 dB and 5 dB SNR penalty for a target BER of 10^{-6} , respectively.

In addition to spatial diversity, time diversity or subcarrier delay diversity (SDD) was also introduced in order to improve the error rate performance of a SIM OWC system in atmospheric turbulence condition. In a SDD scheme, different subcarriers of different frequencies are used to transmit the delayed version of the original data, and they are combined at the receiver by using an EGC combiner. The error rate performance of a BPSK SIM system over lognormal turbulence channel using SDD was presented in [30]. However, in order to achieve an optimal performance by using SDD, the delay between consecutive subcarriers should be larger than the channel coherence time so that each subcarrier experiences independent channel fading. Since the atmospheric turbulence channel varies slowly with a coherence time on the order of milliseconds, SDD can introduce several delays in the system that may eventually outweigh the benefits of SDD in terms of the improved error rate performance. For this reason, SDD is not recommended for those OWC applications where delay is an important design concern.

4.2 Adaptive Transmission

Although spatial diversity is an effective fading mitigation technique, it imposes some limitations on system design. Increasing the number of transmit or the receive apertures will increase the implementation cost. Since outdoor OWC requires a line-of-sight communication link, maintaining alignment between multiple transmitters and receiver terminals requires a complicated tracking system [6]. Moreover, the effectiveness of a spatial diversity is restricted by the spatial correlation among multiple receivers. Adaptive transmission is a suitable alternative fading mitigation solution where transmission parameters (rate, power etc.) are varied according to the channel states in order to make efficient utilization of the channel capacity. The adaptive transmission solutions were originally proposed for RF wireless communications. In order to implement adaptive transmission over the fading channels, the channels should vary slowly. If the channel is fast changing, frequent feedback from the receiver to the transmitter will be needed. Moreover, frequent update of transmission parameters will also be required, which will significantly increase the system complexity and degrade the performance. Because an OWC channel has a

Subcarrier Intensity Modulated Optical Wireless Communications: A Survey from Communication Theory Perspective

Md. Zoheb Hassan, Md. Jahangir Hossain, Julian Cheng, and Victor C. M. Leung

slow fading process with channel coherence time from 0.1-100 msec, the implementation of adaptive transmission over OWC channel does not require frequent channel feedback from the receiver to the transmitter. Therefore, adaptive transmission is a feasible fading mitigation solution for the outdoor OWC systems. For SIM OWC systems, a variable-rate, constant-power adaptive transmission scheme was proposed by considering MPSK and R-QAM based SIM over the Gamma-Gamma and lognormal turbulence channels [31], [32]. In this scheme, the transmission power was kept constant, and the rate was varied by adapting the modulation order based on the received SNR (i.e., a higher order modulation was transmitted when the received SNR is high, a lower order modulation was transmitted when the received SNR is low, and transmission is suspended when received SNR falls below a cutoff value). The results of this work show that an adaptive transmission scheme significantly improves spectral efficiency compared to the non-adaptive BPSK while maintaining a target BER. Following [31] and [32], an adaptive transmission scheme for parallel OWC (employing PSK SIM) and millimeter wave communications was investigated in [33]. OWC and millimeter wave communications are complimentary: the performance of an OWC link is mainly degraded by fog and atmospheric turbulence, and that of the millimeter wave communication link is mainly degraded by the heavy rainfall. Consequently, the proposed adaptive transmission scheme in [33] offers an improved throughput and link availability in all weather conditions compared to the adaptive rate SIM OWC systems proposed in the previous studies.

4.3 Relay Assisted Transmission

Atmospheric turbulence induced fading severely degrades the performance of a SIM OWC system with a link longer than 1 km. Relay assisted transmission can improve the performance of such a SIM OWC system in two ways. First, a multi-hop relay assisted transmission (also known as the serial relaying) can enhance the coverage (i.e., the link range) of SIM OWC systems. Second, a parallel relaying scheme can create N independent fading links (where N is the number of parallel relays employed in the system) between source and destination nodes which eventually create a virtual multiple aperture system, and can offer a diversity gain (also known as the cooperative diversity gain). In particular, the shorter length hops created by a multi-hop relaying scheme help improve the performance (in terms of diversity gain) of a relayed-OWC system because of the distance-dependent behavior of the atmospheric turbulence fading. This is different from conventional RF wireless communications since multi-hop transmission does not provide any diversity gain for RF wireless communications over the fading channels. Recently, a mixed RF/OWC relaying scheme was introduced in order to facilitate radio over free space optical (RoFSO) communications. In the uplink direction, the mixed RF/OWC relaying scheme facilitates the multiplexing of a large number of RF devices into a single OWC

link. Such a system can transmit maximum possible RF messages over OWC links (since an OWC link has much higher capacity compared to a RF link), and increase the end-to-end throughput. The outage performance of an asymmetric dual-hop relay transmission was investigated in [34]. A dual branch transmission system composed of a direct RF transmission link and fixed gain RF/OWC mixed relay aided dual hop link with SIM was considered in [35]. The simulation results show that the diversity combining scheme improves the outage and BER performance compared to a single RF link based transmission scheme.

4.4 Multiple-Subcarrier Modulation

In OWC systems, multiple-subcarrier modulation (MSM) refers to the modulation of information data onto multiple electrical subcarriers which are then modulated onto a single optical carrier [36]. Due to simplicity, the electrical subcarriers are usually modulated onto the intensity of the optical carrier, and the system is referred as the multiple-subcarrier intensity modulation. For an OWC system, multiple-subcarrier intensity modulation offers a number of advantages. Multiple-subcarrier intensity modulation is more bandwidth efficient compared to the OOK and M -ary PPM based IM/DD, and it also offers an opportunity of multiplexing multiple user data onto a single optical carrier. Moreover, multiple-subcarrier intensity modulation can minimize the inter symbol interference (ISI) because several narrowband subcarriers are used, and can also provide immunity to fluorescent-light induced noise [37]. As a result, multiple-subcarrier intensity modulation can be used in indoor OWC applications where optical signals suffer reflection and scattering from multiple objects, and the system performance is limited by ISI and fluorescent-light induced noise. Multiple-subcarrier intensity modulation was first proposed for non-directed infrared wireless communications in [38]. The performance of multiple-subcarrier intensity modulated OWC in atmospheric turbulence was investigated in [37]. The major challenge of multiple-subcarrier intensity modulation is poor optical average power efficiency. In particular, since the input to the optical intensity modulator must be non-negative, a sufficient DC-bias should be added with the electrical subcarriers that have both negative and positive parts. Adding DC-bias with the electrical subcarriers reduces the power efficiency of multiple-subcarrier intensity modulation. Moreover, the amount of required DC-bias increases as the number of subcarriers increases, and the power efficiency of multiple-subcarrier intensity modulation worsens as the number of subcarriers increases. Because of eye-safety and power consumption of the portable transmitter, the transmit power of a typical OWC system must be limited within some threshold value. As a result, due to poor power efficiency, multiple-subcarrier intensity modulation is forced to use a small number of subcarriers, which may degrade the data rate performance. BPSK and quadrature PSK (QPSK) modulations were used and two techniques were pro-

Subcarrier Intensity Modulated Optical Wireless Communications: A Survey from Communication Theory Perspective

Md. Zoheb Hassan, Md. Jahangir Hossain, Julian Cheng, and Victor C. M. Leung

posed in [39] to improve the power efficiency of multiple-subcarrier intensity modulation employing. The first technique uses block coding between the information bits and modulated symbols on the subcarriers so that the minimum value of electrical subcarriers increases and the required DC bias is reduced. However, this technique results in the expansion of the required bandwidth. The second technique introduces a symbol-by-symbol DC adaptive bias replacing the fixed DC bias, and this technique does not require bandwidth expansion. These two techniques can be used separately or together in order to improve the power efficiency of multiple-subcarrier intensity modulation.

4.5 Optical-Orthogonal Frequency Division Multiplexing

O-OFDM is a special case of the multiple-subcarrier intensity modulation, and in recent years it has gained attention for both outdoor and indoor OWC systems. OFDM is one of the most popular fading mitigation solutions for RF wireless communications due to its excellent resistance capability of multipath induced ISI. Moreover, OFDM uses inverse fast Fourier transform (IFFT)/fast Fourier transform (FFT) blocks at the transceiver and supports cost effective implementation. However, the OFDM signal used in RF wireless communications cannot be directly applied to the OWC systems. The main difference between these two systems is that the OFDM signal for RF wireless communications is a bipolar signal and that for an OWC system has to be unipolar signal (the O-OFDM signal cannot contain negative parts because it is modulated on the intensity). However, the use of unipolar signals reduces power efficiency of the O-OFDM system. The power efficiency of O-OFDM worsens as the number of subcarrier increases. In addition, the channel between the transmitter IFFT input and receiver FFT output is linear in RF wireless communication system. However, the linearity of channels does not hold in an OWC system since the receivers in the system employ square law detectors and introduce non-linear signal distortion [40]. In order to successfully apply OFDM to OWC, several modifi-

cations to the original OFDM signals were proposed. Examples of these modified OFDM signals are DC-biased O-OFDM (DCO-OFDM), asymmetrically clipped O-OFDM (ACO-OFDM), and flipped-OFDM. Subcarrier based PSK and QAM modulated O-OFDM were employed in IM/DD OWC systems in order to transport the WiMAX traffic to densely populated area where RF signal exhibits severe attenuation and multipath distortion [41]. The theoretical BER and outage performance were studied for subcarrier PSK and QAM based O-OFDM using IM/DD over Gamma-Gamma and M -turbulence channels considering transmitter non-linearity, inter-modulation distortion, and non-linear clipping [42], [43]. Results of these research works suggest that, due to laser diode non-linearity, the number of subcarriers and the optical modulation index for SIM need to be carefully chosen in order to minimize the performance loss due to non-linear signal distortion. Powerful error correction coding schemes with interleaving such as low-density-parity-check (LDPC) were also considered for IM/DD OWC employing O-OFDM technique in order to mitigate the scintillation effect [44].

In **Table 1**, we present a summary of different techniques that are useful for mitigating turbulence fading effects in SIM OWC systems.

5 SIM OWC Systems Subject to Various Channel and System Impairments

In addition to atmospheric turbulence induced fading, OWC systems also experience other system and channel impairments. We present a brief review of the pointing error and carrier phase synchronization error, and the impact of these impairments on the performance of SIM OWC systems.

5.1 Performance of SIM OWC in Presence of Pointing Error

Outdoor OWC systems are typically installed on the top of buildings, and a pointing error (i.e., the misalignment between

▼ **Table 1. Atmospheric turbulence induced fading mitigation solutions for SIM OWC**

Fading mitigation solutions	Literatures	Advantage	Challenges
Spatial diversity	[27], [28], [29]	Improves BER and outage performance through diversity combining	Increases system cost and complexity with the increase of terminals; Performance is affected by spatial correlation among multiple terminals.
Subcarrier delay diversity	[30]	Improves BER and outage performance through combining subcarriers that have different delays	Increases end-to-end delay
Adaptive transmission	[31]–[33]	Improves spectral efficiency while maintaining a target BER requirement, and thus utilizes channel capacity in an efficient way	Requires ideal feedback on CSI from the receiver; Performance degrades when there is a feedback delay and transmission parameters are adapted based on outdated CSI.
Relay assisted transmission	[34], [35]	Improves BER and outage performance through cooperative diversity and facilitates non-line-of-sight communications	Synchronization of multiple distributed relay nodes for cooperative diversity gain is challenging.
Multiple-subcarrier intensity modulations	[36]–[39]	Offers high data rate, and provides immunity to fluorescent-light induced noise for the indoor OWC	Poor power efficiency
Optical-orthogonal frequency division multiplexing	[40]–[44]	Offers high data rate, and mitigates ISI in the scattered propagation environment	Signal distortion due to non-linearity of the transceivers

BER: bit-error rate

CSI: channel state information

OWC: optical wireless communication

Subcarrier Intensity Modulated Optical Wireless Communications: A Survey from Communication Theory Perspective

Md. Zoheb Hassan, Md. Jahangir Hossain, Julian Cheng, and Victor C. M. Leung

the transmitter and receiver terminals) may occur in such OWC systems due to building sway caused by the thermal expansion, wind load, small earthquake, and building vibration. Since the optical beam usually has a narrow beam width and the receiver has a narrow field of view, the pointing error may lead to the beam deviation at the receiver plane, which will significantly degrade the received SNR performance and link outage.

A pointing error consists of boresight and jitter. Boresight refers to the fixed displacement of the beam center from the detector center at receiver. Although typical OWC systems are installed with zero boresight, random thermal expansion may result in non-zero boresight. Jitter refers to the random vibration of the beam center around the center of detector, and it is mainly caused by building sway and building vibration. Different pointing error models are proposed in the literature.

Assuming zero boresight error and identical jitter in both horizontal and vertical directions, Farid and Hranilovic proposed an analytical pointing error model that has been widely used [45]. Using this model, the same authors proposed a closed-form expression for the probability density function (PDF) of composite channel impaired by the lognormal turbulence, and an integral expression for the PDF of the composite channel impaired by the Gamma-Gamma turbulence fading. Later, using the same model, a closed-form PDF expression of the composite channel impaired by the Gamma-Gamma turbulence was proposed in [46]. Assuming non-identical jitter in horizontal and vertical directions, a pointing error model was derived in [47] where the authors modeled the PDF of the composite channel using Hoyt distribution. Moreover, assuming non-zero boresight and identical jitter in both horizontal and vertical directions, a generalized pointing error model was presented in [48].

The performance of SIM OWC in the presence of pointing error and atmospheric turbulence was first analyzed in [49] where the authors used the pointing error model developed in [45]. The asymptotic high SNR analysis reveals that it is possible to make the diversity order of the SIM systems independent of the pointing error by choosing the equivalent beamwidth larger than $2\sigma_s\sqrt{\min(\alpha,\beta)}$, where σ_s is the jitter standard deviation, and α, β are the two channel parameters of the Gamma - Gamma turbulence fading. Besides, the authors showed that the pointing error severely degrades the performance of a SIM OWC system if an appropriate tracking is not employed. It was shown that diversity order of the system scales up with the number of transmitters and receivers, and consequently, the average BER performance improves by employing spatial diversity with pointing error. Relay assisted transmission (cooperative diversity) was also considered for investigating the performance of SIM OWC in the presence of pointing error. Outage probability and BER performance of a mixed RF/OWC system using an AF relay and SIM OWC was reported in [50] by considering both Gamma-Gamma turbu-

lence and a zero boresight pointing error.

5.2 Performance of SIM OWC in Presence of Carrier Phase Synchronization Error

Most SIM OWC systems use coherent digital modulation schemes; therefore, carrier phase needs to be tracked at the receiver for demodulating the received signal. In these systems, the received optical signal is first being converted to an electrical signal, and then the phase of modulated signal is tracked by a phase locked loop (PLL). An error in phase tracking, known as carrier phase recovery error (CPE), degrades the error rate performance of a SIM OWC system. The BER performance of SIM OWC employing PSK over the lognormal turbulence channels with CPE was analyzed in [51]. The authors modeled the PDF of CPE using a Trikhonov distribution. The asymptotic analysis reveals that for lognormal turbulence fading, the performance loss of BPSK SIM due to CPE is 0 dB. The asymptotic performance loss of MPSK SIM ($M > 2$) due to CPE was also quantified in this work, and it reveals that the performance loss increases as the value of M (modulation order) increases or the value of PLL SNR coefficient decreases.

6 Conclusions

SIM OWC is an excellent candidate for next generation IM/DD OWC systems because it improves the error rate performance when compared to conventional OOK IM/DD OWC with fixed detection threshold, and it is able to offer a larger data transmission rate by using multiple subcarriers. In this review article, we provide a comprehensive survey of the recent research works on SIM OWC systems. This survey covers three important aspects of the state-of-the-art research on SIM OWC systems, namely, modulation schemes and channel coding techniques, fading mitigation solutions, and performance of the SIM OWC systems with pointing error and carrier phase synchronization error.

Several interesting options can be carried out to further the research on SIM OWC systems. One is to further explore the adaptive SIM systems. In particular, the proposed adaptive SIM OWC considers the transmission parameters adaptation based on the instantaneous SNR that requires an increased channel feedback rate. Since atmospheric turbulence experiences a slow fading process, adaptation of transmission parameters based on the average SNR instead of instantaneous SNR is of practical interest, because the former has the potential to reduce the channel feedback rate. Another interesting topic is to design energy-efficient multiple subcarrier intensity modulations. Since one major disadvantage of multiple subcarrier intensity modulation is the poor power efficiency, a potential research topic is to develop joint power and rate allocation for multiple subcarrier intensity modulations in order to maximize the energy efficiency subject to transmit power constraint and other QoS constraints. The joint power and rate allocation

Subcarrier Intensity Modulated Optical Wireless Communications: A Survey from Communication Theory Perspective

Md. Zoheb Hassan, Md. Jahangir Hossain, Julian Cheng, and Victor C. M. Leung

schemes proposed for RF multi-carrier communications cannot be applied here because those schemes were proposed based on the assumption that the system can achieve Shannon capacity, and such an assumption is not applicable to SIM systems. Therefore, it is necessary to take into account the underlying properties of multiple-subcarrier intensity modulation for developing joint power and rate allocation for the multiple subcarrier intensity modulations. Finally, in almost all the aforementioned works, only physical layer performance metrics of SIM OWC are investigated. However, it is also important to analyze different cross-layer queuing performance metrics, such as the packet drop rate, packet delay, and effective capacity (the achievable traffic arrival rate in order to support a given delay bound). Therefore, developing an appropriate queuing model and analyzing different queuing performance metrics for SIM OWC in atmospheric turbulence fading and pointing error is a potential research direction.

References

- [1] Z. Ghassemlooy, S. Arnon, M. Uysal, Z. Xu, and J. Cheng, "Emerging optical wireless communications—advances and challenges," *IEEE Journal on Selected Areas in Communications*, vol. 33, no. 9, pp. 1738–1740, Sep. 2015. doi: 10.1109/JSAC.2015.2458511.
- [2] M. A. Khalighi and M. Uysal, "Survey on free space optical communication: A communication theory perspective," *IEEE Communications Survey & Tutorials*, vol. 16, no. 4, pp. 2231–2258, fourth quarter 2014. doi: 10.1109/COMST.2014.2329501.
- [3] D. Keddar and S. Arnon, "Urban optical wireless communication networks: the main challenges and possible solutions," *IEEE Communications Magazine*, vol. 42, no. 5, pp. 51–57, May 2004. doi: 10.1109/MCOM.2004.1299334.
- [4] V. W. S. Chan, "Free-space optical communications," *IEEE/OSA Journal of Lightwave Technology*, vol. 24, no. 12, pp. 4750–4762, Dec. 2006. doi: 10.1109/JLT.2006.885252.
- [5] N. Cvijetic, D. Qian, and T. Wang, "10 Gb/s free-space optical transmission using OFDM," in *Proc. OFC/NFOEC*, San Diego, USA, 2008, pp. 1–3. doi: 10.1109/OFC.2008.4528442.
- [6] S. Bloom, E. Korevaar, J. Schuster, and H. Willebrand, "Understanding the performance of free space optics," *Journal of Optical Networking*, vol. 2, no. 6, pp. 178–200, Jun. 2003.
- [7] J. Bartelt, G. Fettweis, D. Wübben, M. Boldi, and B. Melis, "Heterogeneous backhaul for cloud-based mobile networks," in *IEEE 78th Vehicular Technology Conference (VTC - Fall)*, Las Vegas, USA, 2013, pp. 1–5. doi: 10.1109/VTC-Fall.2013.6692220.
- [8] Info-Internet. (2015, July 30). New milestones in connectivity lab's aircraft and laser programs [Online]. Available: <https://info.internet.org/en/2015/07/30/new-milestones-in-connectivity-labs-aircraft-and-laser-programs>
- [9] M. Matsumoto, "Next generation free-space optical system by system design optimization and performance enhancement," in *Proc. Progress in Electromagnetics Research Symposium (PIERS)*, KL, Malaysia, 2012, pp. 501–506.
- [10] M. A. Kashani, M. Uysal, and M. Kavehrad, "A novel statistical channel model of turbulence-induced fading in free space optical systems," *IEEE/OSA Journal of Lightwave Technology*, vol. 33, no. 11, pp. 2303–2312, Mar. 2015. doi: 10.1109/JLT.2015.2410695.
- [11] A. Jurado-Navas, J.M. Garrido-Balsells, J.F. Paris and A. Puerta-Notario, "A unifying statistical model for atmospheric optical scintillation," invited chapter in *Numerical Simulations of Physical and Engineering Processes*. Rijeka, Croatia: InTech Press, 2011.
- [12] R. Barrios and F. Dios, "Exponentiated Weibull model for the irradiance probability density function of a laser beam propagating through atmospheric turbulence," *Optics & Laser Technology*, vol. 45, no. 12, pp. 13–20, Jan. 2013. doi: 10.1016/j.optlastec.2012.08.004.
- [13] K. Kiasaleh, "Performance of APD-based, PPM free-space optical communication systems in atmospheric turbulence," *IEEE Transactions on Communications*, vol. 53, no. 9, pp. 1455–1461, Sep. 2005. doi: 10.1109/TCOMM.2011.072011.110001.
- [14] J. Li, J. Q. Liu, and D. P. Tayler, "Optical communication using subcarrier PSK intensity modulation through atmospheric turbulence channels," *IEEE Transactions on Communications*, vol. 55, no. 8, pp. 1598–1606, Aug. 2007. doi: 10.1109/TCOMM.2007.902592.
- [15] W. Huang, J. Takayanagi, T. Sakanaka, and M. Nakagawa, "Atmospheric optical communication system using subcarrier PSK modulation," *IEICE Transaction on Communications*, vol. E76-B, no. 9, pp. 1169–1177, Sep. 1993. doi: 10.1109/ICC.1993.397553.
- [16] X. Song, M. Niu, and J. Cheng, "Error rate of subcarrier intensity modulations for wireless optical communications," *IEEE Communications Letters*, vol. 16, no. 4, pp. 540–543, Apr. 2012. doi: 10.1109/LCOMM.2012.021612.112554.
- [17] X. Song and J. Cheng, "Optical communication using subcarrier intensity modulation in strong atmospheric turbulence," *IEEE/OSA Journal of Lightwave Technology*, vol. 30, no. 22, pp. 3484–3493, Nov. 2012. doi: 10.1109/JLT.2012.2220754.
- [18] X. Song and J. Cheng, "Subcarrier intensity modulated optical wireless communications using noncoherent and differentially coherent modulations," *IEEE/OSA Journal of Lightwave Technology*, vol. 31, no. 12, pp. 1906–1913, Jun. 2013. doi: 10.1109/JLT.2013.2261282.
- [19] X. Song, F. Yang, J. Cheng, and M.-S. Alouini, "BER of Subcarrier MPSK/MDPSK Systems in Atmospheric Turbulence," *IEEE/OSA Journal of Lightwave Technology*, vol. 33, no. 1, pp. 161–170, Jan. 2015. doi: 10.1109/JLT.2014.2384027.
- [20] K. P. Peppas and C. K. Datsikas, "Average symbol error probability of general-order rectangular quadrature amplitude modulation of optical wireless communication systems over atmospheric turbulence channels," *IEEE/OSA Journal of Optical Communications and Networking*, vol. 2, no. 2, pp. 102–110, Feb. 2010. doi: 10.1364/JOCN.2.000102.
- [21] Md. Z. Hassan, X. Song, and J. Cheng, "Subcarrier intensity modulated wireless optical communications with rectangular QAM," *IEEE/OSA Journal of Optical Communications and Networking*, vol. 4, no. 6, pp. 522–532, Jun. 2012. doi: 10.1364/JOCN.4.000522.
- [22] B. T. Vu, N. T. Dang, T. C. Thang, and A. T. Pham, "Bit error rate analysis of rectangular QAM/FSO systems using an APD receiver over atmospheric turbulence channels," *IEEE/OSA Journal of Optical Communications and Networking*, vol. 5, no. 5, pp. 437–446, May 2013. doi: 10.1364/JOCN.5.000437.
- [23] X. Zhu and J. M. Kahn, "Performance bounds for coded free-space optical communications through atmospheric turbulence channels," *IEEE Transactions on Communications*, vol. 51, no. 8, pp. 1233–1239, Aug. 2003. doi: 10.1109/TCOMM.2003.815052.
- [24] L. Yang, J. Cheng, and J. F. Holzman, "Performance of convolutional coded subcarrier intensity modulation over Gamma-Gamma turbulence channels," *IEEE Communications Letters*, vol. 17, no. 12, pp. 2332–2335, Dec. 2013. doi: 10.1109/LCOMM.2013.102913.131461.
- [25] M. T. Malik, Md. J. Hossain, J. Cheng, and M.-S. Alouini, "Performance of BICM-based SIM OWC over Gamma-Gamma turbulence channels," *IEEE Communications Letters*, vol. 19, no. 5, pp. 731–734, May 2015. doi: 10.1109/LCOMM.2015.2405554.
- [26] E. Lee and V. W. S. Chan, "Part I: optical communication over the clear turbulent atmospheric channel using diversity," *IEEE Journal on Selected Areas in Communications*, vol. 22, no. 9, pp. 1896–1906, Nov. 2004. doi: 10.1109/JSAC.2004.835751.
- [27] M. Niu, J. Cheng, and J. F. Holzman, "Error rate performance comparison of coherent and subcarrier intensity modulated wireless optical communications," *IEEE/OSA Journal of Optical Communications and Networking*, vol. 5, no. 6, pp. 554–564, Jun. 2013. doi: 10.1364/JOCN.5.000554.
- [28] X. Song and J. Cheng, "Subcarrier intensity modulated MIMO optical communications in atmospheric turbulence," *IEEE/OSA Journal of Optical Communications and Networking*, vol. 5, no. 9, pp. 1001–1009, Sep. 2013. doi: 10.1364/JOCN.5.001001.
- [29] Z. Ghassemlooy, W.O. Popoola, E. Leitgeb, and V. Ahmadi, "MIMO free space optical communications employing subcarrier intensity modulations in atmospheric turbulence," in *Proc. 1st Int. ICST Conf. EuropeComm*, London, UK, Aug. 2009, pp. 61–73. doi: 10.1007/978-3-642-11284-3_7.
- [30] W. O. Popoola, Z. Ghassemlooy, H. Haas, E. Leitgeb, and V. Ahmadi, "Error performance of terrestrial free space optical links with subcarrier time diversity," *IET Communications*, vol. 6, no. 5, pp. 499–506, Mar. 2012. doi: 10.1049/iet-com.2011.0107.
- [31] N. D. Chatzidiamantis, A. S. Lioumpas, G. K. Karagiannidis, and S. Arnon, "Adaptive subcarrier PSK intensity modulation in free space optical systems,"

Subcarrier Intensity Modulated Optical Wireless Communications: A Survey from Communication Theory Perspective

Md. Zoheb Hassan, Md. Jahangir Hossain, Julian Cheng, and Victor C. M. Leung

- IEEE Transactions on Communications*, vol. 59, no. 5, pp. 1368–1377, May 2011. doi: 10.1109/TCOMM.2011.022811.100078.
- [32] M. Z. Hassan, M. J. Hossain, and J. Cheng, "Performance of non-adaptive and adaptive subcarrier intensity modulations in Gamma - Gamma turbulence," *IEEE Transactions on Communications*, vol. 61, no. 7, pp. 2946–2957, Jul. 2013. doi: 10.1109/TCOMM.2013.041113.120514.
- [33] V. V. Mai and A. T. Pham, "Performance Analysis of Parallel Free-Space Optics/Millimeter-Wave Systems with Adaptive Rate under Weather Effects," in *Proc. 21st Asia-Pacific Conference on Communications (APCC)*, Kyoto, Japan, Oct. 2015. doi: 10.1109/APCC.2015.7412510.
- [34] E. Lee, J. Park, D. Han, and G. Yoon, "Performance analysis of the asymmetric dual-hop relay transmission with mixed RF/FSO links," *IEEE Photonics Technology Letters*, vol. 23, no. 21, pp. 1642–1644, Nov. 2011. doi: 10.1109/LPT.2011.2166063.
- [35] E. Zedini, I. S. Ansari, and M.-S. Alouini, "On the performance of hybrid line of sight RF and RF-FSO fixed gain dual-hop transmission system," in *2014 IEEE Global Communication Conference (GLOBECOM)*, Austin, USA, Dec. 8–12, 2014. doi: 10.1109/GLOCOM.2014.7037121.
- [36] R. You and J. M. Kahn, "Upper-bounding the capacity of optical IM/DD channel with multiple-subcarrier modulation and fixed bias using trigonometric moment space method," *IEEE Transactions on Communications*, vol. 49, no. 2, pp. 2164–2171, Dec. 2001. doi: 10.1109/18.979327.
- [37] T. Ohtsuki, "Multiple-subcarrier modulations in optical wireless communications," *IEEE Communications Magazine*, vol. 41, no. 3, pp. 74–79, Mar. 2013. doi: 10.1109/MCOM.2003.1186548.
- [38] J. B. Carruthers and J. M. Kahn, "Multiple-subcarrier modulation for nondirected wireless infrared communication," *IEEE Journal on Selected Areas in Communications*, vol. 14, no. 3, pp. 538–546, Apr. 1996. doi: 10.1109/49.490239.
- [39] R. Hui, B. Zhu, R. Huang, et al., "Subcarrier multiplexing for high-speed optical transmission," *IEEE/OSA Journal of Lightwave Technology*, vol. 20, no. 3, pp. 417–427, Mar. 2002. doi: 10.1109/50.988990.
- [40] J. Armstrong, "OFDM for optical communications," *IEEE/OSA Journal of Lightwave Technology*, vol. 27, no. 3, pp. 189–204, Feb. 2009. doi: 10.1109/JLT.2008.2010061.
- [41] N. Cuijetic and T. Wang, "WiMAX over free-space optics—evaluating OFDM multi-subcarrier modulation in optical wireless channels," in *IEEE Sarnoff Symposium*, Princeton, USA, Mar. 2006, pp. 1–4. doi: 10.1109/SARNOF.2006.4534760.
- [42] A. Bekkali, C. B. Naila, K. Kazaura, K. Wakamori, and M. Matsumoto, "Transmission analysis of OFDM-based wireless services over turbulent radio-on-FSO links modeled by Gamma-Gamma distribution," *IEEE Photonics Journal*, vol. 2, no. 3, pp. 509–520, Jun. 2010. doi: 10.1109/JPHOT.2010.2050306.
- [43] H. E. Nistazakis, A. N. Stassinakis, S. Sinanovic, W. O. Popoola, and G. S. Tombras, "Performance of quadrature amplitude modulation orthogonal frequency division multiplexing-based free space optical links with non-linear clipping effect over Gamma-Gamma modeled turbulence channels," *IET Optoelectronics*, vol. 9, no. 5, pp. 269–274, Oct. 2015. doi: 10.1049/iet-opt.2014.0150.
- [44] I. B. Djordjevic, B. Vasic, and M. A. Neifeld, "LDPC coded OFDM over the atmospheric turbulence channel," *Optics Express*, vol. 15, no. 10, pp. 6337–6350, May 2007. doi: 10.1364/OE.15.006336.
- [45] A. A. Farid and S. Hranilovic, "Outage capacity optimization for free space optical links with pointing errors," *IEEE/OSA Journal of Lightwave Technology*, vol. 25, no. 7, pp. 1702–1710, July 2007. doi: 10.1109/ACSSC.2007.4487567.
- [46] W. Gappmair, "Further results on the capacity of free-space optical channels in turbulent atmosphere," *IET Communications*, vol. 5, no. 9, pp. 1262–1267, Jun. 2011. doi: 10.1049/iet-com.2010.0172.
- [47] W. Gappmair, S. Hranilovic, and E. Leitgeb, "OOK performance for terrestrial FSO links in turbulent atmosphere with pointing errors modeled by Hoyt distributions," *IEEE Communications Letters*, vol. 15, no. 8, pp. 875–877, Aug. 2011. doi: 10.1109/LCOMM.2011.062911.102083.
- [48] F. Yang, J. Cheng, and T. A. Tsiftsis, "Free-space optical communication with nonzero boresight pointing errors," *IEEE Transactions on Communications*, vol. 62, no. 2, pp. 713–725, Feb. 2014. doi: 10.1109/TCOMM.2014.010914.130249.
- [49] X. Song, F. Yang, and J. Cheng, "Subcarrier intensity modulated optical wireless communications in atmospheric turbulence with pointing errors," *IEEE/OSA Journal of Optical Communications and Networking*, vol. 5, no. 4, pp. 349–358, Apr. 2013. doi: 10.1364/JOCN.5.000349.
- [50] I. S. Ansari, F. Yilmaz, and M.-S. Alouini, "Impact of pointing errors on the performance of mixed RF/FSO dual-hop transmission systems," *IEEE Wireless Communications Letters*, vol. 2, no. 3, pp. 351–354, Jun. 2013. doi: 10.1109/WCL.2013.042313.130138.
- [51] X. Song, F. Yang, J. Cheng, N. Al-Dhahir, and Z. Xu, "Subcarrier phase-shift keying systems with phase errors in Lognormal turbulence channels," *IEEE/OSA Journal of Lightwave Technology*, vol. 33, no. 9, pp. 1896–1904, May 2015. doi: 10.1109/JLT.2015.2398847.

Manuscript received: 2016-02-12

Biographies

Md. Zoheb Hassan (mdzoheb@ece.ubc.ca) obtained his BSc degree in electrical and electronics engineering from Bangladesh University of Engineering and Technology, Bangladesh in 2011, and MSc degree in electrical engineering from The University of British Columbia, Canada in 2013. He is currently working towards his Ph.D. degree in the department of electrical and computer engineering, The University of British Columbia, Vancouver, BC, Canada. He is the recipient of 2014 four year fellowship at The University of British Columbia, Canada. His research interests include wireless optical communications, optimization and resource allocation in wireless communication networks, and digital communications over fading channels.

Md. Jahangir Hossain (jahangir.hossain@ubc.ca) received his BSc degree in electrical and electronics engineering from Bangladesh University of Engineering and Technology (BUET), Bangladesh, the MSc degree from the University of Victoria, Canada in August 2003, and the PhD degree from the University of British Columbia (UBC), Canada in 2007. He served as a lecturer at BUET. He was a research fellow with McGill University, Canada, the National Institute of Scientific Research, Canada, and the Institute for Telecommunications Research, University of South Australia, Australia. His industrial experiences include a senior systems engineer position with Redline Communications, Canada, and a research intern position with Communication Technology Lab, Intel, Inc. He is currently working as an assistant professor with the School of Engineering, UBC Okanagan campus, Canada. His research interests include bit interleaved coded modulation, spectrally efficient and power-efficient modulation schemes, cognitive radio, and cooperative communication systems. He is currently serving as an editor for the *IEEE Transactions on Wireless Communications*. He received the Natural Sciences and Engineering Research Council of Canada Postdoctoral Fellowship.

Julian Cheng (julian.cheng@ubc.ca) received his BEng degree (First Class) in electrical engineering from the University of Victoria, Canada in 1995, the MSc (Eng) degree in mathematics and engineering from Queens University, Canada in 1997, and the PhD degree in electrical engineering from the University of Alberta, Canada in 2003. He is currently an associate professor in the School of Engineering, The University of British Columbia, Canada. From 2005 to 2006, he was an assistant professor with the Department of Electrical Engineering, Lakehead University, Canada. Previously he worked for Bell Northern Research and Northern Telecom (later known as NORTEL Networks). His current research interests include digital communications over fading channels, orthogonal frequency division multiplexing, spread spectrum communications, statistical signal processing for wireless applications, and optical wireless communications. Currently, he serves as an editor for *IEEE Communication Letters*, *IEEE Transactions on Communications*, an associate editor for *IEEE Access*, and a guest editor for a special issue of *IEEE Journal on Selected Areas in Communications* on optical wireless communications. Dr. Cheng is also a senior member of IEEE.

Victor C. M. Leung (vleung@ece.ubc.ca) is a professor of Electrical and Computer Engineering and the holder of the TELUS Mobility Research Chair at The University of British Columbia (UBC), Canada. His research is in the areas of wireless networks and mobile systems. He has co-authored more than 800 technical papers in archival journals and refereed conference proceedings, several of which had won best paper awards. Dr. Leung is a fellow of IEEE, a fellow of the Royal Society of Canada, a fellow of the Canadian Academy of Engineering and a fellow of the Engineering Institute of Canada. He is serving or has served on the editorial boards of *JCN*, *IEEE JSAC*, *Transactions on Computers*, *Wireless Communications*, and *Vehicle Technology*, *Wireless Communications Letters*, and several other journals. He has provided leadership to the technical program committees and organizing committees of numerous international conferences. Dr. Leung was the recipient of the 1977 APEBC Gold Medal, NSERC Postgraduate Scholarships from 1977–1981, a 2012 UBC Killam Research Prize, and an IEEE Vancouver Section Centennial Award.

Short-Range Optical Wireless Communications for Indoor and Interconnects Applications

WANG Ke^{1,2,3}, Ampalavanapillai Nirmalathas², Christina Lim², SONG Tingting^{2,4}, LIANG Tian², Kamal Alameh⁵, and Efstratios Skafidas^{1,2}

(1. Center for Neural Engineering (CfNE), The University of Melbourne, VIC 3010, Australia;

2. Department of Electrical and Electronic Engineering, The University of Melbourne, VIC 3010, Australia;

3. Department of Electrical Engineering, Stanford University, CA 94305, USA;

4. National Key Laboratory of Tunable Laser Technology, Harbin Institute of Technology, Harbin 150001, China;

5. Electron Science Research Institute (ESRI), Edith Cowan University, WA 6027, Australia)

Abstract

Optical wireless communications have been widely studied during the past decade in short-range applications, such as indoor high-speed wireless networks and interconnects in data centers and high-performance computing. In this paper, recent developments in high-speed short-range optical wireless communications are reviewed, including visible light communications (VLCs), infrared indoor communication systems, and reconfigurable optical interconnects. The general architecture of indoor high-speed optical wireless communications is described, and the advantages and limitations of both visible and infrared based solutions are discussed. The concept of reconfigurable optical interconnects is presented, and key results are summarized. In addition, the challenges and potential future directions of short-range optical wireless communications are discussed.

Keywords

indoor infrared communications; optical wireless communications; reconfigurable optical interconnects; visible light communications

1 Introduction

Broadband access networks have been widely deployed, mainly using the passive optical network (PON) architecture, and high-speed connectivity has been provided to door steps of users' premises [1]. Therefore, high-speed communications within personal working/living spaces are highly demanded. The popularity and availability of high-performance portable communication devices such as smartphones and tablets has brought more demands on wireless connectivity that supports mobility than those based on wired connections.

Several technologies have been investigated to provide over gigabit-per-second wireless connections to users in indoor environments. The millimeter-wave (mm-wave) system using the 60 GHz range is a promising solution which utilizes the several GHz license-free bandwidth available [2], [3]. One advantage

of 60 GHz mm-wave systems is the possibility of realizing compact integrated transceivers, including mixers, phase-locked loops, amplifiers and phased-array antennas, by using complementary metal-oxide-semiconductor (CMOS), which is the dominant technology in the semiconductor industry. However, the distribution of 60 GHz mm-wave signals to indoor scenarios is challenging, mainly due to the high free-space propagation loss and the line-of-sight propagation requirement. Typically, it is also challenging to realize broadband CMOS based mm-wave transceivers. Therefore, the license-free bandwidth available needs to be divided into several sub-bands and the data to be transmitted needs to be fit into a limited sub-band. This results in the use of comparatively complicated modulations and signal processing algorithms. Another type of widely investigated high-speed indoor wireless communication technology is the ultra-wideband (UWB) based system, which has low power spectral density (PSD) spread over a wide range of frequencies and can share the RF spectrum with other existing communication systems [4], [5]. However, there is a fundamental trade-off between the bit rate and the communication distance that can be achieved.

In addition to mm-wave and UWB systems, the optical wire-

This work is supported under Australian Research Council's Discovery Early Career Researcher Award (DECRA) funding scheme (project number DE150100924), The University of Melbourne's Early Career Researcher (ECR) funding scheme (project number 602702), and the Victoria Fellowship (D2015/35025).

Short-Range Optical Wireless Communications for Indoor and Interconnects Applications

WANG Ke, Ampalavanapillai Nirmalathas, Christina Lim, SONG Tingting, LIANG Tian, Kamal Alameh, and Efstratios Skafidas

less technology has also been widely studied to realize high-speed indoor communications, where the optical signal propagates through the free-space directly to the subscriber side [6]–[8]. Based on the carrier wavelength, indoor optical wireless systems can be divided into two broad categories, namely visible light communication (VLC) systems and infrared systems [9], [10]. In VLC systems, LEDs are used as light sources and they can be used for illumination and data transmission simultaneously. In infrared systems, the light source is typically laser which has much broader modulation bandwidth and higher cost compared to LEDs. In this paper, both systems will be discussed.

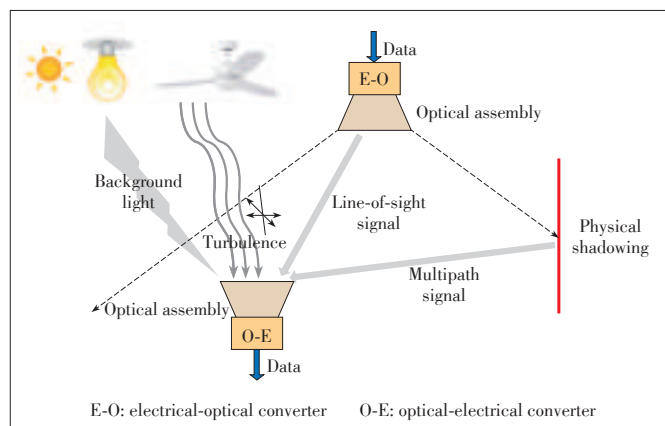
The optical wireless technology has also been applied in another short-range scenario—board-to-board optical interconnects in data centers and for high-performance computing [11]–[13]. With the rapid development of semiconductor integrated circuits such as processors and with the increasing data-intensive applications such as high-definition video in demand, high-speed interconnects are highly needed and the use of optical interconnects have been widely studied. According to the data transmission distance, optical interconnects can be divided into chip-to-chip, board-to-board, and rack-to-rack interconnects. The silicon photonics technology has been widely used in chip-to-chip interconnects, and high-speed transmissions have been realized through silicon waveguides [14]–[17]. For rack-to-rack interconnects, single-mode optical fiber is considered to increase both transmission speed and distance [18], [19]. Several solutions based on polymer waveguides, multi-mode fiber ribbons and free-space optics are considered for board-to-board optical interconnects [11]–[13], [20]–[22]. Compared with other solutions to board-to-board optical interconnects, the optical wireless based scheme is capable of providing the reconfigurability and flexibility through free-space beam steering. This scheme will be discussed in this paper.

2 High-Speed Indoor Optical Wireless Communications

2.1 Typical System Architecture and Model

Indoor optical wireless communication systems are typically modeled by the architecture shown in **Fig. 1**. The data to be transmitted (in the electrical domain) is first converted to the optical domain through an electrical-optical (E-O) conversion unit, where either LEDs or lasers can be used. Then the modulated optical signal passes through an optical assembly to generate the desired beam pattern for free-space propagation. The optical assembly can be used to generate collimated beams, fully diffusive beams, partially diffusive beams, or other special patterns such as multiple beam spots [6]. Then the optical signal propagates through the free-space link before being collected at the receiver side.

Optical signals arrive at the receiver side via two possible



▲ **Figure 1. Typical model of indoor optical wireless communication systems.**

links: the direct line-of-sight link and the non line-of-sight (multipath) link [23]. The multipath signal is mainly due to the reflections of physical shadowing items, such as walls, ground, ceiling, and cubicle partitions. For high-speed operations, the direct line-of-sight signals are always preferred because the multipath signals limit the channel bandwidth due to different propagation delays. However, when the direct line-of-sight link is blocked, multipath signals can be used to maintain wireless connections, although at much lower communication speed.

In addition to line-of-sight and multipath signals, background light is also collected at the receiver end. Both sunlight and illuminating lamps contribute to the collected background light. In order to reduce the impact of background light, optical bandpass filters are used at the receiver side to reject most of the out-of-band (signal band) background light. However, the in-band background light cannot be avoided and results in additional noise and performance degradation in the optical wireless communication system [24], [25].

In typical indoor optical wireless communication systems, an optical assembly is used at the receiver side for signal collection and focusing. The signal is converted back to the electrical domain by an optical-electrical (O-E) converter for further signal processing and characterization. It is desirable that the receiving optical assembly can collect large signal power with minimum multipath dispersion and background light power, and provide high optical gain to the O-E converter. In order to provide mobility to end users, a reasonable field-of-view (FOV) is also required for the receiving optical assembly. However, there is a trade-off between the FOV and the optical gain [23]. The receiver with a large FOV also collects high background light power. In addition, a large FOV may result in the collection of substantial multipath signals, limiting the system communication bandwidth [26]. To overcome this limitation, a number of advanced receiver designs have been proposed and investigated, such as angle-diversity receivers [27], imaging receivers [28], single-channel imaging receivers [29], [30], and steering-mirror assisted receivers [31], [32]. These solutions

Short-Range Optical Wireless Communications for Indoor and Interconnects Applications

WANG Ke, Ampalavanapillai Nirmalathas, Christina Lim, SONG Tingting, LIANG Tian, Kamal Alameh, and Efstratios Skafidas

use different mechanisms to limit the FOV of receiving elements (or each element). They can reduce the impact of background light, improve the optical gain, and enhance the transmission channel bandwidth. However, the cost is more complicated structure and operation.

Air turbulence is another possible source of performance degradation in indoor optical wireless communications. Although the indoor channel status is typically stable, turbulence still exists due to local environmental changes such as the change of local temperature because of air-conditioners or heaters. The scintillation and beam wandering effects are negligible in indoor short-range applications due to the relatively weak turbulence and short link distance, although these effects are limiting factors in outdoor long-range optical wireless systems. Turbulence also changes the polarization status of the optical signal at the receiver side. In general, the power penalty due to polarization dependent loss in indoor optical wireless systems is minimal.

Compared with RF based wireless communication systems such as Wi-Fi, mm-wave and UWB systems, indoor optical wireless communication systems have unique advantages. First of all, almost unlimited license-free bandwidth is available in optical wireless systems, ranging from ultra-violet (UV) and visible to infrared bands (the UV band is typically not used in indoor applications). Therefore, high-speed communications can be realized without spectrum limitations. Moreover, optical wireless systems are immune to electromagnetic interferences (EMIs). As a result, the optical wireless technology can be used in RF hostile environments, such as in hospitals or on aircrafts.

According to the link configuration, indoor optical wireless communication systems can be divided into two categories, namely directed systems and diffusive systems [23], as shown in Fig. 2a and Fig. 2b. In directed systems, a narrow signal beam is used to establish a point-to-point link between the transmitter and the receiver. Such a system has minimum multipath dispersion and can achieve high data transmission rate. In addition, the energy efficiency is high as well. However, strict alignment between transceivers is required in the directed system, which limits the mobility of end users. In diffusive systems, the entire room is covered by diffusive signal beams to provide full mobility to end users. However, the severe multipath dispersion limits the communication bandwidth and the

energy efficiency is low. Therefore, hybrid partial diffusive systems (Fig. 3c) have been proposed and demonstrated. In a hybrid system, the partial diffusive signal beam covers the user's location and surrounding areas to realize limited mobility and simultaneously maintains broad channel bandwidth and relatively high energy efficiency [33], [34].

2.2 Visible Light Communications

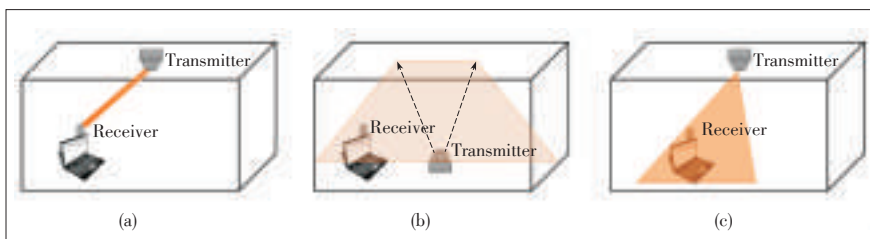
In indoor optical wireless communication systems, the use of visible wavelength range has been widely investigated [9], [35]–[55]. VLC systems generally use the wavelength range from 380 nm to 780 nm and LEDs serve as the light source in the systems. Because LEDs are more energy efficient compared with traditional illumination lights and widely deployed as headlights, the possibility of using LEDs for data transmissions has attracted intensive research interests. Different types of LEDs have been used for data transmission and they have different modulation bandwidths, ranging from a few tens of MHz (phosphorus LEDs), to about 100 MHz (RGB LEDs), and up to a few hundreds of MHz (resonant cavity enhanced LEDs). At the receiver (user) side, a photodiode (PD) or photodiode array is typically used for signal detection.

LEDs are incoherent light sources and transmitting information can only be realized by the optical intensity change. Therefore, intensity modulation and direct detection (IM/DD) is used in VLC systems. This also implies that the signal used to modulate LEDs needs to be real-valued, non-negative, and unipolar.

LEDs in VLC systems have limited modulation bandwidth, and other techniques are therefore needed to provide high-speed wireless connections to end users. A number of potential solutions have been proposed and investigated.

When the phosphor-based LED is used, a blue optical filter can be added at the receiver side to remove the yellow component that has slower frequency response, with the cost of higher link attenuation [36]. The communication speed can also be improved by using equalizations at the transmitter, receiver, or both sides [36]–[42]. The transmitter equalization is used to compensate for the LED fast roll-off frequency response, improving the modulation bandwidth. The equalization can also be applied at the receiver side to achieve higher data rates.

In addition, advanced modulation formats with better spectral efficiency can be used in VLC systems to further enhance the channel capacity [43], [44]. One widely used advanced modulation is the orthogonal frequency division multiplexing (OFDM). However, conventional OFDM signals are bipolar and complex, and cannot be directly applied to VLC systems with IM/DD scheme. Therefore, modifications are required, such as discrete multi-tone (DMT) modulation [45], [46], direct current optical OFDM (DCO-OFDM) [47], and asymmetrically clipped optical OFDM (ACO-OFDM) [48]–[50]. Another way to increase



▲ Figure 2. Different types of indoor optical wireless communication systems: (a) directed systems; (b) diffusive systems; and (c) partial diffusive systems.

Short-Range Optical Wireless Communications for Indoor and Interconnects Applications

WANG Ke, Ampalavanapillai Nirmalathas, Christina Lim, SONG Tingting, LIANG Tian, Kamal Alameh, and Efstratios Skafidas

the VLC system speed is the Multi-Input Multi-Output (MIMO) technique. This technique uses an array of LEDs and an array of photodiodes and can realize parallel communications [51], [52].

The VLC system is an attractive option for realizing high-speed indoor wireless communications, because it is able to provide illumination and data transmission simultaneously. Several solutions to its bandwidth limit have been proposed and the achievable bit rate has been significantly enhanced to well beyond 1 Gb/s. More detailed review on VLC systems can be found in [53]–[55].

2.3 Indoor Infrared Optical Wireless Communication Systems

Indoor optical wireless communication systems also use the near-infrared bands including 850 nm, 980 nm, and 1510 nm regions. In this type of systems, the laser is used as the light source. The laser has much broader modulation bandwidth compared with the LED. Therefore, high-speed operation can be achieved even using the simplest on-off-keying (OOK) modulation format without equalizations. The vertical cavity surface emitting laser (VCSEL) is a low-cost option for the optical transmitter. However, because of the laser eye and skin safety regulations, the transmission power is generally limited.

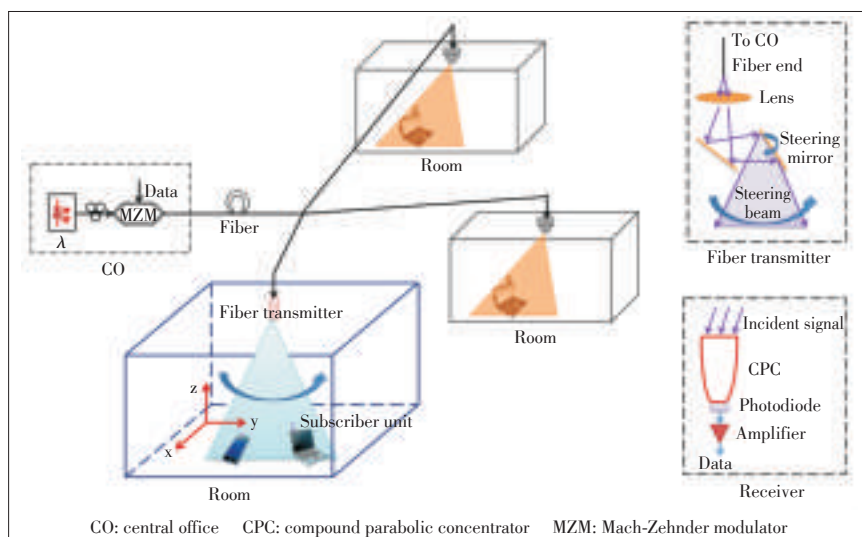
Considerable research attention has been devoted to the diffusive indoor infrared communication systems [23], [26]–[32]. Here, high-power laser is used to cover the entire room, providing full mobility to end users. However, the inherent multipath dispersion in the system results in limited channel bandwidth. A large FOV is also typically required at the receiver side, which also collects a large amount of background light. Furthermore, the high power laser leads to safety concerns. In order to overcome these limitations, a number of advanced schemes have been studied. At the transmitter side, the multi-spots technique has been proposed to provide better channel bandwidth, and at the receiver side, the diversity scheme has been employed for better channel impulse response and smaller collected background light [28]–[31], [56]. Adaptive power and beam spots/angular allocation mechanism based on the user location has also been investigated, with which over gigabit-per-second data rates become possible [57], [58].

In the previously mentioned VLC and diffusive indoor infrared communication systems, the light sources, either LEDs or lasers, are always placed inside each room and the distribution of data to each room is challenging, especially when the data is in the electrical domain. Although optical fibers can be used for signal distribution, additional optical-electrical-optical (O-E-O) conversion unit is needed at

each transmitter, which results in additional cost and control issues. In addition, complicated mechanisms, possibly advanced modulation format, MIMO, equalizations, advanced transceivers, and adaptive allocation schemes, are needed in the previously discussed systems to achieve high-speed data transmission.

To overcome these challenges, we have proposed a hybrid indoor optical wireless communication system using the near-infrared wavelength range in previous studies, and its basic architecture is shown in **Fig. 3** [7], [34]. Here, a centralized architecture is utilized where a central office (CO) serves multiple rooms through the in-building fiber distribution network. All expensive components and complicated control functions are placed in the CO, so the cost and complexity can be shared by multiple rooms and users. Inside each room, the ceiling mounted fiber transmitter is used and partially diffusive optical beam is used for data transmission. The beam covers the user location and surrounding areas to provide limited mobility. The fiber transmitter mainly consists of a fiber end connected with the CO, a lens for controlling the beam divergence angle, and MEMS-based steering mirrors to change the orientation of optical signal according to the user location. After free-space propagation, the optical signal from direct line-of-sight link is collected and detected. The simplest subscriber unit is a non-imaging receiver, which consists of a non-imaging compound parabolic concentrator (CPC) and a photodiode.

In this system, the user location is required to provide limited mobility. The user tracking function is also needed to change the beam orientation and to maintain high-speed wireless connectivity. The indoor localization function has been realized by using a number of technologies, such as RF based, imaging sensor based, infrared beams based and pyro-electric sensors based systems [59]–[62]. The indoor localization function can also be realized based on the optical wireless technology.



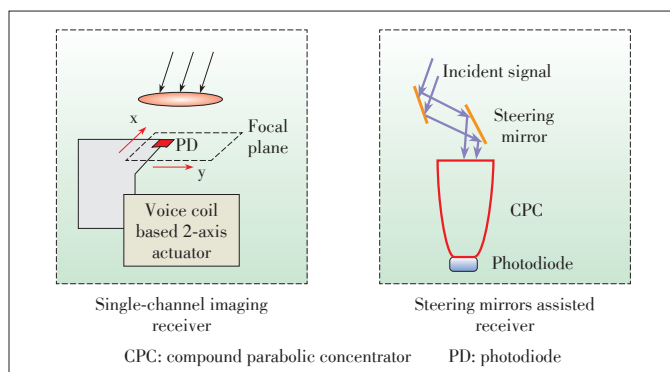
▲ **Figure 3. Centralized architecture of the hybrid indoor infrared optical wireless communication system.**

gy, using either VLC or infrared systems. The optical wireless indoor localization is out of the scope of this paper, and more details can be found in [63]–[65].

Similar with VLC systems, the background light is also a fundamental limiting factor in hybrid indoor infrared communication systems [25]. Advanced receivers, such as the single-channel imaging receiver and the steering mirrors assisted receiver, are used to reduce the impact of background light (**Fig. 4**) [29]–[32]. The single-channel imaging receiver mainly consists of an imaging lens for signal collection and focusing, and a small photo-sensitive area PD placed on a 2-axis actuator at the back focal plane of the lens [29], [30]. The actuator can be voice-coil based and move the PD on the focal plane to search for the focused signal spot. The receiver FOV is further limited due to the small size of PD, and this receiver is capable of rejecting most of the background light and improving the system performance. A similar concept is applied in the steering mirrors assisted receiver, where steering mirrors are used in front of the simple non-imaging receiver [31], [32]. The mirrors are steered according to the user location to reduce the incident angle of signal light into the CPC. Therefore, smaller FOV CPCs can be utilized which have higher optical gain and lower collected background light power. In addition, the steering mirrors further limit the receiver FOV for better system performance.

3 Reconfigurable Board-to-Board Optical Interconnects

Traditionally, electrical cables are used to realize board-to-board interconnects in data centers and for high performance computing. However, the electrical cables encounter a number of fundamental limitations with high-speed operations, including limited bandwidth, high transmission loss and latency, and weight and heat dissipation problems. To overcome these issues, optical interconnects based on polymer waveguides and multi-mode fiber ribbons have been proposed and investigated [20]–[22]. These proposed solutions are capable of high-speed data transmission between fixed ports/boards. However, high-



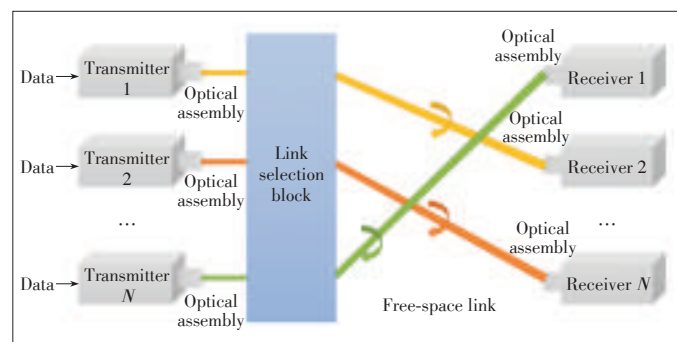
▲ **Figure 4.** Advanced receivers for hybrid indoor infrared optical wireless communication system.

speed O-E-O conversions are required for data re-routing to other destinations.

The optical wireless technology has been studied for realizing reconfigurable and flexible board-to-board optical interconnects [11]–[13], [66]–[70]. **Fig. 5** shows a typical architecture of optical wireless based interconnects. The electrical data to be transmitted first modulates optical transmitters, and low-cost VCSELs or VCSEL arrays are good choices for optical transmitters. Then the modulated optical beams pass through optical assemblies for collimation. A link selection block is then used which can dynamically change the beam orientation to different receivers according to requirements. After free-space propagation, signal beams arrive at the receiver side and are collected and focused by receiving optical assemblies. Optical signals are finally converted back to the electrical domain with photodiodes or photodiode arrays.

It can be seen that the flexibility and reconfigurability in optical wireless interconnects are realized by the link selection block, which dynamically steers signal beams to different destinations in the optical domain. The link selection block has been realized by using liquid crystal on silicon or opto Very Large Scale Integrated Circuits (opto-VLSIs) [66], [67]. However, both the solutions are based on optical signal diffractions and the beam steering range is limited. Furthermore, high order diffractions need to be used for large beam steering angles, which results in considerably large signal loss. To overcome these limitations, a link selection block based on MEMS steering mirrors has been proposed and investigated [68]–[70]. MEMS mirrors have simple link reconfiguration mechanism based on signal reflections. In addition, the signal loss after passing through such the link selection block is minimal because the MEMS mirrors reflection efficiency can be high through coating. Furthermore, the large beam steering range can be easily realized with the link selection block based on MEMS steering mirrors.

Multiple wavelength channels through wavelength division multiplexing (WDM) and multiple parallel free-space channels with the same operation wavelengths are used to realize ultra-high-speed board-to-board interconnections. Compared with the WDM solution, the solution based on multiple parallel



▲ **Figure 5.** Typical architecture of reconfigurable board-to-board optical interconnects based on the optical wireless technology.

Short-Range Optical Wireless Communications for Indoor and Interconnects Applications

WANG Ke, Ampalavanapillai Nirmalathas, Christina Lim, SONG Tingting, LIANG Tian, Kamal Alameh, and Efstratios Skafidas

free-space channels has the advantages of lower cost and simpler operation, because precise wavelength control circuits and wavelength multiplexers/demultiplexers are not needed. Therefore, the solution based on parallel channels is typically utilized.

Based on multiple parallel channels and MEMS steering mirrors, we have proposed and experimentally demonstrated a reconfigurable board-to-board optical interconnects [68]–[70]. The proposed interconnects architecture is shown in **Fig. 6**. One dedicated optical interconnect module is integrated onto each electronic card, which is typically a printed circuit board (PCB). Inside the optical interconnect module, a VCSEL array serves as the light sources for optical interconnects, and each VCSEL element is directly modulated by the data to be transmitted. The generated optical beams pass through a micro-lens array for collimation before being steered by the link selection block based on MEMS steering mirrors along arbitrary directions to the destinations. After free-space propagation, the optical beams are steered with another MEMS mirror array towards corresponding receivers, which consist of a micro-lens array for optical beam focusing and a photodiode array for detection.

To further increase the data rate of optical wireless based interconnects, advanced modulation formats can be used. However, this modulation format needs to support direct modulation of VCSELs and simple signal processing for keeping the low cost and low complexity of the system. The carrierless-amplitude-phase (CAP) modulation format can satisfy these requirements and have been applied in reconfigurable free-space optical interconnects. Up to 3–40 Gb/s interconnects have been experimentally demonstrated with 16-CAP [71].

In free-space based reconfigurable board-to-board optical interconnects, moderate or even strong turbulence exists due to the heat generated by electronic components and the fans for heat dissipation. The air turbulence results in refractive index fluctuations along the optical interconnection path and leads to signal scintillation, beam wandering and beam broadening effects [72]. Experimental results show that the power penalty is about 0.5 dB with moderate turbulence and about 1.6 dB with

comparatively strong turbulence [73].

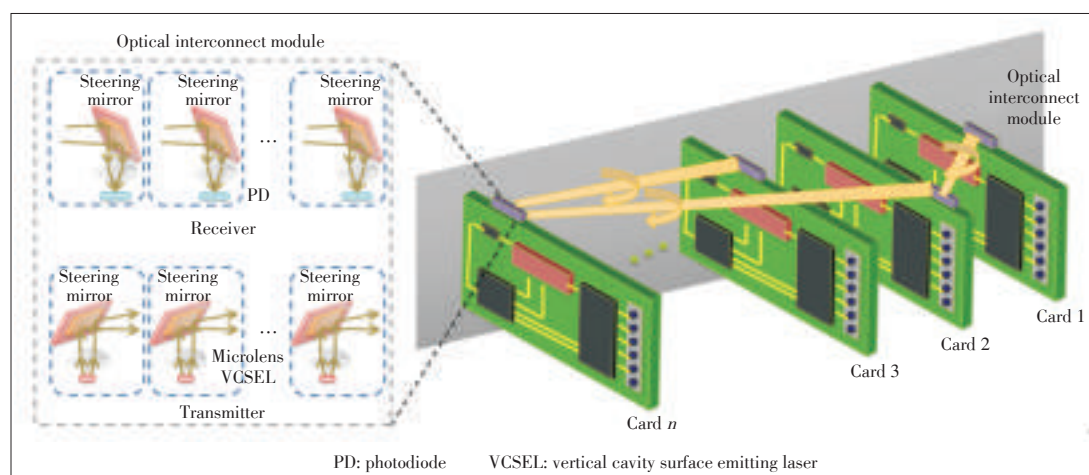
4 Discussions

The application of optical wireless technology in short-range applications has attracted considerable research attention and achieved significant advances during the past years. High-speed data transmissions have been demonstrated in both VLC, infrared and interconnect systems. However, there are still considerable aspects that require further innovative research efforts and some of these are discussed in this section.

4.1 Hybrid Indoor Optical Wireless Communication Systems with Multiple Users

In previous studies of hybrid high-speed indoor optical wireless communication systems with partial diffusive beams, especially systems using the infrared wavelength region as discussed in Section 2.3, typically the scenario with only one user is considered. However, in practical personal working/living spaces, multiple users may need to be connected simultaneously. Therefore, further studies on multiple users' scenarios are needed.

With safety considerations, partial diffusive beams are required and transmission power is limited. In this way, high-speed wireless connectivity can only be provided to a limited area. When multiple users are located in the same area of a room that can be covered by the signal beam, providing data transmission to all users can be achieved by simply using the time-division-multiplexing (TDM) scheme. However, when the multiple users are located in different areas inside the room, providing wireless connections becomes challenging. The TDM scheme can still be used by steering the signal beam to different users at different time slots. However, the throughput is reduced significantly due to the limited MEMS mirrors steering speed (in the millisecond or tens of milliseconds scale). In addition, the use of TDM decreases the data transmission speed to each user, and the situation becomes worse when the number of users increases. Therefore, other solutions are demand-



◀ **Figure 6.** Architecture of proposed reconfigurable board-to-board optical interconnects with MEMS mirrors and parallel channels.

Short-Range Optical Wireless Communications for Indoor and Interconnects Applications

WANG Ke, Ampalavanapillai Nirmalathas, Christina Lim, SONG Tingting, LIANG Tian, Kamal Alameh, and Efstratios Skafidas

ed and some of the possible candidates include the spatial-division-multiplexing scheme with which multiple fiber transmitters are used to connect different users or user groups, and the WDM scheme that uses different wavelengths to cover multiple users or user groups. However, detailed investigations are necessary, especially taking the cost into consideration. Furthermore, corresponding media access control (MAC) protocols need to be considered.

4.2 Dimming Requirements in VLC Systems

In VLC systems, LEDs are used for illumination and data transmission simultaneously, and typically a higher illumination level results in faster wireless connectivity. However, in practical applications, the LEDs may be preferred to be operated at a low illumination level, such as during day time where the sunlight is sufficient for illuminations. In this case, both the data transmission distance and bit rate are affected [74]–[77]. Therefore, further studies are needed using advanced techniques, such as the pulse width modulation (PWM) mechanism.

4.3 Indoor Optical Wireless Communication Systems with Physical Link Blocking

In indoor optical wireless communication systems, line-of-sight link is generally required for high-speed operations. However, in practice, the line-of-sight free-space link can be blocked, resulting in communication interruptions. Therefore, novel solutions are needed to maintain wireless data transmissions. Several schemes have been proposed and investigated, such as using the diffusive signal to maintain connectivity in case the line-of-sight link is blocked. Nevertheless, the data rate needs to be reduced significantly. Recently, we have proposed and demonstrated a space-time-coding based solution by exploiting the spatial diversity [78]. However, the system is more complicated and additional hardware is needed, leading to the cost concern. Another possibility is using the existing RF indoor communication systems, such as Wi-Fi systems, as the lower-speed backup, and switching data transmissions to the RF backup channel when the optical wireless line-of-sight link is blocked. However, the handover also requires further investigations.

4.4 Extending Optical Wireless Interconnection Range

In an optical wireless system for board-to-board interconnects, one fundamental limiting factor is the beam divergence during the free-space link propagation, which results in much larger beam size. Since high data density is required in interconnects applications, the VCSEL, PD and micro-lens arrays typically have a pitch size of a few hundred micro-meters. Therefore, after the free-space propagation, only a small amount transmitted by VCSELs can be collected by receiving micro-lenses for further signal detection, which limits the interconnection range. For larger scale applications, the intercon-

nection range needs to be extended and this requires further studies.

5 Conclusions

In this paper, the basic concepts and recent developments on short-range optical wireless communication systems have been reviewed and summarized. Modulated optical beams in optical wireless systems can directly propagate through the free space towards receivers to provide wireless connectivity. The optical wireless technology has been proposed to be applied in indoor personal area communications as well as in interconnects for data centers and high-performance computing. In indoor optical wireless communication systems, both VLC and infrared systems have been widely investigated and high-speed wireless data transmissions have been demonstrated in both types of systems. In optical wireless interconnects, the free-space signal propagation has been utilized to provide link re-configuration capability through beam steering. In addition to the exciting achievements in this area, several aspects that require further research attention have been discussed as well.

References

- [1] Y. Luo, X. Zhou, F. Effenberger, et al., "Time- and wavelength-division multiplex passive optical network (TWDM-PON) for next-generation PON stage 2 (NG-PON2)," *Journal of Lightwave Technology*, vol. 31, no. 4, pp. 587–593, Feb. 2013. doi: 10.1109/JLT.2012.2215841.
- [2] T. Mitomo et al., "A 2-Gb/s throughput CMOS transceiver chipset with in-package antenna for 60-GHz short-range wireless communication," *IEEE Journal of Solid-State Circuits*, vol. 47, no. 12, pp. 3160–3171, Dec. 2012. doi: 10.1109/JSSC.2012.2216694.
- [3] R. Minami et al., "A 60-GHz 16QAM 11Gbps direct-conversion transceiver in 65nm CMOS," in *Asia and South Pacific Design Automation Conference*, Sydney, Australia, Jan. 2012, pp. 467–468. doi: 10.1109/ASPAC.2012.6164993.
- [4] D. Porcino and W. Hirt, "Ultra-wideband radio technology: potential and challenges ahead," *IEEE Communications Magazine*, vol. 41, no. 7, pp. 66–74, Jul. 2003. doi: 10.1109/MCOM.2003.1215641.
- [5] H. Xu and L. Yang, "Ultra-wideband technology: yesterday, today, and tomorrow," in *IEEE Radio and Wireless Symposium*, Orlando, USA, Jan. 2008, pp. 715–718. doi: 10.1109/RWS.2008.4463592.
- [6] H. Elgala, R. Mesleh, and H. Hass, "Indoor optical wireless communication: potential and state-of-the-art," *IEEE Communications Magazine*, vol. 49, no. 9, pp. 56–62, Sept. 2011. doi: 10.1109/MCOM.2011.6011734.
- [7] K. Wang, A. Nirmalathas, C. Lim, and E. Skafidas, "High-speed optical wireless communication system for indoor applications," *IEEE Photonics Technology Letters*, vol. 23, no. 8, pp. 519–521, Apr. 2011. doi: 10.1109/LPT.2011.2113331.
- [8] A. M. Street, P. N. Stavrinou, D. C. O'Brien, and D. J. Edwards, "Indoor optical wireless systems—a review," *Optical and Quantum Electronics*, vol. 29, no. 3, pp. 349–378, Mar. 1997. doi: 10.1023/A:1018530828084.
- [9] T. Komine and M. Nakagawa, "Fundamental analysis for visible-light communication system using LED lights," *IEEE Transactions on Consumer Electronics*, vol. 50, no. 1, pp. 100–107, Feb. 2004. doi: 10.1109/TCE.2004.1277847.
- [10] M. Kavehrad, "Sustainable energy-efficient wireless applications using light," *IEEE Communications Magazine*, vol. 48, no. 12, pp. 66–73, Dec. 2010. doi: 10.1109/MCOM.2010.5673074.
- [11] E. M. Strzelecka, D. A. Loderback, B. J. Thibeault, et al., "Parallel free-space optical interconnect based on arrays of vertical-cavity lasers and detectors with monolithic microlenses," *Applied Optics*, vol. 37, no. 14, pp. 2811–2821, May 1998. doi: 10.1364/AO.37.002811.
- [12] A. G. Kirk, D. G. Plant, M. H. Ayliffe, M. Chateaufneuf, and F. Lacroix, "Design rules for highly parallel free-space optical interconnects," *IEEE Journal of Selected Topics in Quantum Electronics*, vol. 9, no. 2, pp. 531–547, Mar.–Apr.

Short-Range Optical Wireless Communications for Indoor and Interconnects Applications

WANG Ke, Ampalavanapillai Nirmalathas, Christina Lim, SONG Tingting, LIANG Tian, Kamal Alameh, and Efstratios Skafidas

2003. doi: 10.1109/JSTQE.2003.812482.
- [13] R. Wang, A. D. Rakic, and M. L. Majewski, "Design of microchannel free-space optical interconnects based on vertical-cavity surface-emitting laser arrays," *Applied Optics*, vol. 41, no. 17, pp. 3469–3478, Jun. 2002. doi: 10.1364/AO.41.003469.
- [14] L. Chen, K. Preston, S. Manipatruni, and M. Lipson, "Integrated GHz silicon photonic interconnect with micrometer-scale modulators and detectors," *Optics Express*, vol. 17, no. 17, pp. 15248–15256, Aug. 2009. doi: 10.1364/OE.17.015248.
- [15] C. Gunn, "CMOS photonics for high-speed interconnects," *IEEE Micro*, vol. 26, no. 2, pp. 58–66, Mar.–Apr. 2006. doi: 10.1109/MM.2006.32.
- [16] F. Xia, M. Rooks, L. Sekaric, and Y. Vlasov, "Ultra-compact high order ring resonator filters using submicron silicon photonic wires for on-chip optical interconnects," *Optics Express*, vol. 15, no. 19, pp. 11934–11941, Sept. 2007. doi: 10.1364/OE.15.011934.
- [17] M. J. R. Heck et al., "Hybrid silicon photonics for optical interconnects," *IEEE Journal of Selected Topics in Quantum Electronics*, vol. 17, no. 2, pp. 333–346, Mar.–Apr. 2011. doi: 10.1109/JSTQE.2010.2051798.
- [18] A. F. Benner, M. Ignatowski, J. A. Kash, D. M. Kuchta, and M. B. Ritter, "Exploitation of optical interconnects in future server architectures," *IBM Journal of Research and Development*, vol. 49, no. 4.5, pp. 755–775, Jul. 2005. doi: 10.1147/rd.494.0755.
- [19] M. A. Taubenblatt, "Optical interconnects for high-performance computing," *Journal of Lightwave Technology*, vol. 30, no. 4, pp. 448–457, Feb. 2012. doi: 10.1109/JLT.2011.2172989.
- [20] N. Bamiedakis, J. Beals, R. V. Pentz, I. H. White, et al., "Cost-effective multi-mode polymer waveguides for high-speed on-board optical interconnects," *IEEE Journal of Quantum Electronics*, vol. 45, no. 4, pp. 415–424, Apr. 2009. doi: 10.1109/JQE.2009.2013111.
- [21] M. Tan et al., "OPTOPUS: optical backplane for data center switches," in *Optical Fiber Communications Conference and Exhibition*, San Francisco, USA, Mar. 2014, pp. M3E.3. doi: 10.1364/OFC.2014.M3E.3.
- [22] F. E. Doany et al., "160 Gb/s bidirectional polymer-waveguide board-level optical interconnects using CMOS-based transceivers," *IEEE Transactions on Advanced Packaging*, vol. 32, no. 2, pp. 345–359, May 2009. doi: 10.1109/TADVP.2009.2014877.
- [23] J. M. Kahn and J. R. Barry, "Wireless infrared communications," *Proceedings of the IEEE*, vol. 85, no. 2, pp. 265–298, Feb. 1997. doi: 10.1109/5.554222.
- [24] A. J. C. Moreira, R. T. Valadas, and A. M. de Oliveira Duarte, "Characterization and modelling of artificial light interference in optical wireless communication systems," in *IEEE International Symposium on Personal, Indoor and Mobile Radio Communications*, Toronto, Canada, Sept. 1995, pp. 326–331 vol. 1. doi: 10.1109/PIMRC.1995.476907.
- [25] K. Wang, A. Nirmalathas, C. Lim, and E. Skafidas, "Impact of background light induced shot noise in high-speed full-duplex indoor optical wireless communication systems," *Optics Express*, vol. 19, no. 22, pp. 21321–21332, Oct. 2011. doi: 10.1364/OE.19.021321.
- [26] J. B. Carruthers and J. M. Kahn, "Modelling of nondirected wireless infrared channels," *IEEE Transactions on Communications*, vol. 45, no. 10, pp. 1260–1268, Oct. 1997. doi: 10.1109/26.634690.
- [27] J. B. Carruthers and J. M. Kahn, "Angle diversity for nondirected wireless infrared communication," *IEEE Transactions on Communications*, vol. 48, no. 6, pp. 960–969, Jun. 2000. doi: 10.1109/26.848557.
- [28] P. Djahani and J. M. Kahn, "Analysis of infrared wireless links employing multibeam transmitters and imaging diversity receivers," *IEEE Transactions on Communications*, vol. 48, no. 12, pp. 2077–2088, Aug. 2002. doi: 10.1109/26.891218.
- [29] M. Castillo-Vazquez and A. Puerta-Notario, "Single-channel imaging receiver for optical wireless communications," *IEEE Communications Letters*, vol. 9, no. 10, pp. 897–899, Oct. 2005. doi: 10.1109/LCOMM.2005.10021.
- [30] K. Wang, A. Nirmalathas, C. Lim, and E. Skafidas, "High-speed indoor optical wireless communication system with single channel imaging receiver," *Optics Express*, vol. 20, no. 8, pp. 8442–8456, Apr. 2012. doi: 10.1364/OE.20.008442.
- [31] K. Wang, A. Nirmalathas, C. Lim, and E. Skafidas, "High-speed optical wireless communication system with steering-mirror based receiver for personal area communications," in *IEEE Photonics Conference*, Burlingame, USA, Sept. 2012, pp. 638–639. doi: 10.1109/IPC.2012.6358783.
- [32] K. Wang, A. Nirmalathas, C. Lim, and E. Skafidas, "High-speed indoor optical wireless communication system with a steering mirror based up-link receiver," in *European Conference and Exhibition on Optical Communications*, Amsterdam, Sept. 2012, pp. We.3.B.3. doi: 10.1364/ECEOC.2012.We.3.B.3.
- [33] C. W. Oh, E. Tangdiongga, and A. M. J. Koonen, "Steerable pencil beams for multi-Gbps indoor optical wireless communications," *Optics Letters*, vol. 39, no. 18, pp. 5427–5430, Sept. 2014. doi: 10.1364/OL.39.005427.
- [34] K. Wang, A. Nirmalathas, C. Lim, and E. Skafidas, "High-speed duplex optical wireless communication systems for indoor personal area networks," *Optics Express*, vol. 18, no. 24, pp. 25199–25216, Nov. 2010. doi: 10.1364/OE.18.025199.
- [35] K. Lee, H. Park, and J. R. Barry, "Indoor channel characteristics for visible light communications," *IEEE Communications Letters*, vol. 15, no. 2, pp. 217–219, Feb. 2011. doi: 10.1109/LCOMM.2011.010411.101945.
- [36] H. L. Minh et al., "100-Mb/s NRZ visible light communications using a post-equalized white LED," *IEEE Photonics Technology Letters*, vol. 21, no. 15, pp. 1063–1065, Aug. 2009. doi: 10.1109/PTL.2009.2022413.
- [37] H. L. Minh et al., "High-speed visible light communications using multiple-resonant equalization," *IEEE Photonics Technology Letters*, vol. 20, no. 14, pp. 1243–1245, Jul. 2008. doi: 10.1109/PTL.2008.926030.
- [38] T. Komine, J. H. Lee, S. Haruyama, and M. Nakagawa, "Adaptive equalization system for visible light wireless communication using multiple white LED lighting equipment," *IEEE Transactions on Wireless Communications*, vol. 8, no. 6, pp. 2892–2900, Jun. 2009. doi: 10.1109/TWC.2009.060258.
- [39] H. Li, X. Chen, B. Huang, D. Tang, and D. Chen, "High bandwidth visible light communications based on a post-equalization circuit," *IEEE Photonics Technology Letters*, vol. 26, no. 2, pp. 119–122, Jan. 2014. doi: 10.1109/LPT.2013.2290026.
- [40] Y. Wang, X. Huang, L. Tao, J. Shi, and N. Chi, "4.5-Gb/s RGB-LED based WDM visible light communication system employing CAP modulation and RLS based adaptive equalization," *Optics Express*, vol. 23, no. 10, pp. 13626–13633, May 2015. doi: 10.1364/OE.23.013626.
- [41] Y.-F. Liu, Y. C. Chang, C.-W. Chow, and C.-H. Yeh, "Equalization and pre-distorted schemes for increasing data rate in in-door visible light communication systems," in *Optical Fiber Communication Conference/National Fiber Optic Engineers Conference*, Los Angeles, USA, Mar. 2011, pp. JWA083. doi: 10.1364/NFOEC.2011.JWA083.
- [42] X. Huang, Z. Wang, J. Shi, Y. Wang, and N. Chi, "1.6 Gbit/s phosphorescent white LED based VLC transmission using a cascaded pre-equalization circuit and a differential outputs PIN receiver," *Optics Express*, vol. 23, no. 17, pp. 22034–22042, Aug. 2015. doi: 10.1364/OE.23.022034.
- [43] C. W. Chow, C. H. Yeh, Y. F. Liu, P. Y. Huang, and Y. Liu, "Adaptive scheme for maintaining the performance of the in-home white-LED visible light wireless communications using OFDM," *Optics Communications*, vol. 292, pp. 49–52, Apr. 2013. doi: 10.1016/j.optcom.2012.11.081.
- [44] Z. Wang, C. Yu, W. D. Zhong, and J. Chen, "Performance improvement by tilting receiver plane in M-QAM OFDM visible light communications," *Optics Express*, vol. 19, no. 14, pp. 13418–13427, Jul. 2011. doi: 10.1364/OE.19.013418.
- [45] J. Vucic, C. Kottke, S. Nerreter, K.-D. Langer, and J. W. Walewski, "513 Mbit/s visible light communications link based on DMT-modulation of a white LED," *Journal of Lightwave Technology*, vol. 28, no. 24, pp. 3512–3518, Dec. 2010. doi: 10.1109/JLT.2010.2089602.
- [46] G. Cossu, A. M. Khalid, P. Choudhury, R. Corsini, and E. Ciarabella, "3.4 Gbit/s visible optical wireless transmission based on RGB LED," *Optics Express*, vol. 20, no. 26, pp. B501–B506, Dec. 2012. doi: 10.1364/OE.20.00B501.
- [47] H. Zhang, Y. Yuan, and W. Xu, "PAPR reduction for DCO-OFDM visible light communications via semidefinite relaxation," *IEEE Photonics Technology Letters*, vol. 26, no. 17, pp. 1718–1721, Sept. 2014. doi: 10.1109/LPT.2014.2331360.
- [48] X. Li, J. Vucic, V. Jungnickel, and J. Armstrong, "On the capacity of intensity-modulated direct-detection systems and the information rate of ACO-OFDM for indoor optical wireless applications," *IEEE Transactions on Communications*, vol. 60, no. 3, pp. 799–809, Mar. 2012. doi: 10.1109/TCOMM.2012.020612.090300.
- [49] S. Dimitrov and H. Hass, "On the clipping noise in an ACO-OFDM optical wireless communication system," in *IEEE Global Telecommunications Conference*, Miami, USA, Dec. 2010, pp. 1–5. doi: 10.1109/GLOCOM.2010.5684301.
- [50] R. Mesleh and H. Hass, "On the performance of different OFDM based optical wireless communication systems," *Journal of Optical Communications and Networking*, vol. 3, no. 8, pp. 620–628, Aug. 2011. doi: 10.1364/JOCN.3.000620.
- [51] A. H. Azhar, T. Tran, and D. O'Brien, "A gigabit/s indoor wireless transmission using MIMO-OFDM visible-light communications," *IEEE Photonics Technology Letters*, vol. 25, no. 2, pp. 171–174, Jan. 2013. doi: 10.1109/LPT.2012.2231857.
- [52] T. Q. Wang, Y. A. Sekercioglu, and J. Armstrong, "Analysis of an optical wireless receiver using a hemispherical lens with application in MIMO visible light communications," *Journal of Lightwave Technology*, vol. 31, no. 11, pp. 1744–

Short-Range Optical Wireless Communications for Indoor and Interconnects Applications

WANG Ke, Ampalavanapillai Nirmalathas, Christina Lim, SONG Tingting, LIANG Tian, Kamal Alameh, and Efstratios Skafidas

- 1754, Jun. 2013. doi: 10.1109/JLT.2013.2257685.
- [53] D. Tsonev, S. Videv, and H. Hass, "Light fidelity (Li-Fi): towards all optical networking," *Proc. SPIE 9007*, Broadband Access Communication Technologies VIII, 900792, Dec. 2013. doi: 10.1117/12.2044649.
- [54] H. Burchardt, N. Serafimovski, D. Tsonev, S. Videv, and H. Hass, "VLC: beyond point-to-point communication," *IEEE Communications Magazine*, vol. 52, no. 7, pp. 98–105, Jul. 2014. doi: 10.1109/MCOM.2014.6852089.
- [55] L. Grobe et al., "High-speed visible light communication systems," *IEEE Communications Magazine*, vol. 51, no. 12, pp. 60–66, Dec. 2013. doi: 10.1109/MCOM.2013.6685758.
- [56] A. G. Al-Ghamdi and J. M. H. Elmirghani, "Line strip spot-diffusing transmitter configuration for optical wireless systems influenced by background noise and multipath dispersion," *IEEE Transactions on Communications*, vol. 52, no. 1, pp. 37–45, Jan. 2004. doi: 10.1109/TCOMM.2003.822160.
- [57] F. E. Alsaadi and J. M. H. Elmirghani, "Mobile multigigabit indoor optical wireless systems employing multibeam power adaptation and imaging diversity receivers," *Journal of Optical Communications and Networking*, vol. 3, no. 1, pp. 27–39, Jan. 2011. doi: 10.1364/JOCN.3.000027.
- [58] M. T. Alresheedi and J. M. H. Elmirghani, "Performance evaluation of 5 Gbit/s and 10 Gbit/s mobile optical wireless systems employing beam angle and power adaptation with diversity receivers," *IEEE Journal on Selected Areas in Communications*, vol. 29, no. 6, pp. 1328–1340, Jun. 2011. doi: 10.1109/JSAC.2011.110620.
- [59] C.-H. Lim, Y. Wan, B.-P. Ng, and C.-M. S. See, "A real-time indoor WiFi localization system using smart antennas," *IEEE Transactions on Consumer Electronics*, vol. 53, no. 2, pp. 618–622, May. 2007. doi: 10.1109/TCE.2007.381737.
- [60] S. Lee, K. N. Ha, and K. C. Lee, "A pyroelectric infrared sensor-based indoor location-aware system for the smart home," *IEEE Transactions on Consumer Electronics*, vol. 52, no. 4, pp. 1311–1317, Nov. 2006. doi: 10.1109/TCE.2006.273150.
- [61] P.-W. Chen, K.-S. Ou, and K.-S. Chen, "IR indoor localization and wireless transmission for motion control in smart building applications based on Wiimote technology," in *SICE Annual Conference*, Taipei, China, Aug. 2010, pp. 1781–1785.
- [62] J. Kim and H. Jun, "Vision-based location positioning using augmented reality for indoor navigation," *IEEE Transactions on Consumer Electronics*, vol. 54, no. 3, pp. 954–962, Aug. 2008. doi: 10.1109/TCE.2008.4637573.
- [63] T. Q. Wang, Y. A. Sekercioglu, A. Nelid, and J. Armstrong, "Position accuracy of time-of-arrival based ranging using visible light with application in indoor localization systems," *Journal of Lightwave Technology*, vol. 31, no. 20, pp. 3302–3308, Oct. 2013. doi: 10.1109/JLT.2013.2281592.
- [64] K. Wang, A. Nirmalathas, C. Lim, and E. Skafidas, "Experimental demonstration of a novel indoor optical wireless localization system for high-speed personal area networks," *Optics Letters*, vol. 40, no. 7, pp. 1246–1249, Apr. 2015. doi: 10.1364/OL.40.001246.
- [65] K. Wang, A. Nirmalathas, C. Lim, and E. Skafidas, "Experimental demonstration of optical wireless indoor localization system with background light power estimation," in *Optical Fiber Communication Conference*, Los Angeles, USA, Mar. 2015, pp. W2A.63. doi: 10.1364/OFC.2015.W2A.63.
- [66] C. J. Henderson, D. G. Leyva, and T. D. Wilkinson, "Free space adaptive optical interconnect at 1.25 Gb/s, with beam steering using a ferroelectric liquid-crystal SLM," *Journal of Lightwave Technology*, vol. 24, no. 5, May 2006. doi: 10.1109/JLT.2006.871015.
- [67] M. Aljida, K. E. Alameh, Y.-T. Lee, and I.-S. Chung, "High-speed (2.5 Gbps) reconfigurable inter-chip optical interconnects using opto-VLSI processors," *Optics Express*, vol. 14, no. 15, pp. 6823–6836, Jul. 2006. doi: 10.1364/OE.14.006823.
- [68] K. Wang, A. Nirmalathas, C. Lim, E. Skafidas, and K. Alameh, "Experimental demonstration of 3–3 10 Gb/s reconfigurable free space optical card-to-card interconnects," *Optics Letters*, vol. 37, no. 13, pp. 2553–2555, Jul. 2012. doi: 10.1364/OL.37.002553.
- [69] K. Wang, A. Nirmalathas, C. Lim, E. Skafidas, and K. Alameh, "Experimental demonstration of high-speed free-space reconfigurable card-to-card optical interconnects," *Optics Express*, vol. 21, no. 3, pp. 2850–2861, Feb. 2013. doi: 10.1364/OE.21.002850.
- [70] K. Wang, A. Nirmalathas, C. Lim, E. Skafidas, and K. Alameh, "High-speed free-space based reconfigurable card-to-card optical interconnects with broadcast capability," *Optics Express*, vol. 21, no. 13, pp. 15395–15400, Jul. 2013. doi: 10.1364/OE.21.015395.
- [71] K. Wang, A. Nirmalathas, C. Lim, E. Skafidas, and K. Alameh, "Experimental demonstration of free-space based 120 Gb/s reconfigurable card-to-card optical interconnects," *Optics Letters*, vol. 39, no. 19, pp. 5717–5720, Oct. 2014. doi: 10.1364/OL.39.005717.
- [72] R. Rachmani, A. Ziberman, and S. Arnon, "Computer backplane with free space optical links: air turbulence effects," *Journal of Lightwave Technology*, vol. 30, no. 1, pp. 156–162, Jan. 2012. doi: 10.1109/JLT.2011.2177442.
- [73] K. Wang, A. Nirmalathas, C. Lim, E. Skafidas, and K. Alameh, "Performance of high-speed reconfigurable free-space card-to-card optical interconnect under air turbulence," *Journal of Lightwave Technology*, vol. 31, no. 11, pp. 1687–1693, Jun. 2013. doi: 10.1109/JLT.2013.2256459.
- [74] H. Sugiyama, S. Haruyama, and M. Nakagawa, "Brightness control methods for illumination and visible-light communication systems," in *International Conference on Wireless and Mobile Communications*, Guadeloupe, France, Mar. 2007, pp. 78. doi: 10.1109/ICWMC.2007.26.
- [75] Z. Wang, W. D. Zhong, Y. Yu, J. Chen, C. P. S. Francois, and W. Chen, "Performance of dimming control scheme in visible light communication system," *Optics Express*, vol. 20, no. 17, pp. 18861–18868, Aug. 2012. doi: 10.1364/OE.20.018861.
- [76] J. K. Kwon, "Inverse source coding for dimming in visible light communications using NRZ-OOK on reliable links," *IEEE Photonics Technology Letters*, vol. 22, no. 19, pp. 1455–1457, Oct. 2010. doi: 10.1109/LPT.2010.2062498.
- [77] J.-Y. Sung, C.-W. Chow, and C.-H. Yeh, "Dimming-discrete-multi-tone (DMT) for simultaneous color control and high speed visible light communication," *Optics Express*, vol. 22, no. 7, pp. 7538–7543, Apr. 2014. doi: 10.1364/OE.22.007538.
- [78] K. Wang, A. Nirmalathas, C. Lim, T. Song, and E. Skafidas, "Experimental demonstration of space-time-coded robust high-speed indoor optical wireless communication system," in *IEEE Photonics Conference*, Reston, USA, Oct. 2015, pp. 417–418. doi: 10.1109/IPCon.2015.7323467.

Manuscript received: 2016-01-27

Biographies

WANG Ke (ke.wang@unimelb.edu.au) received his BSc degree from Huazhong University of Science and Technology (HUST), China in 2009, and the PhD degree in Electrical and Electronic Engineering from The University of Melbourne, Australia in 2014. He is currently an Australian Research Council (ARC) Discovery Early Career Researcher Award (DECRA) fellow at Center for Neural Engineering (CiNE), Department of Electrical and Electronic Engineering, The University of Melbourne. He is also a Visiting Assistant Professor at Stanford University, USA. He has authored or co-authored over 70 papers in peer-reviewed journals and conferences. His current research interests include silicon photonics integration, optical wireless technology, high-speed personal area networks, and optical interconnects. He has been awarded the IEEE Photonics Society Postgraduate Student Fellowship, the Marconi Society Paul Baran Young Scholar Fellowship, the ARC DECRA Fellowship, and the Victoria Fellowship.

Ampalavanapillai Nirmalathas (nirmalat@unimelb.edu.au) is a professor of Electrical and Electronic Engineering at The University of Melbourne, Australia. He is also the director of Melbourne Networked Society Institute—an interdisciplinary research institute focusing on challenges and opportunities arising from the society's transition towards a networked society. He also co-founded and provides academic leadership to the Australia's first university based start-up accelerator—Melbourne Accelerator Program, aimed at promoting entrepreneurship culture on campus.

Prof Nirmalathas obtained his BEng and PhD in Electrical and Electronic Engineering from the University of Melbourne in 1993 and 1998 respectively. Between 2010 and 2013, he was the Head of Department of Electrical and Electronic Engineering. Between 2013 and 2014, He was the associate director for the Institute for Broadband-Enabled Society.

He has written more than 400 technical articles and currently hold three active international patents. His current research interests include energy efficient telecommunications, access networks, optical-wireless network integration and broadband systems and devices. He has held many editorial roles with *IEICE Transactions in Communications*, *IEEE/OSA Journal of Lightwave Technology and Photonics* and *Networks SPIE Journal*. He is a Senior Member of IEEE, a member of Optical Society of America and a fellow of the Institution of Engineers Australia.

Short-Range Optical Wireless Communications for Indoor and Interconnects Applications

WANG Ke, Ampalavanapillai Nirmalathas, Christina Lim, SONG Tingting, LIANG Tian, Kamal Alameh, and Efstratios Skafidas

Christina Lim (chrislim@unimelb.edu.au) received the BE and PhD degrees in Electrical and Electronic Engineering from the University of Melbourne, Australia in 1995 and 2000, respectively. She is currently a professor at the Department of Electrical and Electronic Engineering, the University of Melbourne, Australia. She served as the director of the Photonics and Electronics Research Laboratory at the same department from 2011–2015. She was awarded the Australian Research Council (ARC) Australian Research Fellowship from 2004–2008 and the ARC Future Fellow (2009–2013). Between 2003 and 2005, she was a key researcher and also the project leader of the Australian Photonics CRC Fiber-to-the-Premises Challenge Project. Her research interests include fiber-wireless access technology, modeling of optical and wireless communication systems, microwave photonics, application of mode-locked lasers, optical network architectures and optical signal monitoring. She is a member of the IEEE Photonics Society Board of Governors (2015–2017). She is also a member of the Steering Committee for the IEEE Topical Meeting on Microwave Photonics Conference. She is currently an associate editor for the *IEEE Photonics Society Newsletter*, *IEEE Photonics Technology Letter* and *IET Electronics Letter*. She is also a member of the IEEE Microwave Theory and Technique Subcommittee 3 (MTT3) - Microwave Photonics Technical Committee.

SONG Tingting (tingting.song@unimelb.edu.au) is a PhD student in Optical Engineering at the Harbin Institute of Technology, China. Currently, she is working as a visiting PhD student at the Department of Electrical and Electronic Engineering at The University of Melbourne, Australia. She received the BE degree in Measurement Technology and Instrument from the Northeastern University, China, in 2010, and the ME degree in Detection Technology and Automation Instrument from the Northeastern University, China, in 2012. Her previous studies were in fiber-optic sensor design and optical sensing component design, and her current research interests include optical wireless communication system design, optical component design and integration for optical communication and optical sensing, and free space optical technology.

LIANG Tian (liang2@student.unimelb.edu.au) received BE and BE (Hons) degrees in optoelectronics engineering from Beijing Institute of Technology, China, and electronic and communication systems from Australian National University, Australia, respectively. She is currently working towards the Ph.D degree in electrical and electronic engineering at Department of Electrical and Electronic Engineering, The

University of Melbourne, Melbourne, Australia. She received Chancellor's Letters of Commendation, CEA Technologies Prize in Telecommunications, College Dean's List Prize and International Student Scholarship of ANU during her undergraduate period. She held a research internship at network group of National ICT Australia (NICTA) Canberra Research Laboratory in 2014. Her research interests include indoor optical wireless communication systems, converged fibre-wireless access network and broadband optical access networks.

Kamal Alameh (k.alameh@ecu.edu.au) received the MEng degree in photonics from the University of Melbourne, Australia in 1989, and the PhD degree in photonics from the University of Sydney, Australia in 1993. He is currently a professor of microphotonics and the director of the Electron Science Research Institute, Edith Cowan University, Australia. He has pioneered the integration of microelectronic and photonic sciences and developed a new and practical research area, "MicroPhotonics," and he is currently involved in research and development on Opto-VLSI, optoelectronics, and micro/nanophotonics targeting innovative solutions to fundamental issues in ICT, agriculture, health, energy, consumer electronics, and security and defence. He has authored or co-authored more than 350 peer-reviewed journals and conference papers, including three book chapters, and filed 28 patents. He received the WA Inventor of the Year (Early Stage) Award in 2007, Inaugural Vice-Chancellor Award for Excellence in Research, Edith Cowan University, Australia, in 2008, and Khalil Gibran International Award for Outstanding Contributions to Research, in 2010.

Efstratios Skafidas (sskaf@unimelb.edu.au) has focused his research in the areas of novel nanoelectronic systems, communications technologies and smart antenna theory, since completing his PhD in 1998. His work has led to innovative new millimeter wave communication systems on CMOS and is the basis on new biomedical devices. His research is currently incorporated in multiple international communication standards and has led to the establishment of two start up companies. Professor Skafidas is the Clifford Chair in Neural Engineering and Director for the Center for Neural Engineering (CfNE) at the University of Melbourne. Professor Skafidas played an integral role in establishing the CfNE, an interdisciplinary center established to undertake research in neuroscience and neural diseases by drawing together Australia's leading neuroscientists, neurologists, psychiatrists, chemists, physicists and engineers.

Roundup

Introduction to *ZTE Communications*



ZTE Communications is a quarterly, peer-reviewed international technical journal (ISSN 1673– 5188 and CODEN ZCTOAK) sponsored by ZTE Corporation, a major international provider of telecommunications, enterprise and consumer technology solutions for the Mobile Internet. The journal publishes original academic papers and research findings on the whole range of communications topics, including communications and information system design, optical fiber and electro-optical engineering, microwave technology, radio wave propagation, antenna engineering, electromagnetics, signal and image processing, and power engineering. The journal is designed to be an integrated forum for university academics and industry researchers from around the world. *ZTE Communications* was founded in 2003 and has a readership of 5500. The English version is distributed to universities, colleges, and research institutes in more than 140 countries. It is listed in Inspec, Cambridge Scientific Abstracts (CSA), Index of Copernicus (IC), Ulrich's Periodicals Directory, Norwegian Social Science Data Services (NSD), Chinese Journal Fulltext Databases, Wanfang Data — Digital Periodicals, and China Science and Technology Journal Database. Each issue of *ZTE Communications* is based around a Special Topic, and past issues have attracted contributions from leading international experts in their fields.

Optimal Transmission Power in a Nonlinear VLC System

ZHAO Shuang^{1,2,3}, CAI Sunzeng^{1,2,3}, KANG Kai⁴, and QIAN Hua⁴

(1. Shanghai Institute of Microsystem and Information Technology, Chinese Academy of Sciences, Shanghai 200050, China;

2. Key Laboratory of Wireless Sensor Network & Communication, Chinese Academy of Sciences, Shanghai 200335, China;

3. Shanghai Research Center for Wireless Communications, Shanghai 201210, China;

4. Shanghai Advanced Research Institute, Chinese Academy of Sciences, Shanghai 201210, China)

Abstract

In a visible light communication (VLC) system, the light emitting diode (LED) is nonlinear for large signals, which limits the transmission power or equivalently the coverage of the VLC system. When the input signal amplitude is large, the nonlinear distortion creates harmonic and intermodulation distortion, which degrades the transmission error vector magnitude (EVM). To evaluate the impact of nonlinearity on system performance, the signal to noise and distortion ratio (SNDR) is applied, defined as the linear signal power over the thermal noise plus the front end nonlinear distortion. At a given noise level, the optimal system performance can be achieved by maximizing the SNDR, which results in high transmission rate or long transmission range for the VLC system. In this paper, we provide theoretical analysis on the optimization of SNDR with a nonlinear Hammerstein model of LED. Simulation results and lab experiments validate the theoretical analysis.

Keywords

nonlinearity; light emitting diode (LED); SNDR

1 Introduction

Visible light communication (VLC) systems become attractive as they utilize the unlicensed visible light spectrum that has 1000 times larger bandwidth than the conventional radio frequency (RF) spectrum [1]. Moreover, existing illumination devices and illumination infrastructure can be easily upgraded to accommodate wireless data transmission [2].

In a VLC system, spectrum efficiency is very critical because the frequency response of the light emission diode (LED) is limited. Orthogonal frequency division modulation (OFDM), which is widely used in wireless communications because of its high spectral efficiency, can be applied to the VLC system with modifications. In the VLC system, the signal is modulated on light intensity (IM) of LED [3]. At the receiver side, the photon detector (PD) is applied with direct detection (DD) of the light intensity. Since the LED at the transmitter and the PD at the receiver only deal with real and positive signals, conventional OFDM signals need to be modified to meet such the re-

quirement. The real-valued OFDM can be obtained by introducing Hermitian symmetry, such as direct current biased optical OFDM (DCO-OFDM) [4], asymmetrically clipped optical OFDM (ACO-OFDM) [5], pulse-amplitude-modulated discrete multitone modulation (PAM-DMT) [6], and unipolar OFDM (U-OFDM) [7].

Many efforts have been made to improve the transmission rate of the VLC system. The authors in [8] achieved 40 Mb/s data rate on 25 MHz bandwidth at a distance of 2 m with the normal room illumination level. In [9], 1.1 Gb/s data rate was achieved at a distance of 23 cm by employing carrier-less amplitude and phase modulation (CAP). Besides, 4.2 Gb/s data rate was achieved using wavelength multiplexing division with red-green-blue (RGB) LED at a distance of 10 cm [10]. It can be found that there is an inverse relationship between the transmission range and data rate. In conventional wireless communication systems, the data rate and transmission range can be improved simultaneously if the transmission signal power increases. However, nonlinear effects in the VLC system are more severe with large input signals than those with small signals. The nonlinear effects significantly degrade system performance and limit the application of spectral efficient modulation schemes. Therefore, the research on nonlinear effects in the VLC system is necessary.

This work was supported in part by the National Key Science and Technology "863" Project under Grant No. SS2015AA011303 and the Science and Technology Commission Foundation of Shanghai under Grant No. 14511100200.

Optimal Transmission Power in a Nonlinear VLC System

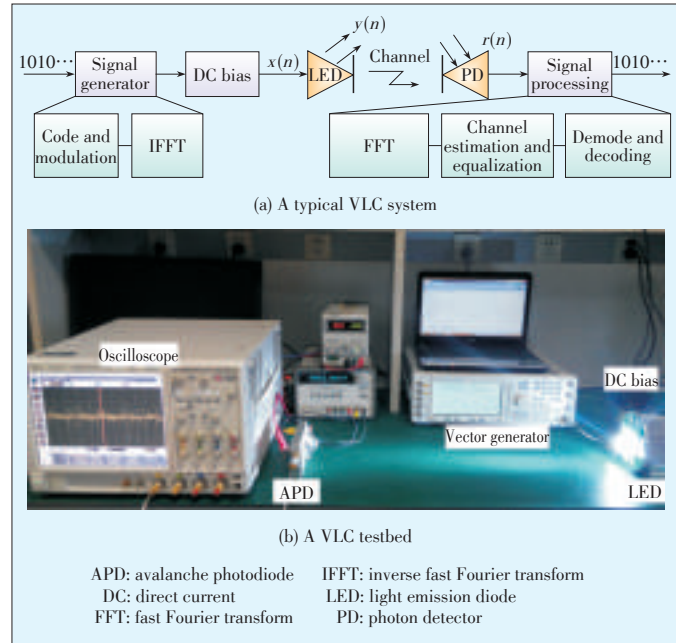
ZHAO Shuang, CAI Sunzeng, KANG Kai, and QIAN Hua

The authors in [11] studied the VLC system performance with clipping effects. In order to compensate for the nonlinear effects of LED, digital predistortion (DPD) was applied in the transmitter at the expense of an additional feedback path [12], [13]. Adaptive post-distortion algorithm for nonlinear LEDs delivered similar performance as the DPD at no additional hardware cost [14]. The Volterra equalization used to compensate for the nonlinearity of LED with memory effects was discussed in [15]. The authors in [16] optimized the SNDR in the family of dynamic-constrained memoryless nonlinearities and found out the optimal nonlinear mapping. In order to mitigate the nonlinearity of LED, we have also proposed two methods. We used a one-bit sigma-delta modulator to convert the multi-level input signal into the binary input signal with signal LED, thus avoiding LED nonlinearity [17]. Moreover, a new system architecture was proposed with micro-LED arrays, which provides digital controls to each element. The multi-level signal is realized with multiple elements in the micro-LED array, and a linear transmission is achieved for signals with large peak-to-average power ratio (PAPR) [18]. In this paper, we study the LED nonlinearity and provide theoretical analysis on the optimization of SNDR with a general nonlinear Hammerstein model of LED.

The rest of paper is organized as follows. Section 2 provides a setup of VLC system. The performance metric SNDR is introduced for the nonlinear LED model. The optimal transmission power is obtained with theoretical derivation. Section 3 shows simulation results as well as experiment measurements of the SNDR optimization. These results validate the theoretical analysis. Section 4 concludes this paper.

2 Optimization of SNDR

In a typical VLC system (**Fig. 1a**), the information bits are coded and modulated first. The transmit signal is generated by the inverse discrete Fourier transform (IDFT), which is realized by inverse Fast Fourier transform (IFFT) algorithm. A direct current (DC) bias is applied to ensure that the LED works properly as an illumination device. The input signal $x(n)$ directly modulates the lighting intensity of the LED and generates the lighting signal $y(n)$. A typical power delay profile of the VLC channel with additive white Gaussian noise (AWGN) is considered [19]. The received signal $r(n)$ is obtained by PD at the receiver. The DC component is ignored since it carries no information. The received information bits can be obtained by the baseband processing including synchronization, discrete Fourier transform (DFT), channel estimation, equalization, and demodulation. Similar with IDFT, the DFT is realized by the Fast Fourier transform (FFT) algorithm. **Fig. 1b** shows an experimental VLC system. The vector signal generator Agilent E4438 is used to generate the baseband signal. With a bias power amplifier, the signal is applied to drive the LED. At the receiver side, the avalanche photodiode (APD) is used for



▲ **Figure 1.** Setup of a visible light communication system.

reception. The digital signal analyzer Agilent DSA 90804 is used to capture the received signal.

The LED and PD are both nonlinear devices. At a reasonable radiant flux range, the nonlinearity of the PD is not significant and is ignored during the analysis of this paper. Besides, the PD works in linear region in our simulation and experiment. For the intensity modulated LED, the output signal is a nondecreasing function of the input signal, and the output becomes saturate when the input signal is large. Furthermore, most LEDs have limited bandwidths (from kHz to MHz) and the frequency response or the memory effect shows up. The nonlinearity with memory effects between input voltage and output luminous flux can be described by the Hammerstein model that consists of a memoryless polynomial nonlinear block and a linear time-invariant (LTI) system block [20].

The memoryless nonlinearity can be described by a polynomial model $f(\cdot)$:

$$f(x(n)) = \sum_{p=1}^P a_p x(n)^p \quad (1)$$

The LTI system can be modeled by an FIR filter $g(\cdot)$ as

$$y(n) = g(f(x(n))) = \sum_{l=0}^{L-1} b_l f(x(n-l)) \quad (2)$$

In (1) and (2), $y(n)$ is the output luminous flux of LED; $x(n)$ is the input voltage signal; a_p is the p th order coefficient of polynomial model, where the model coefficients can be estimated with LS/RLS solution adaptively, and the computational complexity of RLS algorithm is on the order of $O((K*(D+1))^2)$ [14]; l is the maximum delay tap; and b_l is the coefficient of filter.

Optimal Transmission Power in a Nonlinear VLC System

ZHAO Shuang, CAI Sunzeng, KANG Kai, and QIAN Hua

Decomposing the output of polynomial nonlinearity $f(x(n))$ into the linear signal part and the distortion part, the nonlinear mapping (1) can be rewritten as [21]

$$f(x(n)) = \alpha x(n) + d(n) \quad (3)$$

where $d(n)$ is the distortion term that is orthogonal to $x(n)$, i.e., $E[x(n)d(n)] = 0$; α is a constant given by $\alpha = E[xf(x)]/E[x^2]$

$E[x^2] = E[xf(x)]/\sigma_x^2$, where σ_x^2 is the variance of $x(n)$. By definition, we have $E[f^2(x(n))] = \alpha^2 \sigma_x^2 + \sigma_d^2$.

For a typical VLC channel, the received signal $r(n)$ is

$$r(n) = h(y(n)) + v(n) = h(g(f(x(n)))) + v(n) \quad (4)$$

where $h(\cdot)$ is channel model for VLC [19] and $v(n)$ is the total noise including ambient lighting noise and thermal noise.

Without loss of generality, we assume that the frequency response of the LED and that of the channel are perfectly equalized with conventional equalization algorithms. We have

$$\mathcal{O}(r(n)) = \alpha x(n) + d(n) + \text{Gain}_{\mathcal{O}(\cdot)} v(n) \quad (5)$$

where $\mathcal{O}(\cdot)$ is the inverse function of the cascaded frequency response of the LED and the channel response. $\mathcal{O}(\cdot)$ satisfies

$$\mathcal{O}(\cdot) \star h(g(\cdot)) = 1 \quad (6)$$

where \star denotes the time domain convolutional.

Normalizing the channel gain of the VLC system $\mathcal{O}(\cdot)$, the variance of the noise remains the same as σ_v^2 . The optics SNDR is defined as the linear signal power over the noise power and the distortion power, or

$$SNDR = \frac{\alpha^2 \sigma_x^2}{\sigma_x^2 + \sigma_v^2} = \frac{E[xf(x(n))]^2 / \sigma_x^2}{E[f^2(x(n))] - \frac{E[x(n)f(x(n))]^2}{\sigma_x^2} + \sigma_v^2} \quad (7)$$

From (7), we observe that the SNDR is determined by the input baseband signal power, nonlinearity of the LED and the noise power. Intuitively, when the input signal is small, the SNDR is small, and vice versa. However, when the input signal becomes very large, the nonlinear distortion dominates and the SNDR degrades. There exists an optimal transmission power for a given noise level.

To simplify the discussion, we assume that the input signal $x(n)$ follows a Gaussian distribution. This assumption is quite accurate if modified OFDM signal, which significantly improves the spectral efficiency, is used for VLC systems [5]. For a Gaussian random variable, the expectation on the polynomial term $E[xp(n)]$ is given by [22]:

$$E[x^p(n)] = \begin{cases} (p-1)!! \sigma_x^p & p \text{ even} \\ 0 & p \text{ odd} \end{cases} \quad (8)$$

where $(\cdot)!!$ denotes the double factorial operation and $(p-1)!! = (p-1)(p-3)\cdots 3\cdot 1$ when p is even.

Substituting (1) and (8) into (7), we have (9).

$$SNDR = \frac{E\left[\sum_{p=1}^P a_p x^{p+1}(n)\right]^2 / \sigma_x^2}{E\left[\left(\sum_{p=1}^P a_p x^p(n)\right)^2\right] - E\left[\sum_{p=1}^P a_p x^{p+1}(n)\right]^2 / \sigma_x^2 + \sigma_v^2} = \frac{\sum_{i=1}^P \sum_{j=1}^P a_i a_j E[x^{i+1}(n)] E[x^{j+1}(n)] / \sigma_x^2}{\sum_{i=1}^P \sum_{j=1}^P a_i a_j E[x^{i+j}(n)] - \sum_{i=1}^P \sum_{j=1}^P a_i a_j E[x^{i+1}(n)] E[x^{j+1}(n)] / \sigma_x^2 + \sigma_v^2} = \frac{\sum_{i, \text{odd}} \sum_{j, \text{odd}} i!! j!! a_i a_j \sigma_x^{i+j}}{\sum_{i, \text{odd}} \sum_{j, \text{odd}} ((i+j-1)!! - i!! j!!) a_i a_j \sigma_x^{i+j} + \sum_{i, \text{even}} \sum_{j, \text{even}} (i+j-1)!! a_i a_j \sigma_x^{i+j} + \sigma_v^2} \quad (9)$$

As an example, for a 5th order nonlinearity, $P = 5$. The SNDR in (9) reduces to (10).

$$SNDR = \frac{a_1^2 \sigma_x^2 + 6a_1 a_3 \sigma_x^4 + (9a_3^2 + 30a_1 a_5) \sigma_x^6 + 90a_3 a_5 \sigma_x^8 + 225a_5^2 \sigma_x^{10}}{3a_2^2 \sigma_x^4 + 6a_3^2 \sigma_x^6 + (105a_4^2 + 120a_3 a_5) \sigma_x^8 + 720a_5^2 \sigma_x^{10} + \sigma_v^2} \quad (10)$$

The nonlinear function of LED is nondecreasing and convex for the input signal range, which implies the first-order derivative $\partial f(x)/\partial x > 0$ and the second - order derivative $\partial^2 f(x)/\partial x^2 < 0$. After some mathematical derivations, the numerator of (9) is concave and the denominator of (9) is convex. From [23], we conclude that the SNDR expression is pseudo-concave, which guarantees that a global maximum can be achieved within the input signal range. Optimization tools can be used to find the optimal value numerically [24].

As an example, for a 3th order nonlinearity, $P = 3$. The SNDR in (9) reduces to (11)

$$SNDR = \frac{a_1^2 \sigma_x^2 + 6a_1 a_3 \sigma_x^4 + 9a_3^2 \sigma_x^6}{3a_2^2 \sigma_x^4 + 6a_3^2 \sigma_x^6 + \sigma_v^2} \quad (11)$$

$$SNDR = \frac{1.9557 \sigma_x^2 - 15.7179 \sigma_x^4 + 31.5799 \sigma_x^6}{0.0022 \sigma_x^4 + 21.0541 \sigma_x^6 + \sigma_v^2} \quad (12)$$

We define (13) and (14) and have (15) and (16)

$$P(\sigma_x^2) = a_1^2 \sigma_x^2 + 6a_1 a_3 \sigma_x^4 + 9a_3^2 \sigma_x^6, \quad (13)$$

$$Q(\sigma_x^2) = 3a_2^2 \sigma_x^4 + 6a_3^2 \sigma_x^6 + \sigma_v^2 \quad (14)$$

$$\frac{\partial P(\sigma_x^2)}{\partial \sigma_x^2} = a_1^2 + 12a_1 a_3 \sigma_x^2 + 27a_3^2 \sigma_x^4 = 1.9558 - 31.4360 \sigma_x^2 + 94.7397 \sigma_x^4, \quad (15)$$

$$\frac{\partial Q(\sigma_x^2)}{\partial \sigma_x^2} = 6a_2^2 \sigma_x^2 + 18a_3^2 \sigma_x^4 = 0.0044 \sigma_x^2 + 63.1623 \sigma_x^4 \quad (16)$$

Optimal Transmission Power in a Nonlinear VLC System

ZHAO Shuang, CAI Sunzeng, KANG Kai, and QIAN Hua

When the signal-to-noise ratio (SNR) is estimated, σ_v^2 can be express as σ_x^2/SNR , the optimal signal power σ_x^2 is calculated by

$$\frac{\partial SNDR}{\partial \sigma_x^2} = \frac{\partial P(\sigma_x^2)/\partial \sigma_x^2 \cdot Q(\sigma_x^2) - P(\sigma_x^2) \cdot \partial Q(\sigma_x^2)/\partial \sigma_x^2}{Q(\sigma_x^2)^2} \quad (17)$$

The valid input range of signal for the nonlinear coefficient a_1, a_2, a_3 is $[-0.5, 0.5]$. When the thermal noise is 0 dBm, $\sigma_v^2 = 0.001$. When the optimal input signal power is -15.93 dB, $\sigma_x^2 = 0.0255$.

3 Simulation and Experiment

To validate the optimal SNDR result, a VLC system was set up for simulation (Fig. 1b). A white LED (LE UW S2LN) from OSRAM was used in our experiment [25]. The LED's turn on voltage (TOV) is 2.7 V. The maximum input voltage is 3.7 V, which is limited by the maximum permissible current of the LED. The input signal is clipped when it is above the maximum voltage 3.7 V. A DC bias with VDC = 3.2 V is superimposed on the input signal using a bias power amplifier (LZY-22+) from Minicircuits to obtain a reasonable operation region. The normalized polynomial model coefficients with highest nonlinear order $P = 5$ and the frequency response of the LED are obtained by the real-time measurement. The coefficients of polynomial model are shown in **Table 1**, and the coefficients of the LTI system shown in **Table 2**. **Fig. 2a** compares the P-V transfer characteristics of the polynomial model and the combination of P-I and I-V curves from the datasheet. The APD C12702-12 from Hamamatsu is used in the receiver. The communication distance of the VLC system is 50 cm during the experiment, which make the PD works in linear region. The blue solid line in the figure shows the combined P-V curve from the datasheet, while the red dotted line shows the P-V curve obtained by the curve fitting of a 5th order polynomial model. The approximation error can be ignored between the blue line and the red dash line. **Fig. 2b** shows the measured frequency response of LTI system for the Hammerstein model.

A DCO-OFDM signal is applied in Fig. 1a [4]. The information bits are modulated with uncoded 64-quadrature amplitude modulation (QAM). The IDFT size of the DCO-OFDM is 256; the positive subcarriers are assigned with modulated data symbols and the negative subcarriers are loaded with their complex conjugates. The signal bandwidth is 10 MHz. We consider a typical realization of the DCO-OFDM signal, and the average power is at least 10 dB lower than the peak power, that is $\sigma_x^2 < 0.3$, to avoid the clipping distortion at the analog-to-digital converter (ADC). With the measured model coefficients in Table 1, the SNDR in (10) can be expressed as (18).

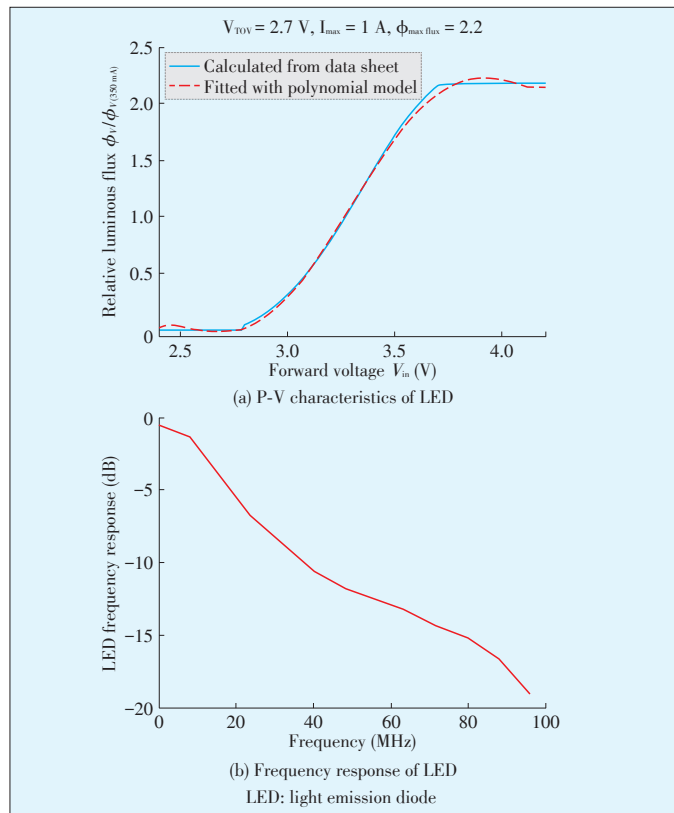
$$SNDR = \frac{1.9557\sigma_x^2 - 15.7179\sigma_x^4 + 73.5396\sigma_x^6 - 168.61\sigma_x^8 + 225.0496\sigma_x^{10}}{0.0022\sigma_x^4 + 21.0541\sigma_x^6 - 224.6562\sigma_x^8 + 720.1587\sigma_x^{10} + \sigma_v^2} \quad (18)$$

▼ **Table 1.** Normalized polynomial coefficients of a measured white LED

Model coefficient	a_1	a_2	a_3	a_4	a_5
Normalized value	1.3985	0.0269	-1.8732	-0.0387	1.0001

▼ **Table 2.** LTI coefficients of a measured white LED (spectrum response)

Coefficient	b_0	b_1	b_2	b_3	b_4	b_5
Value	0.0189	0.2976	0.2288	0.1348	0.1176	0.0695
Coefficient	b_6	b_7	b_8	b_9	b_{10}	b_{11}
Value	0.0578	0.0374	0.0258	0.0189	0.0133	0.0097



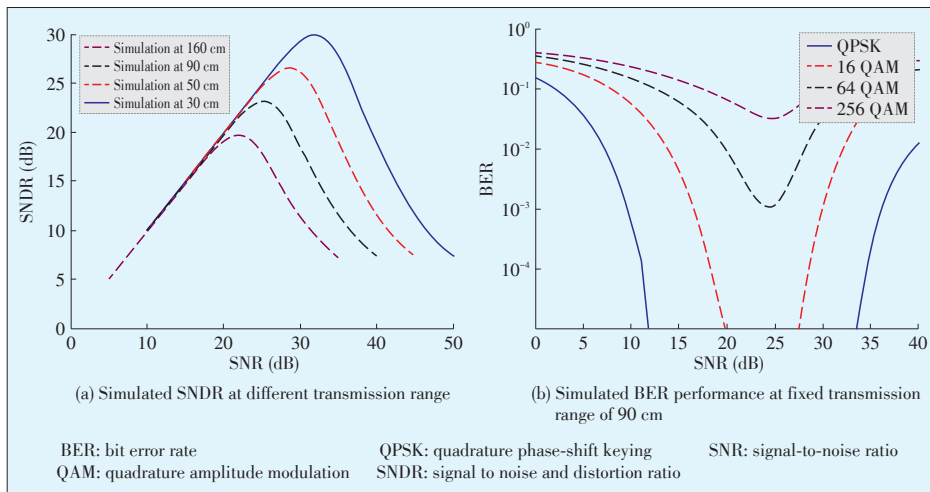
▲ **Figure 2.** Characteristics of LED in experiment.

The numerical results show that the second order derivative of the numerator in (18) is negative when $\sigma_x^2 < 0.37$, and the second order derivative of the denominator is positive when $\sigma_x^2 < 0.56$. The numerator in (18) is concave and the denominator in (18) is convex during the input signal range within $\sigma_x^2 < 0.3$. From the previous discussion, we know that the SNDR expression is pseudo-concave and hence a global optimum can be efficiently found via numerical methods.

Fig. 3a shows the SNDR results from SNR with the transmission ranges of 30 cm, 50 cm, 90 cm, and 160 cm. The signal power is determined by the transmission range and the constant noise comes from APD and the ambient lighting noise. According to Fig. 3a, the SNR is determined by the communication distance, with a constant noise level which comes from

Optimal Transmission Power in a Nonlinear VLC System

ZHAO Shuang, CAI Sunzeng, KANG Kai, and QIAN Hua



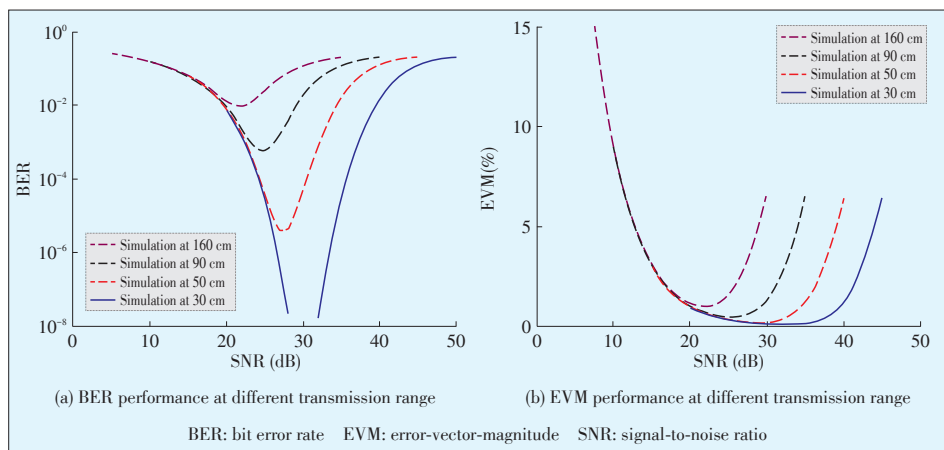
▲ Figure 3. System performance of a 5th order nonlinear DCO-OFDM system with uncoded QAM modulation.

LED and APD. In addition, there always exists an optimal value for the SNDR. When the input signal is very small, the distortion is negligible. The SNDR increases with the SNR increase. When the signal power increases, the distortion also increases. For the red dashed line, a maximum SNDR of 27 dB is achieved when the SNR is 28 dB. When the signal is too large, the SNDR decreases and the system performance is degraded. Moreover, different optimal SNDR values are achieved at different communication distances in Fig. 3a. Higher optimal SNDR can be achieved at a higher SNR level with shorter communication distance, which agrees with our theoretical analysis.

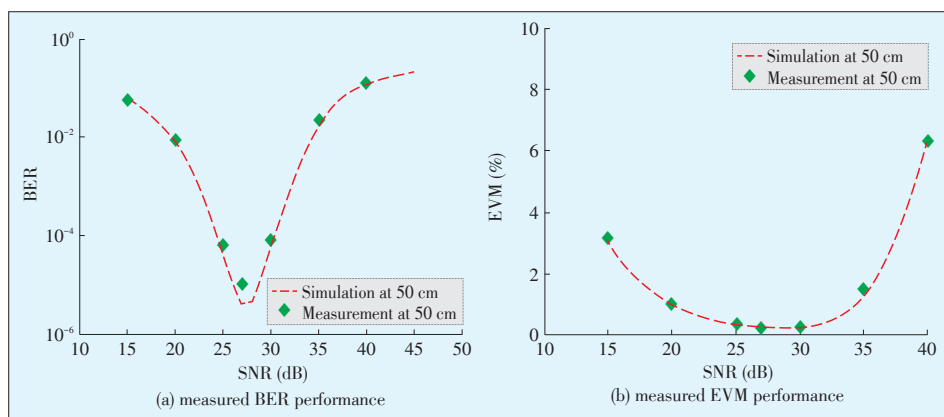
The optimal transmission power for the maximum SNDR can be validated by the bit error rate (BER) performance. Fig. 3b shows system BER performance for different modulations. The transmission range is fixed at 90 cm. A total number of 1.92×10^8 information bits are transmitted. In Fig. 3b, the lines from top to bottom show the BER performance of QPSK, 16QAM, 64QAM and 256QAM signals, respectively. The optimal BER performance is yielded at SNR of 25 dB (or SNDR of 23.2 dB). To achieve the same BER level, a higher order modulation requires higher SNR than a lower order modulation. At the same transmission range, the nonlinearity limits the application of high-order modulation schemes. In

other words, the nonlinearity of the LED becomes the bottleneck of the communication range of the system.

The optimal transmission power for the maximum SNDR was also validated by error-vector-magnitude (EVM) performance. A total number of 1.92×10^8 information bits are transmitted for each test. Fig. 4 shows the BER and EVM performance of QPSK, 16QAM, 64QAM and 256QAM modulation, while Fig. 5 shows the measured performance at distance of 50 cm (the green diamond dots) and the simulated performance for the same communication distance (the red dashed lines). EVM in Fig. 4 gets the same system performance as the SNDR in Fig. 3. Besides, the measurement results agree with the simulation results (Fig. 5). According to Fig. 4a, with the 64QAM modulation, the VLC transmission range is limited within 1 meter. The nonlinearity



▲ Figure 4. System performance of a 5th order nonlinear DCO-OFDM system with uncoded QAM modulation.



▲ Figure 5. System performance of a 5th order nonlinear DCO-OFDM system with uncoded QAM modulation at 50 cm transmission range.

Optimal Transmission Power in a Nonlinear VLC System

ZHAO Shuang, CAI Sunzeng, KANG Kai, and QIAN Hua

becomes the bottleneck of the system performance. The long communication range demands high transmission power, which in turn creates large nonlinearity and limits the overall system performance. Compensation of the system nonlinearity is needed to improve the transmission data rate or extend the transmission range.

4 Conclusions

The nonlinear distortion created by LED limits the performance of VLC systems. Large signals are distorted by the nonlinearity and small signals are vulnerable to noise. In this paper, we perform theoretical analysis on the optimization of SNDR, which provides a guidance of choosing optimal transmission power for a given thermal noise level. Simulation results and experimental measurements validate our theoretical analysis. Compensation of the system nonlinearity is critical for improving the transmission data rate or extending the transmission range.

References

- [1] Cisco, "Cisco visual networking index: Forecast and methodology, 2013–2018," Cisco System, San Jose, USA, June 2013.
- [2] H. Elgala, R. Mesleh, and H. Haas, "Indoor optical wireless communication: potential and state-of-the-art," *IEEE Communications Magazine*, vol. 49, no. 9, pp. 56–62, 2011. doi: 10.1109/MCOM.2011.6011734.
- [3] H. Yu, Z. Dong, X. Xiao, C. H. Chien, and N. Chi, "Generation of coherent and frequency-locked multi-carriers using cascaded phase modulators for 10 Tb/s optical transmission system," *Journal of Lightwave Technology*, vol. 30, no. 4, pp. 458–465, 2012.
- [4] J. Armstrong and B. Schmidt, "Comparison of asymmetrically clipped optical OFDM and DC-biased optical OFDM in AWGN," *IEEE Communications Letters*, vol. 12, no. 5, pp. 343–345, 2008. doi: 10.1109/LCOMM.2008.080193.
- [5] J. Armstrong and A. Lowery, "Power efficient optical OFDM," *IET Electronics Letters*, vol. 42, no. 6, pp. 370–372, 2006.
- [6] D. J. Barros, S. K. Wilson, and J. M. Kahn, "Comparison of orthogonal frequency-division multiplexing and pulse-amplitude modulation in indoor optical wireless links," *IEEE Transactions on Communications*, vol. 60, no. 1, pp. 153–163, 2012. doi: 10.1109/LCOMM.2008.080193.
- [7] D. Tsonev, S. Sinanovic, and H. Haas, "Novel unipolar orthogonal frequency division multiplexing (U-OFDM) for optical wireless," in *IEEE 75th Vehicular Technology Conference (VTC Spring)*, Yokohama, Japan, 2012, pp. 1–5. doi: 10.1109/VETECS.2012.6240060.
- [8] H. Le Minh, D. O'Brien, G. Faulkner, et al., "High-speed visible light communications using multiple-resonant equalization," *IEEE Photonics Technology Letters*, vol. 20, no. 14, pp. 1243–1245, 2008. doi: 10.1109/LPT.2008.926030.
- [9] F.-M. Wu, C.-T. Lin, C.-C. Wei, et al., "1.1-Gb/s white-LED-based visible light communication employing carrier-less amplitude and phase modulation," *IEEE Photonics Technology Letters*, vol. 24, no. 19, pp. 1730–1732, 2012. doi: 10.1109/LPT.2012.2210540.
- [10] Y. Wang, X. Huang, J. Zhang, Y. Wang, and N. Chi, "Enhanced performance of visible light communication employing 512-QAM NSC-FDE and DD-LMS," *Optics Express*, vol. 22, no. 13, pp. 15328–15334, 2014.
- [11] R. Mesleh, H. Elgala, and H. Haas, "On the performance of different OFDM based optical wireless communication systems," *IEEE/OSA Journal of Optical Communications and Networking*, vol. 3, no. 8, pp. 620–628, 2011. doi: 10.1364/JOCN.3.000620.
- [12] K. Asatani and T. Kimura, "Linearization of LED nonlinearity by predistortions," *IEEE Journal of Solid-State Circuits*, vol. 13, no. 1, pp. 133–138, 1978. doi: 10.1109/JSSC.1978.1051007.
- [13] D. Lee, K. Choi, K.-D. Kim, and Y. Park, "Visible light wireless communications based on predistorted OFDM," *Optics Communications*, vol. 285, no. 7, pp. 1767–1770, 2012.
- [14] H. Qian, S. J. Yao, S. Z. Cai, and T. Zhou, "Adaptive postdistortion for nonlinear LEDs in visible light communications," *IEEE Photonics Journal*, vol. 6, no. 4, pp. 1943–1955, 2014. doi: 10.1109/JPHOT.2014.2331242.
- [15] G. Stepniak, J. Siuzdak, and P. Zwiorko, "Compensation of a VLC Phosphorescent White LED Nonlinearity by Means of Volterra DFE," *IEEE Photonics Technology Letters*, vol. 25, no. 16, pp. 1597–1600, 2013. doi: 10.1109/LPT.2013.2272511.
- [16] K. Ying, Z. Yu, R. J. Baxley, and G. T. Zhou, "Optimization of signal-to-noise-plus-distortion ratio for dynamic-range-limited nonlinearities," *Digital Signal Processing*, vol. 36, pp. 104–114, Jan. 2015.
- [17] H. Qian, J. Chen, S. Yao, et al., "One-bit sigma-delta modulator for nonlinear visible light communication systems," *IEEE Photonics Technology Letters*, vol. 27, no. 4, pp. 419–422, 2014. doi: 10.1109/LPT.2014.2376971.
- [18] H. Qian, Z. Shuan, C. Sunzeng, and Z. Ting, "Digital controlled micro-led array for linear visible light communication systems," *IEEE Photonics Journal*, vol. 7, no. 3, 2015. doi: 10.1109/JPHOT.2015.2424398.
- [19] K. Lee, H. Park, and J. R. Barry, "Indoor channel characteristics for visible light communications," *IEEE Communications Letters*, vol. 15, no. 2, pp. 217–219, 2011. doi: 10.1109/LCOMM.2011.010411.101945.
- [20] L. Ding, R. Raich, and G. Zhou, "A Hammerstein predistortion linearization design based on the indirect learning architecture," in *IEEE International Conference on Acoustics, Speech, and Signal Processing (ICASSP)*, Orlando, USA, 2002, vol. 3, pp. 2689–2692. doi: 10.1109/ICASSP.2002.5745202.
- [21] R. Raich, H. Qian, and G.T.Zhou, "Optimization of SNDR for amplitude-limited nonlinearities," *IEEE Transactions on Communications*, vol. 53, pp. 1964–1972, Nov. 2005. doi: 10.1109/TCOMM.2005.857141.
- [22] R. Durrentr, *Probability: Theory and Examples*. Cambridge, UK: Cambridge University Press, 2010. doi: 10.1109/TCOMM.2005.857141.
- [23] S. Schaible, "Fractional programming," *Zeitschrift für Operations Research*, vol. 27, no. 1, pp. 39–54, 1983. doi: 10.1007/BF01916898.
- [24] S. Boyd and L. Vandenberghe, *Convex Optimization*. Cambridge, UK: Cambridge University Press, 2009.
- [25] OSRAM GmbH, "Datasheet: LE UW S2LN," Mar. 2008.

Manuscript received: 2015-12-11

Biographies

ZHAO Shuang (shuang.zhao@wico.sh) received her BS degree from the Department of Sciences, Wuhan University of Technology, China in 2013. She is pursuing her MS degree in Shanghai Institute of Microsystem and Information Technology Research Institute, Chinese Academy of Sciences. Her current research interests include nonlinear signal processing and visible light communications.

CAI Sunzeng (caisunzeng@163.com) received his BS degree from the Department of Communication & Information Engineering, Xi'an University of Posts & Telecommunications, China in 2010. He obtained his PhD degree from Shanghai Institute of Microsystem and Information Technology Research Institute, Chinese Academy of Sciences. His current research interests include nonlinear signal processing and visible light communications.

KANG Kai (kangk@sari.ac.cn) received his PhD degree in electrical engineering from Tsinghua University, China, in 2007. He has been a senior engineer at the Shanghai Advanced Research Institute, Chinese Academy of Sciences since 2015. His research interests include next generation of Wi-Fi and 5G networks.

QIAN Hua (qianh@sari.ac.cn) received his BS and MS degrees from the Department of Electrical Engineering, Tsinghua University, China, in 1998 and 2000, respectively. He obtained his PhD degree from the School of Electrical and Computer Engineering, Georgia Institute of Technology, USA, in 2005. He is currently with Shanghai Advanced Research Institute, Chinese Academy of Sciences as a full professor. His research interests include nonlinear signal processing and system design of wireless communications.

Modulation Techniques for Li-Fi

Mohamed Sufyan Islim and Harald Haas

(Li-Fi Research and Development Centre, Institute for Digital Communications, University of Edinburgh, Edinburgh EH9 3JL, UK)

Abstract

Modulation techniques for light fidelity (Li-Fi) are reviewed in this paper. Li-Fi is the fully networked solution for multiple users that combines communication and illumination simultaneously. Light emitting diodes (LEDs) are used in Li-Fi as visible light transmitters, therefore, only intensity modulated direct detected modulation techniques can be achieved. Single carrier modulation techniques are straightforward to be used in Li-Fi, however, computationally complex equalization processes are required in frequency selective Li-Fi channels. On the other hand, multicarrier modulation techniques offer a viable solution for Li-Fi in terms of power, spectral and computational efficiency. In particular, orthogonal frequency division multiplexing (OFDM) based modulation techniques offer a practical solution for Li-Fi, especially when direct current (DC) wander, and adaptive bit and power loading techniques are considered. Li-Fi modulation techniques need to also satisfy illumination requirements. Flickering avoidance and dimming control are considered in the variant modulation techniques presented. This paper surveys the suitable modulation techniques for Li-Fi including those which explore time, frequency and colour domains.

Keywords

light fidelity (Li-Fi); optical wireless communications (OWC); visible light communication (VLC); intensity modulation and direct detection (IM/DD); orthogonal frequency division multiplexing (OFDM)

1 Introduction

More than half a billion new communication devices were added to the network services in 2015. Globally, mobile data traffic is predicted to reach 30.6 exabytes per month by 2020 (the equivalent of 7641 million DVDs each month), up from 3.7 exabytes per month in 2015 [1]. The radio frequency bandwidth currently used is a very limited resource. The increasing dependency on cloud services for storage and processing means that new access technologies are necessary to allow this huge increase in network utilization. The visible light spectrum on the other hand offers a 10,000 times larger unlicensed frequency bandwidth that could accommodate this expansion of network capacity. Visible light communication (VLC) is the point-to-point high speed communication and illumination system. Light fidelity (Li-Fi) is the complete wireless, bi-directional, multi-user network solution for visible light communications that would operate seamlessly alongside other Long Term Evolution (LTE) and wireless fidelity (Wi-Fi) access technologies [2]. Li-Fi is a green communication method as it reuses the existing lightning infrastructure for communications. Infor-

mation is transmitted by the rapid subtle changes of light intensity that is unnoticeable by the human eye. Recent studies have demonstrated data rates of 14 Gbps for Li-Fi using three off-the-shelf laser diodes (red, green and blue) [3]. It was also predict that a data rate of 100 Gbps is achievable for Li-Fi when the whole visible spectrum is utilized [3]. Li-Fi offers inherent security, and also it can be employed in areas where sensitive electronic devices are present, such as in hospitals. In addition, Li-Fi is a potential candidate for other applications such as underwater communications, intelligent transportation systems, indoor positioning, and the Internet of Things (IoT) [2].

Modulation techniques developed for intensity modulation and direct detection (IM/DD) optical wireless communication (OWC) systems are suitable for Li-Fi communications systems. However, these modulation techniques may not be suitable for all lightning regimes. Li-Fi transceivers are illumination devices enabled for data communications. Therefore adapting IM/DD modulation technique should first satisfy certain illumination requirements before being Li-Fi enabled. For example, modulation techniques should support dimmable illumination so that communication would be still available when the illumination is not required. Li-Fi uses off-the-shelf light emitting diodes (LEDs) and photodiodes (PDs) as channel front-end devices. This restricts signals propagating throughout the channel to

This work is support by the UK Engineering and Physical Sciences Research Council (EPSRC) under Grants EP/K008757/1 and EP/M506515/1.

Modulation Techniques for Li-Fi

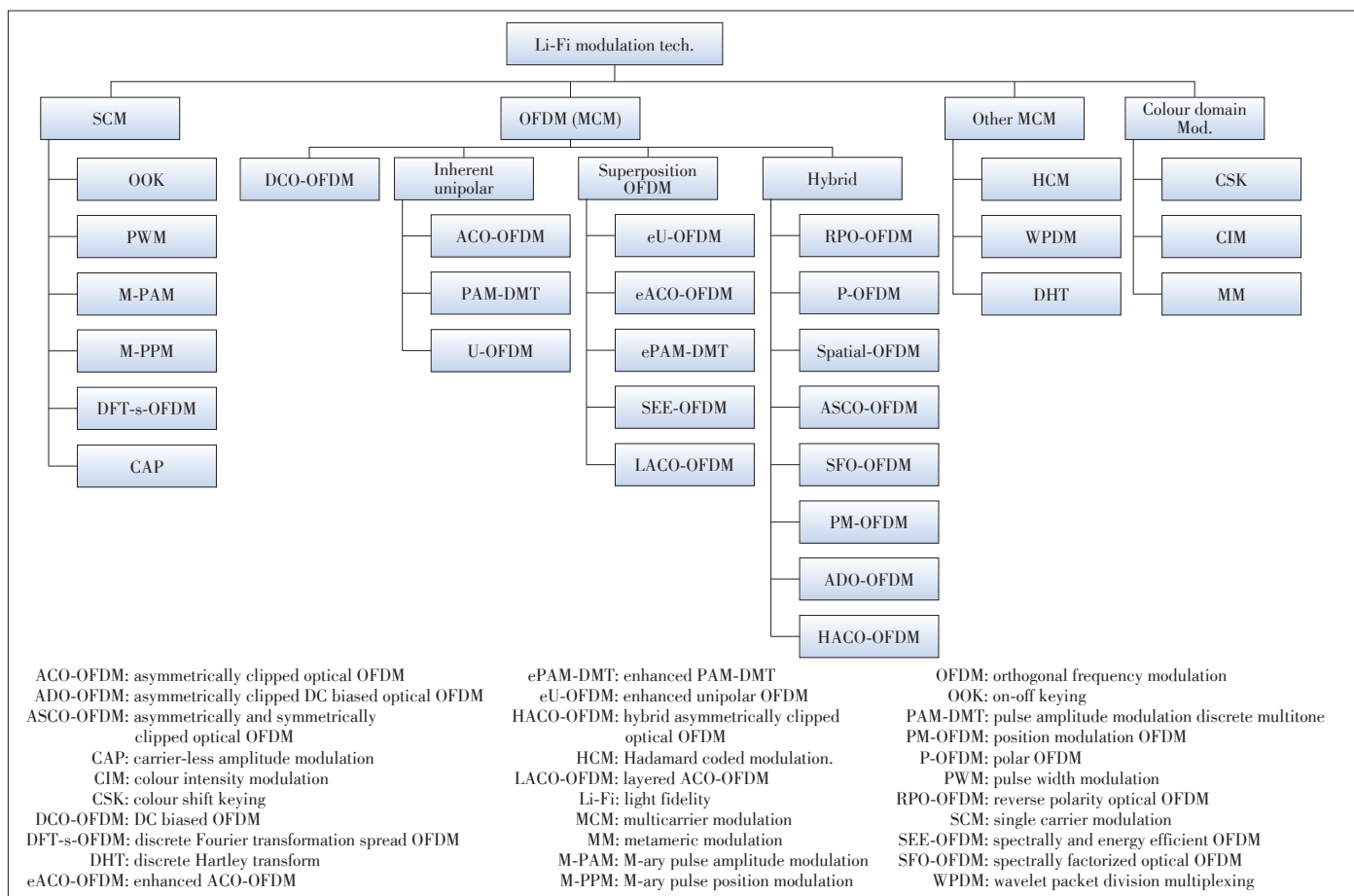
Mohamed Sufyan Islim and Harald Haas

strictly positive signals. Single carrier modulation (SCM) techniques are straight forward to implement in Li-Fi. Modulation techniques, such as on-off keying (OOK), pulse-position modulation (PPM), and M -ary pulse-amplitude modulation (M -PAM), can be easily implemented. However, due to the dispersive nature of optical wireless channels, such schemes require complex equalizers at the receiver. Therefore, the performance of these schemes degrades as their spectral efficiency (SE) increases. On the other hand, multiple carrier modulation (MCM) techniques, such as the orthogonal frequency division multiplexing (OFDM), have been shown to be potential candidates for optical wireless channels since they only require single tap equalizer at the receiver. Adaptive bit and power loading can maximize the achievable data rates of OFDM-based Li-Fi systems by adapting the system loading to the channel frequency response. Moreover, the DC wander and low frequency interference can be easily avoided in OFDM by optimizing the adaptive bit/power loading to avoid the low frequency subcarriers. Colour modulation techniques are unique to Li-Fi communication systems as the information is modulated on the instantaneous colour changes. The colour dimension adds a new degree of freedom to Li-Fi. The various modulation Li-Fi modulation techniques discussed in this paper are shown in **Fig. 1**.

This paper is organized as follows: The main challenges for Li-Fi modulation techniques are summarized in Section 2. SCM techniques for Li-Fi are detailed in Section 3. OFDM-based modulation techniques for Li-Fi are discussed in details in Section 4, including inherent unipolar OFDM techniques, hybrid OFDM modulation techniques and superposition OFDM modulation techniques. Other MCM techniques are revisited in Section 5. The unique colour domain modulation techniques are discussed in Section 6. Finally the conclusion is presented in Section 7. The paper is limited to single input-single output (SISO) Li-Fi communication systems. The space dimension of Li-Fi is not considered in this paper.

2 Li-Fi Modulation Techniques Challenges

Li-Fi is an emerging high-speed, low-cost solution to the scarcity of the radio frequency (RF) spectrum, therefore it is expected to be realized using the widely deployed off-the-shelf optoelectronic LEDs. Due to the mass production of these inexpensive devices, they lack accurate characterizations. In Li-Fi, light is modulated on the subtle changes of the light intensity, therefore, the communication link would be affected by the non-linearity of the voltage-luminance characteristic. As a solution,



▲ Figure 1. Li-Fi modulation techniques considered in this paper.

pre-distortion techniques were proposed to mitigate non-linear distortion [4]. However, as the LED temperature increases the voltage-luminance (V-L) characteristic experiences memory-effects. Therefore, the LED non-linearity mitigation is still an open research problem. The limited bandwidth of Li-Fi communication channel leads to inter-symbol interference (ISI) at high data rates. The LED frequency response is modeled as a low-pass filter, and it is the major contributor to the frequency selectivity of Li-Fi channels. The modulation bandwidth over which the frequency response of most commercially available LEDs can be considered flat is around 2–20 MHz [5], [6]. However, the usable bandwidth in Li-Fi could be extended beyond the 3 dB cut-off frequency.

Therefore, modulation techniques with higher spectral efficiencies are key elements in a Li-Fi system design. Satisfying the illumination requirements is a key element in Li-Fi. Most of the research on modulation techniques has been on the communication system performance of Li-Fi system. Factors such as dimming, illumination level control and flickering have been analyzed as secondary parameters of a Li-Fi system. The Li-Fi systems should be also considered as an illumination system with communications capability, not the reverse.

3 Single Carrier Modulation Techniques

Single carrier modulation techniques were first proposed for IM/DD optical wireless communications based on infrared communications [7]. Modulation techniques, such as OOK, pulse amplitude modulation (PAM), pulse width modulation (PWM), and PPM, are straightforward to implement for Li-Fi systems. In general, single carrier modulation techniques are suitable candidates for Li-Fi when low-to-moderate data rates applications are required. By switching the LED between “on” and “off” states, the incoming bits can be modulated into the light intensity. Illumination control can be supported by adjusting the light intensities of the “on” and “off” states, without affecting the system performance. Compensation symbols are proposed in the visible light communications standard, IEEE 802.15.7 [8], to facilitate the illumination control at the expense of reducing the SE. If the link budget offers high signal to noise ratios (SNR), M -PAM can be used to modulate the incoming bits on the amplitude of the optical pulse [9]. The position of the optical pulse is modulated into shorter duration chips in PPM with a position index that varies depending on the incoming bits. The PPM is more power efficient than OOK, however, it requires more bandwidth than OOK to support equivalent data rates. Differential PPM (DPPM) was proposed to achieve power and/or SE gains [10], however the effect of unequal bit duration for the different incoming symbols could affect the illumination performance. A solution was proposed in [11] to ensure that the duty cycle is similar among the different symbols to prevent any possible flickering. Variable PPM (VPPM) was proposed in the VLC standard IEEE 802.15.7 to

support dimming for the PPM technique and prevent any possible flickering. The pulse dimming in VPPM is controlled by the width of the pulse rather than the pulse amplitude. Therefore, VPPM can be considered as a combination of PPM and PWM techniques. Multiple PPM (MPPM) was proposed [12] as a solution to the dimming capability of PPM, where it was reported that it achieves higher spectral efficiencies than VPPM with less optical power dissipation. The advantages of PAM and PPM are combined in pulse amplitude and position modulation (PAPM) [13].

The performance comparison between single carrier and multicarrier modulation techniques was studied in [14]–[18] for different scenarios and considerations. The results may differ depending on the major considerations and assumptions of each study. However in general, the performance of single carrier modulation techniques deteriorate as the data rates increase, due to the increased ISI. Equalization techniques, such as optimum maximum likelihood sequence detection (MLSD), frequency domain equalizers (FDE), nonlinear decision feedback equalizers (DFE), and linear feed forward equalizer (FFE), are suitable candidates for equalization processes, with different degrees of performance and computational complexity [7], [19], [20]. The single carrier frequency domain equalizer (SC-FDE) was proposed for OWC as a solution to the high peak to average power ratio (PAPR) of OFDM in [12], [21]. PPM-SCFDE was considered in [22], and OOK-SCFDE was considered in [23]. The performance of OOK with minimum mean square error equalization (MMSE) was compared with the performance of asymmetrically clipped optical (ACO)-OFDM and the performance of complex modulation M -ary quadrature amplitude modulation (M -QAM) ACO-SCFDE in [18]. It was reported that the performance of ACO-SCFDE outperforms asymmetrically clipped optical OFDM (ACO-OFDM) and OOK-MMSE due to the high PAPR of ACO-OFDM when the nonlinear characteristics of the LED are considered. The performance of PAM-SCFDE is compared with OFDM in [12], without consideration of the LED nonlinearity. It was shown that PAM-SCFDE achieves higher performance gains when compared with OFDM at spectral efficiencies less than 3 bits/s/Hz.

Discrete Fourier transformation spread (DFT-s) OFDM was also considered for Li-Fi as a SCM that has the benefits of an OFDM multicarrier system with lower PAPR [24]. An extra pair of DFT and inverse discrete Fourier transformation (IDFT) operations are required to achieve DFT-s OFDM. Multiple independent streams of DFT-s OFDM modulated waveforms are separately transmitted through multiple LEDs in a single array. The performance of DFT-s OFDM is reported to be better when compared with DC-biased optical OFDM (DCO-OFDM) in terms of both PAPR and bit error rate (BER) [24]. A novel carrier-less amplitude and phase (CAP) modulation was proposed for Li-Fi in [25]. In order for CAP to suit the frequency response of LEDs, the spectrum of CAP was divided into m sub-carriers by the aid of finite impulse response (FIR) filter. Al-

Modulation Techniques for Li-Fi

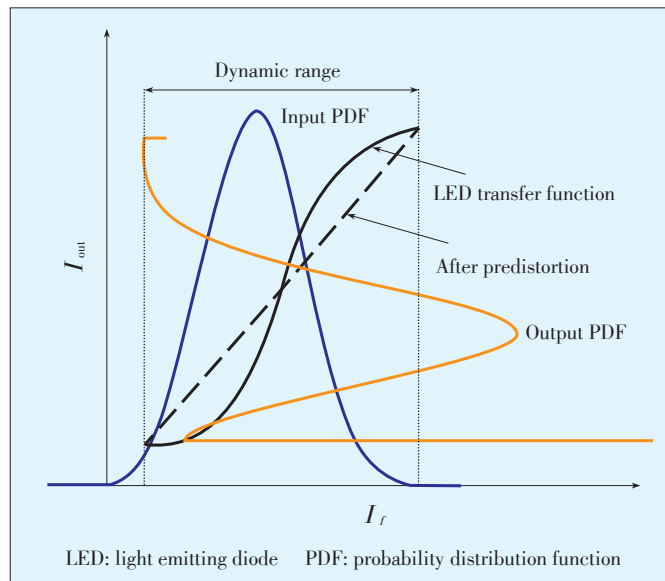
Mohamed Sufyan Islim and Harald Haas

though CAP is computationally complex, it could offer high spectral efficiencies in band-limited Li-Fi channel.

4 Optical OFDM

Single carrier modulation techniques require a complex equalization process when employed at high data rates. In addition, effects such as DC wandering and flickering interference of florescent lights may influence the system performance at the lower frequency regions of the used bandwidth. On the other hand, multicarrier modulation techniques such as OFDM can convert the frequency selective fading of the communication channel into a flat fading by employing the computationally efficient single tap equalizer. In addition, OFDM supports adaptive power and bit loading which can adapt the channel utilization to the frequency response of the channel. This can maximize the system performance. Supporting multiuser communication systems is an inherent advantage of OFDM, where each user could be allocated certain subcarriers. At the OFDM transmitter, the incoming bits are modulated into specific modulation formats such as M -QAM. The M -QAM symbols are loaded afterwards into orthogonal subcarriers with subcarrier spacing equal to multiple of the symbol duration. The parallel symbols can then be multiplexed into a serial time domain output, generally using inverse fast Fourier transformation (IFFT). The physical link of Li-Fi is achieved using off-the-shelf optoelectronic devices such as LED and photo-detectors (PD). Due to the fact that these light sources produce an incoherent light, the OFDM time-domain waveforms are used in Li-Fi to modulate the intensity of the LED source. Therefore, these waveforms are required to be both unipolar and real valued.

Hermitian symmetry is generally imposed on the OFDM input frame to enforce the OFDM time domain signal output into the real domain. Different variants of optical OFDM were proposed to achieve a unipolar OFDM output. DC bias is used in the widely deployed DCO-OFDM [26] to realize a unipolar time-domain OFDM output. However, OFDM signals have a high PAPR, which makes it practically impossible to convert all of the signal samples into unipolar ones. The OFDM time-domain waveform can be approximated with a Normal distribution when the length of the input frame is greater than 64. The DC bias point would be dependent on the V-L characteristic of the LED. Zero level clipping of the remaining negative samples after the biasing would result in a clipping distortion that could deteriorate the system performance. High DC bias would also incur some distortion as a result of the upper clipping of the OFDM waveform due to the V-L characteristic of the ideal LED. The forward-output current characteristic of an LED is shown in **Fig. 2**. Pre-distortion is used to linearize the dynamic range of the LED. The LED input and output probability distribution function (PDF) of the OFDM modulation signal are also shown. The dynamic range of the LED is between the turn-on bias and the maximum allowed current points of the LED. The



▲ **Figure 2.** The forward-output current characteristic of an LED.

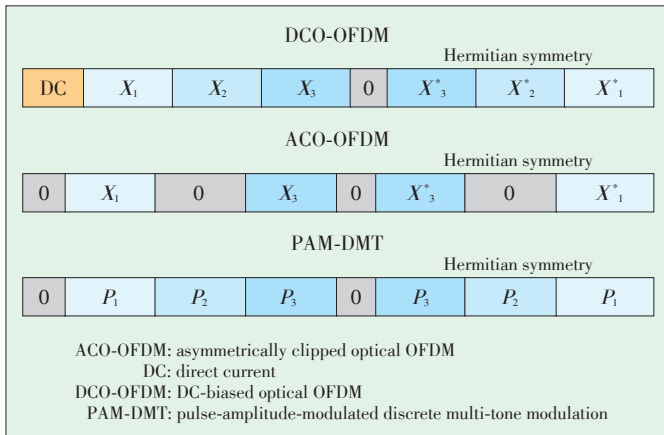
input signal is biased and the output signal is clipped for values outside the dynamic range. The optimization of the DC biasing point was studied in [27]–[29]. The additional dissipation of electrical power in DCO-OFDM compared with bipolar OFDM increases as the modulation order increases. This leads to electrical and optical power inefficiency when DCO-OFDM is used with high M -QAM modulation orders. Illumination is an essential part of VLC, therefore, the DCO-OFDM optical power inefficiency can be justified for some VLC applications. However, when energy efficiency is required, an alternative modulation approach is required.

4.1 Inherent Unipolar Optical OFDM Techniques

Unipolar OFDM modulation schemes were mainly introduced to provide energy efficient optical OFDM alternatives to DCO-OFDM. These schemes include ACO-OFDM [30], pulse-amplitude - modulated discrete multitone modulation (PAM - DMT) [31], flipped OFDM (Flip-OFDM) [32], and unipolar orthogonal frequency division multiplexing (U-OFDM) [33]. They exploit the OFDM input/output frame structure to produce a unipolar time domain waveform output. However, all of these schemes have a reduced SE compared with DCO-OFDM due to the restrictions imposed on their frame structures. In this section, ACO-OFDM, PAM-DMT and U-OFDM/Flip-OFDM modulation schemes are discussed.

4.1.1 ACO-OFDM

A real unipolar OFDM waveform can be achieved by exploiting the Fourier transformation properties on the frequency domain input OFDM frames. The principle of ACO-OFDM [30] is to skip the even subcarriers of an OFDM frame, by only loading the odd subcarriers with useful information (**Fig. 3**). This creates a symmetry in the time domain OFDM signal, which al-

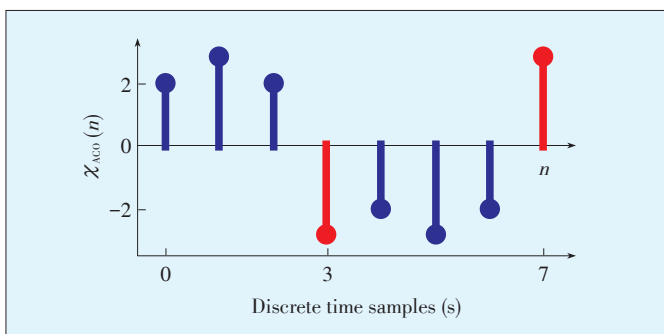


▲ Figure 3. Subcarriers mapping of the input frames for DCO-OFDM, ACO-OFDM and PAM-DMT. X_i represents the M -QAM symbol at the i th subcarrier and P_i represents the M -PAM symbol at the i th subcarrier.

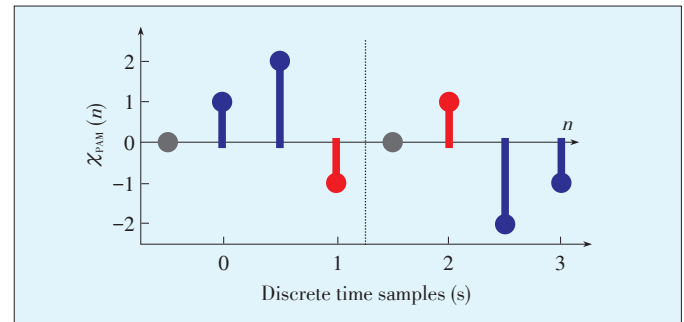
lowers the distortion-less clipping of the negative samples without the need of any DC biasing (Fig. 4). Clipping of the negative values is distortion-less since all of the distortion will only affect the even-indexed subcarriers. However, skipping half of the subcarriers reduces the SE of ACO-OFDM to half of that in DCO-OFDM. A penalty of 3 dB should be applied to the signal-to-noise ratio (SNR) of ACO-OFDM when compared with bipolar OFDM, since half of the signal power is lost due to clipping. Hermitian symmetry is also used to guarantee a real valued ACO-OFDM output. At the receiver, after a fast Fourier transformation (FFT) is applied on the incoming frame, only odd subcarriers are considered.

4.1.2 PAM-DMT

A real unipolar optical OFDM is realized in PAM-DMT by exploiting the Fourier properties of imaginary signals. The real component of the subcarriers is not used in PAM-DMT, which restricts the modulation scheme used to M-PAM (Fig. 3). By only loading M -PAM modulated symbols on the imaginary components of the subcarriers, an antisymmetry in the time-domain waveform of PAM-DMT would be achieved (Fig. 5). This would facilitate the distortion-less zero level clipping of PAM-DMT waveform, as all of the distortion would only affect the re-



▲ Figure 4. The time-domain ACO-OFDM waveform.



▲ Figure 5. The time-domain PAM-DMT waveform.

al component of the subcarriers. Hermitian symmetry is also used to guarantee a real valued PAM-DMT output. PAM-DMT is more attractive than ACO-OFDM when bit loading techniques are considered, as the PAM-DMT performance can be optimally adapted to the frequency response of the channel since all of the subcarriers are used. The SE of PAM-DMT is similar to that of DCO-OFDM. PAM-DMT has a 3 dB fixed penalty when compared with bipolar OFDM at an appropriate constellation size, as half of the power is also lost due to clipping. At the receiver, the imaginary part of the subcarriers is only considered, while the real part is ignored.

4.1.3 U-OFDM/Flip-OFDM

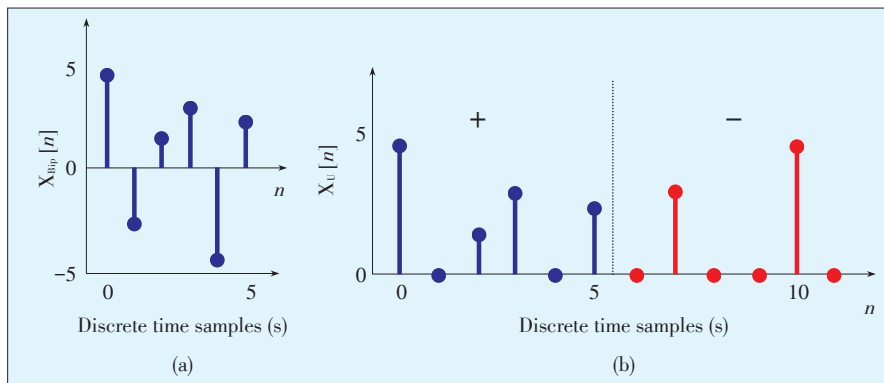
The concept and performance of U-OFDM and Flip-OFDM is identical. In this paper, the term U-OFDM is used, however, all discussion and analysis is applicable to both schemes. Hermitian symmetry is applied on the incoming frame of M -QAM symbols. The bipolar OFDM time-domain frame obtained afterwards is expanded into two time-domain frames in U-OFDM with similar sizes to the original OFDM frame (Fig. 6). The first frame is identical to the original frame, while the second is a flipped replica of the original frame. A unipolar OFDM waveform can be achieved by zero-level clipping without the need of any DC biasing. At the receiver, each second frame would be subtracted from the first frame of the same pair, in order to reconstruct the original bipolar OFDM frame. This would double the noise at the receiver, which leads to a 3 dB penalty when compared with bipolar OFDM at equivalent constellation sizes. The SE of U-OFDM is half of the SE of DCO-OFDM since two U-OFDM frames are required to convey the same information conveyed in a single DCO-OFDM frame. The single tap equalizer can be used for U-OFDM, providing that the ISI effects on the first frame are identical to the ISI effects on the second frame.

4.1.4 Performance of Inherent Unipolar OFDM Techniques

The inherent unipolar OFDM schemes (ACO-OFDM, U-OFDM, and Flip-OFDM) were introduced as power efficient alternatives to DCO-OFDM. However because two time-domain U-OFDM/Flip-OFDM frames are required to convey the information contained in a single DCO-OFDM frame, and because

Modulation Techniques for Li-Fi

Mohamed Sufyan Islim and Harald Haas



▲ Figure 6. (a) Bipolar OFDM waveform; (b) U-OFDM waveform.

half of the subcarriers are skipped in ACO-OFDM, the performance of M -QAM DCO-OFDM should be compared with the performance of M^2 -QAM (ACO-OFDM, U-OFDM, and Flip-OFDM). Additionally, PAM-DMT uses M -PAM on the imaginary part of the subcarriers instead of M -QAM. Since the performance of M -PAM is equivalent to the performance of M^2 -QAM, the BER of PAM-DMT is similar to that of the inherent unipolar schemes. When compared with DCO-OFDM at the same SE, the performance of all of the inherent unipolar OFDM techniques degrades as the constellation size of M -QAM or M -PAM increases. For example, the performance of 1024-QAM ACO-OFDM/U-OFDM/Flip-OFDM and 32-PAM PAM-DMT would be required to be compared with the performance of 32-QAM DCO-OFDM.

Improved receivers for all of the inherent unipolar OFDM techniques were proposed in [33]–[41]. Most of these improved receivers would either require a flat channel to operate or incur additional computational complexities. Two main methods are considered in the design of these improved receivers. In the first method, the time-domain symmetry can be exploited at the receiver to achieve performance gains. An amplitude comparison between the symmetric received signal samples can improve the receiver detection in flat fading channels at the expense of increased computational complexity. The second method is based on the frequency diversity. The even subcarriers in ACO-OFDM and the real part of the subcarriers in PAM-DMT were exploited, respectively, to achieve improved performance at the receiver [33]–[41]. The frequency diversity method can be used in the frequency selective channel, however it has a higher computational complexity. In addition, it cannot be used for U-OFDM/Flip-OFDM because both schemes are based on the time-domain processing of the OFDM frames. Based on their statistical distribution, the inherent unipolar optical OFDM waveforms utilize the lower part of the V-L characteristic. Therefore, these schemes are suitable candidates for Li-Fi dimmable applications since they can operate with lower optical power dissipation. Adaptive bit loading techniques were studied for MCM techniques, DCO-OFDM and ACO-OFDM, and compared with SC-FDE in [42]. It was found that the per-

formance of SC-FDE is worse than ACO-OFDM but better than DCO-OFDM. In addition, SC-FDE is less complex than DCO-OFDM and ACO-OFDM.

4.2 Hybrid OFDM Techniques

OFDM was modified in many studies to tailor several specific aspects of the Li-Fi system parameters. The natural spatial signal summing in the optical domain was proposed in [43]. An array of multiple LEDs is used to transmit the OFDM signal so that the subcarriers are allocated to different LEDs. As the number of the LEDs in the array increases, the PAPR of the electrical OFDM signals reduces. When the number of subcarriers is equal to the number of the LEDs in the array, the PAPR would reach its minimum value of 3 dB as the electrical signal would be an ideal sine wave. The spatial optical OFDM (SO-OFDM) is reported to have BER performance gains over DCO-OFDM at high SNR due to the reduced PAPR and the robustness against LED nonlinearities [43]. Reverse polarity optical OFDM (RPO-OFDM) was proposed to allow a higher degree of illumination control in the OFDM-based Li-Fi systems [44]. RPO-OFDM combines a real-valued optical OFDM broadband technique with slow PWM to allow dimming. The dynamic range of the LED is fully used in RPO-OFDM to minimize any nonlinear distortion. The RPO-OFDM is reported to achieve higher performance gains compared with DCO-OFDM at a large fraction of dimming ranges without limiting the data rate of the system. RPO-OFDM offers a practical solution for the illumination and dimming control for Li-Fi communication systems, however the OFDM signal in RPO-OFDM is based on unipolar OFDM. This means that the SE of RPO-OFDM is half of that of DCO-OFDM. As a result, the power efficiency advantage over DCO-OFDM starts to diminish as the SE increases. In addition, the PWM duty cycle is assumed to be known at the receiver, which means that side-information should be sent before any transmission and this requires perfect synchronization between the transmitting and receiving ends. A novel technique that combines ACO-OFDM on the odd subcarriers with DCO-OFDM on the even subcarriers was proposed in asymmetrically DC-biased optical OFDM (ADO-OFDM) [45]. The clipping noise of the ACO-OFDM falls only into the even subcarriers, and can be estimated and canceled with a 3 dB penalty at the receiver. The power allocation for different constellation sizes between ACO-OFDM and DCO-OFDM streams in ADO-OFDM was investigated in [15]. The optical power efficiency of the optimal settings for ADO-OFDM was better than ACO-OFDM and DCO-OFDM for different configurations. Hybrid asymmetrical clipped OFDM (HACO-OFDM) uses ACO-OFDM on the odd subcarriers and PAM-DMT on the even subcarriers to improve the SE of unipolar OFDM modulation techniques [46]. The asymmetrical clipping

of the ACO-OFDM on the odd symbols would only distort the even subcarriers. At the receiver, ACO-OFDM symbols are demodulated first by only considering the odd subcarriers and then remodulated to estimate the ACO-OFDM distortion on the even subcarriers. This allows the PAM-DMT symbols on the even subcarrier to be demodulated without any distortion. The SE achieved in HACO-OFDM is identical to that of DCO-OFDM, however PAM-DMT uses M -PAM modulation on half of the subcarriers. Equal power was allocated to ACO-OFDM and PAM-DMT. As the performance of M^2 -QAM is equivalent to the performance of M -PAM, the power requirements for both ACO-OFDM and PAM-DMT to achieve the same performance is different. The problem also appears when different modulation orders are used for both schemes. Unequal power allocation for both schemes was investigated in [47] to guarantee that the performance of both schemes in HACO-OFDM is equal. An improved, but computationally complex, receiver was also proposed in [47] based on the time domain symmetry of both ACO-OFDM and PAM-DMT.

Polar OFDM (P-OFDM) is a new method to achieve the IM/DD for OFDM [48]. The main principle of P-OFDM is to convert the complex valued output of the IFFT from the Cartesian coordinates into the polar coordinates. Therefore, the radial and angular coordinate can be sent in the first and second halves of the OFDM frame, successively. It avoids the use of Hermitian symmetry, however, it allocates the M -QAM symbols into the even indexed subcarriers. As a result, P-OFDM has half-wave even symmetry which states that the first half of the complex valued time-domain frame is identical to the other half. Therefore, it is sufficient to transmit the first half of the IFFT output. As a result, the SE is reduced to be identical to that of DCO-OFDM since only half of the subcarriers are used. The performance of P-OFDM was compared to that of ACO-OFDM in [49]. It was reported that P-OFDM achieves better BER performance gains than ACO-OFDM under narrow dynamic ranges when optimal values for the power allocation of the radial and angular information are used. Note that any ISI between the radial and angular samples may deteriorate the system performance, therefore the system performance in frequency selective channels should be investigated. Asymmetrical and symmetrical clipping optical OFDM (ASCO-OFDM) was proposed in [50] for IM/DD Li-Fi systems. The ACO-OFDM is combined with symmetrical clipping optical OFDM (SCO-OFDM) that uses the even subcarriers. The clipping distortion of both ACO-OFDM and SCO-OFDM affects the even subcarriers. However, the clipping distortion of ACO-OFDM can be estimated and canceled at the receiver. The SCO-OFDM clipping noise can be removed at the receiver using U-OFDM/Flip-OFDM time domain processing techniques. The SE of ASCO-OFDM is 75% of the SE of DCO-OFDM. ASCO-OFDM was reported to have better symbol error rate (SER) compared with ADO-OFDM since the ADO-OFDM uses the DC bias for the even subcarriers. FIR filtering technique

termed spectral factorization was used to create a unipolar optical OFDM signal [51]. The amplitude of the subcarriers in spectral factorized optical OFDM (SFO-OFDM) were chosen to form an autocorrelation sequence that was shown to be sufficient to guarantee a unipolar OFDM output. The SFO-OFDM was reported to achieve 0.5 dB gain over ACO-OFDM with 30% PAPR reduction [51]. The position modulation OFDM (PM-OFDM) avoids the Hermitian symmetry and splits the real and imaginary components of the OFDM output into two branches where a polarity separator is used to obtain the positive and negative samples of each branch [52]. The four frames composed of a real positive frame, a real negative one, an imaginary positive one and an imaginary negative one are transmitted as unipolar OFDM frames. The SE is exactly similar to other inherent unipolar OFDM techniques discussed in section 4.1. The performance of PM-OFDM was reported to be identical to U-OFDM in flat channels. However, it was reported to have better BER performance when compared to ACO-OFDM for frequency selective channels [52].

4.3 Superposition OFDM Techniques

Superposition OFDM based modulation techniques rely on the fact that the SE of U-OFDM/Flip-OFDM, ACO-OFDM, and PAM-DMT can be doubled by proper superimposing of multiple layers of OFDM waveforms. Superposition modulation was first introduced for OFDM-based OWC and has led to enhanced U-OFDM (eU-OFDM) [53]. The eU-OFDM compensates for the spectral efficiency loss of U-OFDM by superimposing multiple U-OFDM streams so that the inter-stream-interference is null. The generation method of the first depth in eU-OFDM is exactly similar to that in U-OFDM. Subsequent depths can be generated by U-OFDM modulators before each unipolar OFDM frame is repeated 2^{d-1} times and scaled by $1/2^{d-1}$, where d is the depth number. At the receiver, the information conveyed in the first depth is demodulated and then remodulated to be subtracted from the overall received signal. Then repeated frames which are equivalent at higher depths are recombined and the demodulation procedure continues the same as for the stream at the first depth. Afterwards, the information conveyed in latter depths is demodulated in a similar way. The SE gap between U-OFDM and DCO-OFDM can never be completely closed with eU-OFDM, as this would require a large number of information streams to be superimposed in the modulation signal. Implementation issues, such as latency, computational complexity, power penalty, and memory requirements put a practical limit on the maximum number of available depths. The eU-OFDM was generalized in the Generalized Enhanced Unipolar OFDM (GREENER-OFDM) for configurations where arbitrary constellation sizes and arbitrary power allocations are used [54]. As a result, the SE gap between U-OFDM and DCO-OFDM can be closed completely with an appropriate selection of the constellation sizes in different information streams. The symmetry in U-OFDM lies in frames,

Modulation Techniques for Li-Fi

Mohamed Sufyan Islim and Harald Haas

whilst in ACO-OFDM and PAM-DMT, it lies in subframes.

The superposition concept has also been extended to other unipolar OFDM techniques such as PAM-DMT [55] and ACO-OFDM [56]–[60]. The enhanced asymmetrically clipped optical OFDM (eACO-OFDM) [56] uses the symmetry of ACO-OFDM subframes to allow multiple ACO-OFDM streams to be superimposed. A similar concept was also proposed by Elgala et al. and Wang et al. under the names of spectrally and energy efficient OFDM (SEE-OFDM) [57] and layered asymmetrically clipped optical OFDM (Layered ACO-OFDM) [58], respectively. The receiver proposed in SEE-OFDM [57] results in SNR penalty that could have been avoided by using the symmetry properties of ACO-OFDM streams. The symmetry arrangement in Layered ACO-OFDM [58] is described in the frequency domain, however, it is shown in [58, Fig.2] that it takes place in the time-domain. Recently, an alternative method to achieve superposition modulation based on ACO-OFDM was proposed by Kozu et al. [59] for two ACO-OFDM streams, and Lawery [60] for Layered ACO-OFDM. This is similar in principle to the solutions in [56]–[58], however the superposition is performed in the frequency domain which results in simpler system design. The concept of eACO-OFDM was generalized to close the SE gap between ACO-OFDM and DCO-OFDM. The generation of eACO-OFDM signal starts at the first depth with an ACO-OFDM modulator. Additional depths are generated in a similar way to the first depth, but with an OFDM frame length equal to half of the previous depth frames. Similar to eU-OFDM, all of the generated frames are repeated 2^{d-1} times and appropriately scaled. The demodulation process at the receiver is applied in a similar way as the eU-OFDM. The information at Depth-1 can be recovered directly as in conventional ACO-OFDM because all of the inter-stream-interference falls into the even-indexed subcarriers. After the first stream is decoded, the information can be remodulated again and subtracted from the overall received signal. Then, the frames that are equivalent can be recombined and the demodulation procedure continues as for the stream at first depth.

The enhanced pulse-amplitude-modulated discrete multi-tone (ePAM-DMT) [55] demonstrates that superposition modulation can also be utilized when the antisymmetry of PAM-DMT waveforms is used. Analogous to eU-OFDM and eACO-OFDM, unique time-domain structures are also present in PAM-DMT. If the interference over a single PAM-DMT frame possesses a Hermitian symmetry in the time-domain, its frequency profile falls on the real component of the subcarriers. Hence, the interference is completely orthogonal to the useful information which is encoded in imaginary symbols of the PAM-DMT frames. The concept of superposition modulation was extended to ePAM-DMT for an arbitrary modulation order and an arbitrary power allocation at each depth [55]. The theoretical BER analysis of eACO-OFDM is similar to the analysis of GREENER-OFDM, therefore the optimal modulation sizes and scaling factors are identical. This is an expected result because the

performance of their unipolar OFDM forms, ACO-OFDM and U-OFDM, is also similar. The ePAM-DMT is less energy efficient than GREENER-OFDM and eACO-OFDM, because ePAM-DMT has 3 dB loss in each depth demodulation process and the optimal configurations of ePAM-DMT are suboptimal as the non-squared M -QAM BER performance can never be achieved using the \sqrt{M} -PAM modulation scheme. The ePAM-DMT is more energy efficient than DCO-OFDM in terms of the electrical SNR at SE values above 1 bit/s/Hz. In terms of the optical SNR, the ePAM-DMT is less energy efficient than DCO-OFDM for all of the presented values. Higher optical energy dissipation is a desirable property for illumination based Li-Fi applications, but it is considered as a disadvantage for dimmable-based Li-Fi applications. However, GREENER-OFDM and eACO-OFDM are suitable candidates for dimmable-based Li-Fi applications due to their optical SNR performance.

5 Other Multi-Carrier Modulation Techniques

OFDM has been mainly studied in the context of Li-Fi channels based on FFT. Other transformations such as discrete Hartley transformation (DHT) [61], wavelet packet division multiplexing (WPDM) [62] and Hadamard coded modulation (HCM) [63] have also been considered for Li-Fi channels. A multicarrier IM/DD system based on DHT was proposed in [61]. It was shown that DHT output can be real when an input frame of real modulated symbols such as binary phase shift keying (BPSK) and M -PAM is used. Similar to DCO-OFDM and ACO-OFDM, DC-biasing and asymmetrical clipping can also be used to achieve unipolar output in DHT-based multicarrier modulation technique. As a major advantage over FFT-based conventional OFDM, the DHT-based multicarrier modulation does not require any Hermitian symmetry. However, this fails to improve the SE as real modulated symbols such as M -PAM are used in DHT-based multicarrier modulation. WPDM uses orthogonal wavelet packet functions for symbol modulation where the basis functions are wavelet packet functions with finite length. It was reported that the performance of WPDM is better than that of OFDM in terms of the spectral and power efficiencies when LED nonlinear distortion and channel dispersion are taken into account [62]. The high illumination level of OFDM Li-Fi systems require higher optical power, which may result in clipping due to the peak power constraint of the V-L transfer function of the LED (Fig. 2). HCM was proposed for multicarrier modulation Li-Fi as a solution to the limitation of OFDM modulation at higher illumination levels. The technique is based on fast Walsh-Hadamard transformation (FWHT) as an alternative to the FFT. HCM is reported to achieve higher performance gains when compared with ACO-OFDM and DCO-OFDM at higher illumination levels [63]. However, the performance improvement over RPO-OFDM is modest. An alternative variant of HCM, termed DC reduced

HCM (DCR-HCM), was also proposed to reduce the power consumption of HCM to support dimmable Li-Fi applications, and interleaving with MMSE equalization is used for HCM in dispersive Li-Fi channels.

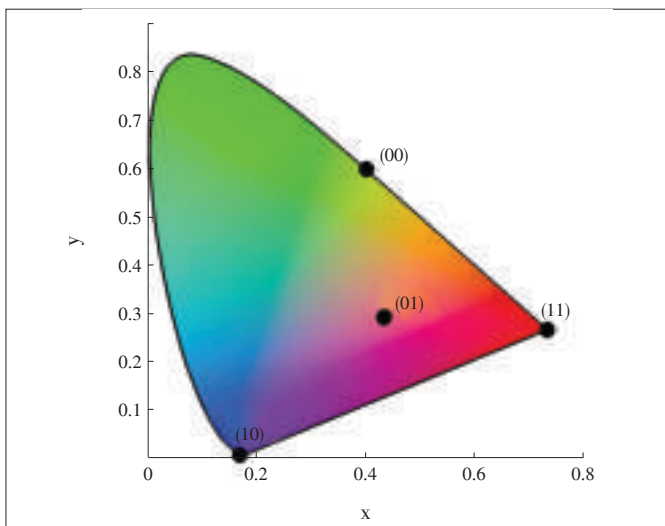
6 Li-Fi Unique Modulation Technique

The modulation frequency in Li-Fi systems does not correspond to the carrier frequency of the LED. All the aforementioned modulation techniques are baseband modulation techniques. It is practically difficult to modulate the carrier frequency of the LEDs, however, it is practically straightforward to change its colour. This feature adds a new degree of freedom to Li-Fi systems. Colour tunable LEDs such as the red green blue LED (RGB-LED) can illuminate with different colours based on the intensity applied on each LED element. The IEEE 802.15.7 standard proposes colour shift keying (CSK) as a modulation technique for VLC [8]. The incoming bits are mapped into a constellation of colours from the chromatic CIE 1931 colour space [64], as shown in **Fig. 7**. The CIE 1931 is the widely used illumination model for human eye colour perception. Any colour in the model can be represented by the chromaticity dimension $[x, y]$. In CSK, the overall intensity of the output colour is constant, however, the relative intensities between the multiple used colours are changed. Therefore the instantaneous colour of the multicolour LED is modulated. Seven wavelengths are defined in IEEE 802.15.7 specify the vertices of a triangle where the constellation point lies in. The intensity of each RGB-LED element is changed to match the constellation point while maintaining a constant optical power and a constant illumination colour. This is desirable in Li-Fi systems, since the constant illumination colour naturally mitigates any flickering. An amplitude dimming is used for brightness control in CSK while the center colour of the colour constella-

tion constant is kept. However, colour shift is possible due to the presence of any improper driving current used for dimming control. Constellation sizes up to 16-CSK were proposed in the IEEE 802.15.7 standard based on tri-colour LEDs. Constellation points design based on CIE 1931 was also investigated by Drost and Sadler using billiard algorithms [65], by Monterio and Hranilovic using interior point method [66], by Singh et al. using quad LED (QLED) [67], and by Jiang et al. using extrinsic transfer (EXIT) charts for an iterative CSK transceiver design [68].

A generalized CSK (GCSK) that operates under varying target colours independent from the number of used LEDs was proposed in [69]. Colour intensity modulation (CIM) was proposed to improve the communication capacity without any loss to the illumination properties (dimming and target colour matching) [70]. The instantaneous intensity of the RGB LED was modulated in CIM while only maintaining a constant perceived colour. Therefore, CIM can be considered as a relaxed version of CSK since a constant perceived power is additionally required in CSK. Metameric modulation (MM) constrains the CSK to have a constant instantaneous perceived ambient light with the aid of an external green LED [70]. An improved control of the RGB output colour was achieved in MM by improving the colour rendering and reducing the colour flickering [71]. A four colour system was used in [67] with the aid of additional IM/DD signaling as a fourth dimension signal. Higher order modulation techniques of 2^{12} -CSK for QLED were achieved in [67]. The CSK was combined with constant rate differential PPM in [72] to simplify the synchronization while maintaining the illumination control and avoiding flickering. A similar approach of combining CSK with complementary PPM was proposed by [73]. A digital CSK (DCSK) was proposed in [74]. Multiple multicolour LEDs were used in DCSK where only one colour is activated in each multicolour LED at a single time. Therefore the information is encoded in the combinations of activated colours. The main advantage of DCSK over conventional CSK is avoiding the need of any digital-to-analog converters, while the main disadvantage is rendering the activated colours which may result in slight changes of the colour perception over time.

The receiver architecture has not been fully addressed in most of the published research on colour domain modulation. CSK is considered to be an expensive and complex modulation technique when compared with OFDM. The colour dimension in Li-Fi can also be used to derive a multicolour LED with different streams of data. The optical summation may turn this coloured parallel stream into a single colour stream output that can be filtered at the receiver into the original transmitted coloured stream.



▲ **Figure 7.** The symbol mapping of 4-CSK on the CIE 1931 colour model based on IEEE 802.15.7.

7 Conclusions

The modulation techniques suitable for Li-Fi are presented

Modulation Techniques for Li-Fi

Mohamed Sufyan Islim and Harald Haas

in this paper. These techniques should satisfy illumination and communication requirements. Single carrier modulation techniques offer a simple solution for frequency-flat Li-Fi channels. Low-to-medium data rates can be achieved using single carrier modulation techniques. Multicarrier modulation techniques offer high data rates solution that can adapt the system performance to the channel frequency response. Many variants of optical OFDM modulation techniques have been proposed in published research to satisfy certain illumination and/or communication requirements. A summary of Li-Fi multicarrier modulation techniques is presented in **Table 1**. The colour di-

▼ **Table 1. Comparison of multicarrier modulation schemes for Li-Fi**

Mod. Tech.	SE as a function of DCO-OFDM	Illumination		Computational complexity	Remarks	Ref.
		Control	Level			
ADO-OFDM	100%	No	Dimmed-medium	High	Requires DC bias	[15]
DCO-OFDM	100%	No	Medium	Low	Requires DC bias	[26]
Inherent unipolar	50%	No	Dimmed	Low	Power efficient at low SE	[30]–[33]
Spatial OFDM	100%	Limited	Medium	High	Low PAPR	[43]
RPO-OFDM	50%	Yes	Dimmed-high	Medium	Requires sync.	[44]
HACO-OFDM	100%	No	Dimmed	High	Power efficient at low-medium SE	[46]
P-OFDM	50%	No	Medium	High	-	[48]
ASCO-OFDM	75%	No	Dimmed	High	-	[50]
SFO-OFDM	Variable	No	Medium	High	Low PAPR	[51]
PM-OFDM	50%	No	Medium	High	-	[52]
Superposition	100%	No	Dimmed	High	Power efficient at low-high SE	[53]–[60]
DHT	50%-100%	No	Dimmed-medium	Low	-	[61]
WPDM	100%	No	Medium	High	-	[62]
HCM	100%	Yes	High	Low	Power inefficient	[63]

mension offers unique modulation formats for Li-Fi and adds to the degrees of freedom of Li-Fi systems. Time, frequency, space, colour dimensions, and the combinations of them can be used for Li-Fi modulation. Li-Fi modulation techniques should offer a high speed communication and be suitable for most illumination regimes.

Acknowledgment

The authors would like to thank Tezcan Cogalan and Liang Yin for their valuable comments and suggestions that improved the presentation of the paper.

References

- [1] Cisco. (2016, Feb.). Global mobile data traffic forecast update, 2015–2020. [Online]. Available: <http://www.cisco.com/c/en/us/solutions/collateral/service-provider/visual-networking-index-vni/mobile-white-paper-c11-520862.pdf>

- [2] S. Dimitrov and H. Haas, *Principles of LED Light Communications: Towards Networked Li-Fi*. Cambridge, England: Cambridge University Press, 2015.
- [3] D. Tsonev, S. Videv, and H. Haas, "Towards a 100 Gb/s visible light wireless access network," *Optics Express*, vol. 23, no. 2, pp. 1627–1637, Jan. 2015. doi: 10.1364/OE.23.001627.
- [4] H. Elgala, R. Mesleh, and H. Haas, "A study of LED nonlinearity effects on optical wireless transmission using OFDM," in *Proc. 6th IEEE International Conference on Wireless and Optical Communications Networks (WOCN)*, Cairo, Egypt, Apr. 28–30, 2009. doi: 10.1109/WOCN.2009.5010576.
- [5] A. M. Khalid, G. Cossu, R. Corsini, et al., "1-Gb/s transmission over a phosphorescent white LED by using rate-adaptive discrete multitone modulation," *IEEE Photonics Journal*, vol. 4, no. 5, pp. 1465–1473, Oct. 2012. doi: 10.1109/JPHOT.2012.2201397.
- [6] G. Cossu, A. M. Khalid, P. Choudhury, et al., "3.4 Gbit/s visible optical wireless transmission based on RGB LED," *Optics Express*, vol. 20, pp. B501–B506, 2012. doi: 10.1364/OE.20.00B501.
- [7] J. M. Kahn and J. R. Barry, "Wireless infrared communications," *Proceedings of the IEEE*, vol. 85, no. 2, pp. 265–298, Feb. 1997.
- [8] *IEEE Standard for Local and Metropolitan Area Networks, Part 15.7: Short-Range Wireless Optical Communication Using Visible Light*, IEEE Std. 802.15.7-2011, 2011. doi: 10.1109/IEEESTD.2011.6016195.
- [9] S. Randel, F. Breyer, S. C. J. Lee, et al., "Advanced modulation schemes for short-range optical communications," *IEEE Journal of Selected Topics in Quantum Electronics*, vol. PP, no. 99, pp. 1–10, 2010. doi: 10.1109/JSTQE.2010.2040808.
- [10] D. Shan Shiu and J. Kahn, "Differential pulse-position modulation for power-efficient optical communication," *IEEE Transactions on Communications*, vol. 47, no. 8, pp. 1201–1210, Aug. 1999. doi: 10.1109/26.780456.
- [11] F. Delgado, I. Quintana, J. Rufo, et al., "Design and implementation of an Ethernet-VLC interface for broadcast transmissions," *IEEE Communications Letters*, vol. 14, no. 12, pp. 1089–1091, Dec. 2010. doi: 10.1109/LCOMM.2010.12.100984.
- [12] S. H. Lee, S.-Y. Jung, and J. K. Kwon, "Modulation and coding for dimmable visible light communication," *IEEE Communications Magazine*, vol. 53, no. 2, pp. 136–143, Feb. 2015. doi: 10.1109/MCOM.2015.7045402.
- [13] Y. Zeng, R. Green, and M. Leeson, "Multiple pulse amplitude and position modulation for the optical wireless channel," in *Proc. 10th Anniversary International Conference on Transparent Optical Networks (ICTON'08)*, vol. 4, Athens, Greece, Jun. 22–26 2008, pp. 193–196. doi: 10.1109/ICTON.2008.4598766.
- [14] R. Mesleh, H. Elgala, and H. Haas, "On the performance of different OFDM based optical wireless communication systems," *IEEE/OSA Journal of Optical Communications and Networking*, vol. 3, no. 8, pp. 620–628, Aug. 2011. doi: 10.1364/JOCN.3.000620.
- [15] S. Dissanayake and J. Armstrong, "Comparison of ACO-OFDM, DCO-OFDM and ADO-OFDM in IM/DD systems," *Journal of Lightwave Technology*, vol. 31, no. 7, pp. 1063–1072, Apr. 2013. doi: 10.1109/JLT.2013.2241731.
- [16] D. Barros, S. Wilson, and J. Kahn, "Comparison of orthogonal frequency-division multiplexing and pulse-amplitude modulation in indoor optical wireless links," *IEEE Transactions on Communications*, vol. 60, no. 1, pp. 153–163, 2012. doi: 10.1109/TCOMM.2011.112311.100538.
- [17] J. Armstrong and B. J. C. Schmidt, "Comparison of asymmetrically clipped optical OFDM and DC-biased optical OFDM in AWGN," *IEEE Communications Letters*, vol. 12, no. 5, pp. 343–345, May 2008. doi: 10.1109/LCOMM.2008.080193.
- [18] M. Kashani and M. Kavehrad, "On the performance of single- and multi-carrier modulation schemes for indoor visible light communication systems," in *IEEE Global Communications Conference (GLOBECOM)*, Austin, USA, Dec. 2014, pp. 2084–2089. doi: 10.1109/GLOCOM.2014.7037115.
- [19] J. B. Carruthers and J. M. Kahn, "Angle diversity for nondirected wireless infrared communication," *IEEE Transactions on Communications*, vol. 48, no. 6, pp. 960–969, Jun. 2000. doi: 10.1109/26.848557.
- [20] J. G. Proakis, *Digital Communications*, 4th ed. New York, USA: McGraw-Hill, 2000.
- [21] K. Acolatse, Y. Bar-Ness, and S. K. Wilson, "Novel techniques of single-carrier frequency-domain equalization for optical wireless communications," *EURASIP Journal on Advances in Signal Processing*, vol. 2011, pp. 4:1–4:13, Jan. 2011. [Online]. Available: 10.1155/2011/393768.
- [22] C. Chen Hsieh and D. Shan Shiu, "Single carrier modulation with frequency domain equalization for intensity modulation-direct detection channels with intersymbol interference," in *17th IEEE International Symposium on Personal, Indoor and Mobile Radio Communications*, Helsinki, Finland, Sept. 2006, pp. 1–5. doi: 10.1109/PIMRC.2006.254418.

- [23] A. Nuwanpriya, J. Zhang, A. Grant, et al., "Single carrier frequency domain equalization based on on-off-keying for optical wireless communications," in *IEEE Wireless Communications and Networking Conference (WCNC)*, Shanghai, China, Apr. 2013, pp. 4272–4277. doi: 10.1109/WCNC.2013.6555264.
- [24] C. Wu, H. Zhang, and W. Xu, "On visible light communication using led array with DFT-spread OFDM," in *IEEE International Conference on Communications (ICC)*, Sydney, Australia, Jun. 2014, pp. 3325–3330. doi: 10.1109/ICC.2014.6883834.
- [25] P. Haigh, S. T. Le, S. Zvanovec, et al., "Multi-band carrier-less amplitude and phase modulation for bandlimited visible light communications systems," *IEEE Wireless Communications*, vol. 22, no. 2, pp. 46–53, Apr. 2015. doi: 10.1109/MWC.2015.7096284.
- [26] J. B. Carruthers and J. M. Kahn, "Multiple-subcarrier modulation for nondirect wireless infrared communication," *IEEE Journal on Selected Areas in Communications*, vol. 14, no. 3, pp. 538–546, Apr. 1996. doi: 10.1109/49.490239.
- [27] S. Dimitrov and H. Haas, "Information rate of OFDM-based optical wireless communication systems with nonlinear distortion," *IEEE Journal of Lightwave Technology*, vol. 31, no. 6, pp. 918–929, Mar. 2013. doi: 10.1109/JLT.2012.2236642.
- [28] X. Ling, J. Wang, X. Liang, et al., "Offset and power optimization for DCO-OFDM in visible light communication systems," *IEEE Transactions on Signal Processing*, vol. 64, no. 2, pp. 349–363, Jan. 2016. doi: 10.1109/TSP.2015.2477799.
- [29] M. Zhang and Z. Zhang, "An optimum DC-biasing for DCO-OFDM system," *IEEE Communications Letters*, vol. 18, no. 8, pp. 1351–1354, Aug. 2014. doi: 10.1109/LCOMM.2014.2331068.
- [30] J. Armstrong and A. Lowery, "Power efficient optical OFDM," *Electronics Letters*, vol. 42, no. 6, pp. 370–372, Mar. 2006. doi: 10.1049/el:20063636.
- [31] S. C. J. Lee, S. Randel, F. Breyer, et al., "PAM-DMT for intensity-modulated and direct-detection optical communication systems," *IEEE Photonics Technology Letters*, vol. 21, no. 23, pp. 1749–1751, Dec. 2009. doi: 10.1109/LPT.2009.2032663.
- [32] N. Fernando, Y. Hong, and E. Viterbo, "Flip-OFDM for unipolar communication systems," *IEEE Transactions on Communications*, vol. 60, no. 12, pp. 3726–3733, Dec. 2012. doi: 10.1109/TCOMM.2012.082712.110812.
- [33] D. Tsonev, S. Sinanovic, and H. Haas, "Novel unipolar orthogonal frequency division multiplexing (U-OFDM) for optical wireless," in *Proc. IEEE Vehicular Technology Conference (VTC Spring)*, Yokohama, Japan, May 2012. doi: 10.1109/VETECS.2012.6240060.
- [34] L. Chen, B. Krongold, and J. Evans, "Diversity combining for asymmetrically clipped optical OFDM in IM/DD channels," in *IEEE Global Telecommunications Conference (GLOBECOM 2009)*, Hawaii, USA, Nov. 2009, pp. 1–6. doi: 10.1109/GLOCOM.2009.5425293.
- [35] J. Dang, Z. Zhang, and L. Wu, "A novel receiver for ACO-OFDM in visible light communication," *IEEE Communications Letters*, vol. 17, no. 12, pp. 2320–2323, Dec. 2013. doi: 10.1109/LCOMM.2013.111113.132223.
- [36] N. Huang, J.-B. Wang, C. Pan, et al., "Iterative receiver for flip-OFDM in optical wireless communication," *IEEE Photonics Technology Letters*, vol. 27, no. 16, pp. 1729–1732, Aug. 2015. doi: 10.1109/LPT.2015.2438338.
- [37] Y. Zheng, Z. Zhang, J. Dang, et al., "A novel receiver for flip-OFDM in optical wireless communication," in *IEEE 16th International Conference on Communication Technology (ICCT)*, Mumbai, India, Oct. 2015, pp. 620–625. doi: 10.1109/ICCT.2015.7399914.
- [38] J. Dang, Z. Zhang, and L. Wu, "Frequency-domain diversity combining receiver for ACO-OFDM system," *IEEE Photonics Journal*, vol. 7, no. 6, pp. 1–10, Dec. 2015. doi: 10.1109/JPHOT.2015.2496865.
- [39] J. Xu, W. Xu, H. Zhang, et al., "Asymmetrically reconstructed optical OFDM for visible light communications," *IEEE Photonics Journal*, vol. 8, no. 1, pp. 1–18, Feb. 2016. doi: 10.1109/JPHOT.2016.2520818.
- [40] N. Huang, J.-B. Wang, J. Wang, et al., "Receiver design for PAM-DMT in indoor optical wireless links," *IEEE Photonics Technology Letters*, vol. 27, no. 2, pp. 161–164, Jan. 2015. doi: 10.1109/LPT.2014.2363876.
- [41] N. Xiang, Z. Zhang, J. Dang, et al., "A novel receiver design for PAM-DMT in optical wireless communication systems," *IEEE Photonics Technology Letters*, vol. 27, no. 18, pp. 1919–1922, Sept. 2015. doi: 10.1109/LPT.2015.2445793.
- [42] L. Wu, Z. Zhang, J. Dang, et al., "Adaptive modulation schemes for visible light communications," *Journal of Lightwave Technology*, vol. 33, no. 1, pp. 117–125, Jan. 2015. doi: 10.1109/JLT.2014.2374171.
- [43] M. Mossaad, S. Hranilovic, and L. Lampe, "Visible light communications using OFDM and multiple LEDs," *IEEE Transactions on Communications*, vol. 63, no. 11, pp. 4304–4313, Nov. 2015. doi: 10.1109/TCOMM.2015.2469285.
- [44] H. Elgala and T. D. C. Little, "Reverse polarity optical-OFDM (RPO-OFDM): dimming compatible OFDM for gigabit VLC links," *Optics Express*, vol. 21, no. 20, pp. 24288–24299, Oct. 2013. doi: 10.1364/OE.21.024288.
- [45] S. Dissanayake, K. Panta, and J. Armstrong, "A novel technique to simultaneously transmit ACO-OFDM and DCO-OFDM in IM/DD systems," in *IEEE GLOBECOM Workshops (GC Wkshps)*, Houston, USA, Dec. 2011, pp. 782–786. doi: 10.1109/GLOCOMW.2011.6162561.
- [46] B. Ranjha and M. Kavehrad, "Hybrid asymmetrically clipped OFDM-based IM/DD optical wireless system," *IEEE/OSA Journal of Optical Communications and Networking*, vol. 6, no. 4, pp. 387–396, Apr. 2014. doi: 10.1364/JOCN.6.000387.
- [47] Q. Wang, Z. Wang, and L. Dai, "Iterative receiver for hybrid asymmetrically clipped optical OFDM," *Journal of Lightwave Technology*, vol. 32, no. 22, pp. 4471–4477, Nov. 2014. doi: 10.1109/JLT.2014.2358611.
- [48] H. Elgala and T. Little, "P-OFDM: Spectrally efficient unipolar OFDM," in *Optical Fiber Communications Conference and Exhibition (OFC)*, San Francisco, USA, Mar. 2014, pp. 1–3. doi: 10.1364/OFC.2014.Th3G.7.
- [49] H. Elgala and T. D. C. Little, "Polar-based OFDM and SC-FDE links toward energy-efficient GBPS transmission under IM-DD optical system constraints invited," *Journal of Optical Communications and Networking*, vol. 7, no. 2, pp. A277–A284, Feb. 2015. doi: 10.1364/JOCN.7.00A277.
- [50] N. Wu and Y. Bar-Ness, "A novel power-efficient scheme asymmetrically and symmetrically clipping optical (ASCO)-OFDM for IM/DD optical systems," *EURASIP Journal on Advances in Signal Processing*, vol. 2015, no. 1, pp. 1–10, 2015. doi: 10.1186/1687-6180-2015-3.
- [51] K. Asadzadeh, A. Farid, and S. Hranilovic, "Spectrally factorized optical OFDM," in *IEEE 12th Canadian Workshop on Information Theory (CWIT 2011)*, British Columbia, Canada, May 2011, pp. 102–105. doi: 10.1109/CWIT.2011.5872134.
- [52] T. Mao, C. Qian, Q. Wang, et al., "PM-DCO-OFDM for PAPR reduction in visible light communications," in *Opto-Electronics and Communications Conference (OECC)*, Shanghai, China, Jun. 2015, pp. 1–3. doi: 10.1109/OECC.2015.7340207.
- [53] D. Tsonev and H. Haas, "Avoiding spectral efficiency loss in Unipolar OFDM for optical wireless communication," in *Proc. International Conference on Communications (ICC)*, Sydney, Australia, Jun. 2014. doi: 10.1109/ICC.2014.6883836.
- [54] M. Islim, D. Tsonev, and H. Haas, "A generalized solution to the spectral efficiency loss in unipolar optical OFDM-based systems," in *Proc. IEEE International Conference on Communications (ICC)*, London, UK, Jun. 2015. doi: 10.1109/ICC.2015.7249137.
- [55] M. Islim, D. Tsonev, and H. Haas, "Spectrally enhanced PAM-DMT for IM/DD optical wireless communications," in *Proc. IEEE 25th Int. Symp. Pers. Indoor and Mobile Radio Commun (PIMRC)*, Hong Kong, China, 2015, pp. 927–932. doi: 10.1109/PIMRC.2015.7343421.
- [56] M. Islim, D. Tsonev, and H. Haas, "On the superposition modulation for OFDM-based optical wireless communication," in *IEEE Global Conference on Signal and Information Processing (GlobalSIP)*, Orlando, USA, Dec. 2015. doi: 10.1109/GlobalSIP.2015.7418352.
- [57] H. Elgala and T. Little, "SEE-OFDM: Spectral and energy efficient OFDM for optical IM/DD systems," in *IEEE 25th Annual International Symposium on Personal, Indoor, and Mobile Radio Communication (PIMRC)*, Washington DC, USA, 2014, pp. 851–855. doi: 10.1109/PIMRC.2014.7136284.
- [58] Q. Wang, C. Qian, X. Guo, et al., "Layered ACO-OFDM for intensity-modulated direct-detection optical wireless transmission," *Optics Express*, vol. 23, no. 9, pp. 12382–12393, May 2015. doi: 10.1364/OE.23.012382.
- [59] T. Kozu and K. Ohuchi, "Proposal for superposed ACO-OFDM using several even subcarriers," in *9th International Conference on Signal Processing and Communication Systems (ICSPCS)*, Cairns, Australia, Dec. 2015, pp. 1–5. doi: 10.1109/ICSPCS.2015.7391762.
- [60] A. J. Lowery, "Comparisons of spectrally-enhanced asymmetrically-clipped optical OFDM systems," *Optics Express*, vol. 24, no. 4, pp. 3950–3966, 2016. doi: 10.1364/OE.24.003950.
- [61] M. S. Moreolo, R. M. Noz, and G. Junyent, "Novel power efficient optical OFDM based on Hartley transform for intensity-modulated direct-detection systems," *Journal of Lightwave Technology*, vol. 28, no. 5, pp. 798–805, Mar. 2010. doi: 10.1109/JLT.2010.2040580.
- [62] W. Huang, C. Gong, and Z. Xu, "System and waveform design for wavelet packet division multiplexing-based visible light communications," *Journal of Lightwave Technology*, vol. 33, no. 14, pp. 3041–3051, Jul. 2015. doi: 10.1109/JLT.2015.2418752.
- [63] M. Noshad and M. Brandt-Pearce, "Hadamard coded modulation for visible light communications," *IEEE Transactions on Communications*, vol. PP, no. 99,

Modulation Techniques for Li-Fi

Mohamed Sufyan Islim and Harald Haas

- pp. 1–1, 2016. doi: 10.1109/TCOMM.2016.2520471.
- [64] The International Commission on Illumination (CIE). (2008, Aug.). CIE 1931 standard colorimetric observer. [Online]. Available: <http://www.cie.co.at>
- [65] R. Drost and B. Sadler, "Constellation design for color-shift keying using billiards algorithms," in *IEEE GLOBECOM Workshops (GC Wkshps)*, Miami, USA, Dec. 2010, pp. 980–984. doi: 10.1109/GLOCOMW.2010.5700472.
- [66] E. Monteiro and S. Hranilovic, "Design and implementation of color-shift keying for visible light communications," *Journal of Lightwave Technology*, vol. 32, no. 10, pp. 2053–2060, May 2014. doi: 10.1109/JLT.2014.2314358.
- [67] R. Singh, T. O'Farrell, and J. P. R. David, "An enhanced color shift keying modulation scheme for high-speed wireless visible light communications," *Journal of Lightwave Technology*, vol. 32, no. 14, pp. 2582–2592, Jul. 2014. doi: 10.1109/JLT.2014.2328866.
- [68] J. Jiang, R. Zhang, and L. Hanzo, "Analysis and design of three-stage concatenated color-shift keying," *IEEE Transactions on Vehicular Technology*, vol. 64, no. 11, pp. 5126–5136, Nov. 2015. doi: 10.1109/TVT.2014.2382875.
- [69] N. Murata, H. Shimamoto, Y. Kozawa, et al., "Performance evaluation of digital color shift keying for visible light communications," in *IEEE International Conference on Communication Workshop (ICCW)*, London, UK, Jun. 2015, pp. 1374–1379. doi: 10.1109/ICCW.2015.7247370.
- [70] K.-I. Ahn and J. Kwon, "Color intensity modulation for multicolored visible light communications," *IEEE Photonics Technology Letters*, vol. 24, no. 24, pp. 2254–2257, Dec. 2012. doi: 10.1109/LPT.2012.2226570.
- [71] P. Butala, J. Chau, and T. Little, "Metameric modulation for diffuse visible light communications with constant ambient lighting," in *International Workshop on Optical Wireless Communications (IWOW)*, Pisa, Italy, Oct. 2012, pp. 1–3. doi: 10.1109/IWOW.2012.6349697.
- [72] J. Luna-Rivera, R. Perez-Jimenez, V. Guerra-Yañez, et al., "Combined CSK and pulse position modulation scheme for indoor visible light communications," *Electronics Letters*, vol. 50, no. 10, pp. 762–764, May 2014. doi: 10.1049/el.2014.0953.
- [73] S. Pergoloni, M. Biagi, S. Colonnese, et al., "Merging color shift keying and complementary pulse position modulation for visible light illumination and communication," in *Euro Med Telco Conference (EMTC)*, Naples, Italy, Nov. 2014, pp. 1–6. doi: 10.1109/EMTC.2014.6996621.
- [74] F. Delgado Rajol, V. Guerra, J. Rabadañ Borges, et al., "Color shift keying communication system with a modified PPM synchronization scheme," *IEEE*

on *Photonics Technology Letters*, vol. 26, no. 18, pp. 1851–1854, Sept. 2014. doi: 10.1109/LPT.2014.2337953.

Manuscript received: 2016-02-24

Biographies

Mohamed Sufyan Islim (m.islim@ed.ac.uk) received his BSc (1st Hons) in communications technology engineering in 2009, and MSc (Distinction) in communications engineering from Aleppo University, Syria in 2012. Among several scholarships he was awarded in 2013, he was awarded the Global Edinburgh Scholarship from Edinburgh University, UK. In 2014, he received another MSc (Distinction) in signal processing and communications from Edinburgh University. He was the recipient of the 2014 IEEE Communications Chapter Best Master Project Prize. Currently, he is a PhD student, under the supervision of Professor Harald Haas, at the Li-Fi Research and Development Centre, University of Edinburgh. His research interests include optical OFDM, Li-Fi, and optical wireless communications.

Harald Haas (h.haas@ed.ac.uk) holds the chair for Mobile Communications at the School of Engineering, and is the director of the Li-Fi Research and Development Centre, University of Edinburgh, UK. Professor Haas has been working in wireless communications for 20 years and has held several posts in industry. He was an invited speaker at TED Global in 2011 where he demonstrated and coined "Li-Fi". Li-Fi was listed among the 50 best inventions in *TIME Magazine* 2011. Moreover, his work has been covered in other international media such as the *New York Times*, BBC, MSNBC, CNN International, Wired UK, and many more. He is initiator, co-founder and chief scientific officer (CSO) of pureLiFi Ltd. Professor Haas holds 31 patents and has more than 30 pending patent applications. He has published 300 conference and journal papers including a paper in *Science Magazine*. He published two textbooks with Cambridge University Press. His h-index is 43 (Google). In 2015 he was co-recipient of three best paper awards including the IEEE Jack Neubauer Memorial Award. He is CI of programme grant TOUCAN (EP/L020009/1), and CI of SERAN (EP/L026147/1). He currently holds an EPSRC Established Career Fellowship (EP/K008757/1). In 2014, Professor Haas was selected as one of ten EPSRC UK RISE Leaders.

Call for Papers

ZTE Communications Special Issue on

Multi-Gigabit Millimeter-Wave Wireless Communications

The exponential growth of wireless devices in recent years has motivated the exploration of the millimeter-wave frequency spectrum for multi-gigabit wireless communications. Recent advances in antenna technology, RF CMOS process, and high-speed baseband signal processing algorithms make millimeter-wave wireless communication feasible. The multi-gigabit-per-second data rate of millimeter-wave wireless communication systems will lead to applications in many important scenarios, such as WPAN, WLAN, back-haul for cellular system. The frequency bands include 28 GHz, 38 GHz, 45GHz, 60GHz, E-BAND, and even beyond 100 GHz. The upcoming special issue of *ZTE Communications* will present some major achievements of the research and development in multi-gigabit millimeter-wave wireless communications. The expected publication date will be in December 2016. It includes (but not limited to) the following topics:

- Channel characterization and channel models
- Antenna technologies
- Millimeter-wave-front-end architectures and circuits

- Baseband processing algorithms and architectures
- System aspects and applications.

Paper Submission

Please directly send to eypzhang@ntu.edu.sg and use the email subject "ZTE-MGMMW-Paper-Submission".

Tentative Schedule

Paper submission deadline: June 15, 2016

Editorial decision: August 31, 2016

Final manuscript: September 15, 2016

Guest Editors

Prof. Yueping Zhang, Nanyang Technological University, Singapore (eypzhang@ntu.edu.sg)

Prof. Ke Guan, Beijing Jiao Tong University, China (kguan@bjtu.edu.cn)

Prof. Junjun Wang, Beihang University, China (wangjunjun@buaa.edu.cn)

LDPC Decoding for Signal Dependent Visible Light Communication Channels

YUAN Ming, SHA Xiaoshi, LIANG Xiao, JIANG Ming, WANG Jiaheng, and ZHAO Chunming

(National Mobile Communications Research Laboratory, Southeast University, Nanjing, 211189, China)

Abstract

Avalanche photodiodes (APD) are widely employed in visible light communication (VLC) systems. The general signal dependent Gaussian channel is investigated. Experiment results reveal that symbols on different constellation points under official illumination inevitably suffer from different levels of noise due to the multiplication process of APDs. In such a case, conventional log likely-hood ratio (LLR) calculation for signal independent channels may cause performance loss. The optimal LLR calculation for decoder is then derived because of the existence of non-ignorable APD shot noise. To find the decoding thresholds of the optimal and suboptimal detection schemes, the extrinsic information transfer (EXIT) chart is further analyzed. Finally a modified minimum sum algorithm is suggested with reduced complexity and acceptable performance loss. Numerical simulations show that, with a regular (3, 6) low-density parity check (LDPC) code of block length 20,000, 0.7 dB gain is achieved with our proposed scheme over the LDPC decoder designed for signal independent noise. It is also found that the coding performance is improved for a larger modulation depth.

Keywords

VLC; APD; shot noise; LDPC code

1 Introduction

Visible light communication (VLC) is an integrated dual-purpose technology to provide general lighting and high speed communications simultaneously [1]–[3]. Avalanche photodiode (APD), as one of photo detectors (PD), is widely employed in VLC due to its high sensitivity, high internal gain and wide bandwidth [4].

Different from the signal independent noise in radio frequency (RF) systems, noise in VLC systems is often signal dependent. Incident light induced PD shot noise is one of major noise sources in VLC, since a VLC system should provide ample illumination for general lighting. Moreover, the intensity of visible light is modulated by the information symbols in VLC. Therefore, symbols on distinct constellation points are contaminated by different noise levels, especially for transceivers adopting APD devices.

The impact of the shot noise on image processing has been well studied. Based on the inner correlative information of the sources, a locally adaptive DCT filtering method was proposed in [5]. The authors in [6] suggested to take the advantage of cor-

relation of adjacent data. Arsenault et al. in [7] presented a square root method to transform the probability density function (PDF) of signal dependent Gaussian noise into that of approximately signal-independent Gaussian noise. The authors in [8] also tried maximum a-posterior estimation and maximum likelihood estimation to minimize the mean-square estimation error.

The existing works seldom considered the impact of shot noise on VLC systems. In [9], the author presented the capacity results of signal dependent Gaussian noise (SDGN) channels in higher and lower power regions, respectively. In our work, we consider an VLC transceiver encoded by an low-density parity check (LDPC) code [10] with on-off keying (OOK) modulation. A general SDGN channel model is established based on experimental results, which is different from the model proposed in [11], [12] for free space optical channel. We also discuss the optimal log likely-hood ratio (LLR) input for the belief propagation (BP) decoding algorithm in this paper. For the more practical minimum sum (MS) algorithm, we proposes an approximate LLR calculation to decrease the computational complexity and meanwhile increase the robustness. We also present the extrinsic information transfer (EXIT) chart decoding threshold analysis to assist the Monte Carlo simulation [13].

The remainder of this paper is organized as follows. In Section 2, a general SDGN channel model is investigated. Then

This work was supported by "973" project (No. 2013CB329204) and the National Natural Science Foundation of China (No. 61223001, No. 61461136003, and No. 61571118).

LDPC Decoding for Signal Dependent Visible Light Communication Channels

YUAN Ming, SHA Xiaoshi, LIANG Xiao, JIANG Ming, WANG Jiaheng, and ZHAO Chunming

we derive the optimal and approximated LLR for the BP and MS algorithms, respectively, in Section 3. The experimental and numerical simulation results are presented in Section 4 before the conclusions in Section 5.

2 System Model

Fig. 1 illustrates our experimental VLC transceiver. In this work, the information stream is first encoded by an LDPC code. The coded bits are then mapped to 2-PAM symbols with unit amplitude. Before the beam is amplified and superposed on proper offset, it is pre-equalized to mitigate the inter-symbol interference of LED chips [14]. Thus the optical signal x sent by LED can be written as

$$x = \beta(A_s s + I_s) \quad (1)$$

where A_s is the amplitude of symbol set by the power amplifier, I_b is the offset to turn on LED as well as to adjust the luminance, and β is the electro-optical coefficient. Accordingly, the modulation depth m is defined as $A_s/I_b \leq 1$.

At the receiver, following the APD optical-electro conversion, signals are enhanced by the trans-impedance amplifier (TIA) and the post amplifier. Then the symbol for detector can be expressed as

$$y = h \cdot x + n \quad (2)$$

where h represents the channel gain including the optical channel gain, the APD optical-electro coefficient and gain, etc.

In the perspective of noise source, noise n consists of thermal noise and incident light induced shot noise. Generally, dual-purpose illumination light and ambient light are two main sources of shot noise. Furthermore, since the incident visible light is broad-wavelength with ample lighting, the PDF of shot noise can approach Gaussian distribution [9], [15]. Accordingly, the variance of shot noise is proportional to the photocurrent I induced by incident light:

$$\sigma_s^2 = \underbrace{2qBMF}_{\gamma} \cdot I \quad (3)$$

where q is the electron charge, B is the system bandwidth, F is the excess noise factor of APD, and M is the multiplica-

tive ratio or gain of APD. Consequently, n can be formulated as

$$n = n_{sd} + \underbrace{\sqrt{\gamma I_a} \cdot n_a + \sigma_t \cdot n_t}_{n_{si}} \quad (4)$$

On the other hand, in the perspective of detection, the noise may be repartitioned as a signal dependent part $n_{sd} \sim N(0, \sigma_{sd})$ and a signal independent part $n_{si} \sim N(0, \sigma_{si})$. n_{si} comprises n_a and n_t , the independent Gaussian random variables for the ambient light (assumed isotropic) induced shot noise and thermal noise, respectively. The variances are the corresponding weighted factors in (4), where I_a is the photocurrent induced by ambient light and σ_t^2 is the variance of thermal noise.

Known from (3) and (2), the variance of signal dependent noise n_{sd} is proportional to transmit signal x :

$$\sigma_{sd}^2 = \gamma \cdot \underbrace{h \cdot x}_{I_{sd}} \quad (5)$$

where $h \cdot x$ is actually the photocurrent I_{sd} induced by incident signal light x .

Applying (5) and (1), we obtain the averaged variance of signal dependent noise:

$$\bar{\sigma}_{sd}^2 = E_s(\sigma_{sd}^2) = h\gamma\beta I_b \quad (6)$$

Clearly, the averaged variance of signal dependent noise is irrelevant to instantaneous data signal value x .

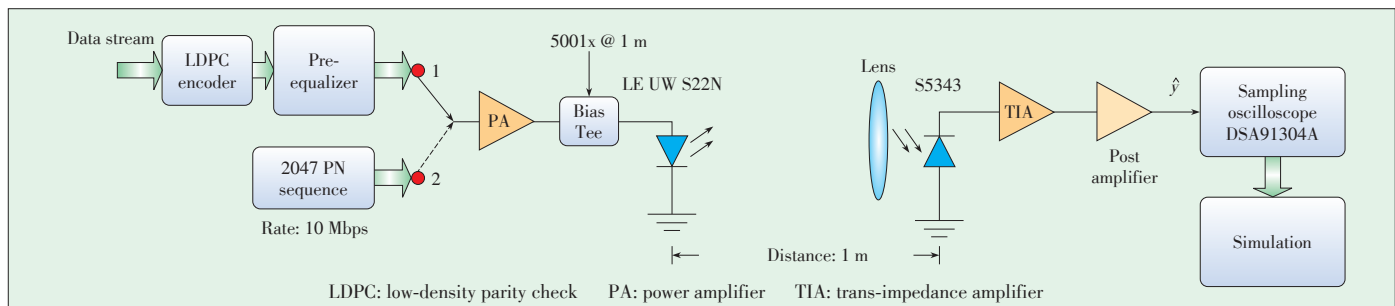
For convenience, we define a parameter f to indicate the ratio of the averaged variance of signal dependent noise to the variance of signal independent noise:

$$f \triangleq \frac{\bar{\sigma}_{sd}^2}{\sigma_{si}^2} \quad (7)$$

In this way, given the averaged variance of received noise $\sigma_n^2 = \bar{\sigma}_{sd}^2 + \sigma_{si}^2$, we could easily evaluate the instantaneous noise variance $\sigma_r^2 = \kappa_r \sigma_n^2, r = 0, 1$ at different constellation points:

$$\begin{cases} \kappa_0 = 1 + \frac{fm}{1+f}, & s = +1; \\ \kappa_1 = 1 - \frac{fm}{1+f}, & s = -1, \end{cases} \quad (8)$$

Usually, the modulation depth m should be close to 1 in a



▲ **Figure 1.** VLC system with OOK modulation. Switch to 1 for general transmission with LDPC channel coding; switch to 2 for SDGN VLC channel model verification.

power efficient VLC system. When the channel is thermal noise dominated, e.g., $f \rightarrow 0$, $\kappa_0 \approx \kappa_1$, we define it as signal independent Gaussian noise (SIGN) channel. On the other hand, when shot noise is strong enough, e.g., $f \gg 0$, $\kappa_0 > \kappa_1$, we define it as signal dependent Gaussian noise (SDGN) channel. Our experiment shows that, in the absence of ambient light, at 500 lux luminance, $f \approx 2.7$; and at 1000 lux luminance, $f \approx 3$. These results indicate that, different from widely adopted SIGN channel model, the VLC channel is actually a SDGN channel. Therefore, the following signal detection and channel decoding algorithm should fully consider the impact of SDGN.

3 Analysis of Detection and Decoding

Optimal and sub-optimal detection strategies are used to calculate the LLR.

The optimal one takes the shot noise into account and is formulated as:

$$\Lambda_{opt} = \frac{1}{2} \log \frac{\kappa_1}{\kappa_0} + \frac{1}{2\sigma_n^2} \left[\frac{(y + h\beta A_s)^2}{\kappa_1} - \frac{(y - h\beta A_s)^2}{\kappa_0} \right] \quad (9)$$

where y is the alternating part of received signal \hat{y} .

The sub-optimal one is to ignore the shot noise and treat the SDGN channel as the conventional SIGN channel. The corresponding LLR is expressed as:

$$\Lambda_{sub} = \log \frac{\frac{1}{\sqrt{2\pi}\sigma_n} \exp\left(-\frac{(y - h\beta A_s)^2}{2\sigma_n^2}\right)}{\frac{1}{\sqrt{2\pi}\sigma_n} \exp\left(-\frac{(y + h\beta A_s)^2}{2\sigma_n^2}\right)} = \frac{2h\beta A_s y}{\sigma_n^2} \quad (10)$$

In conventional SIGN scenarios, the implementation of a LDPC decoder usually uses the MS algorithm, which only requires $\Lambda' = \Lambda \cdot \sigma^2 = 2y$ since only the compare procedure exists in the iterative decoding process.

Similarly, we wish to have an approximated expression Λ'_{opt} without the parameter of σ_n for the MS decoding:

$$\Lambda_{opt} \cdot 2\sigma_n^2 = \frac{1}{2} \log \frac{\kappa_1}{\kappa_0} \cdot 2\sigma_n^2 + \Lambda'_{opt} \quad (11)$$

The first term in (11), $\log \frac{\kappa_1}{\kappa_0} \cdot \sigma_n^2$, is actually ignored based on the following two factors. First, the absolute value of Λ'_{opt} is no less than 10 when the signal to noise ratio (SNR), defined in (13), is greater than 0 dB. Second, in a reasonable range of f and m , $\log \frac{\kappa_1}{\kappa_0}$ is less than 10. Therefore, comparing to

Λ'_{opt} , $\sigma_n^2 \log \frac{\kappa_1}{\kappa_0}$ is small enough to be ignored. The approxima-

ted detection is expressed as:

$$\Lambda'_{opt} = \frac{(y + h\beta A_s)^2}{\kappa_1} - \frac{(y - h\beta A_s)^2}{\kappa_0} \quad (12)$$

Besides, the correction factor α proposed in [16], [17] (usually set to 0.8 for code rate $R=0.5$) should be considered for improving decoding performance.

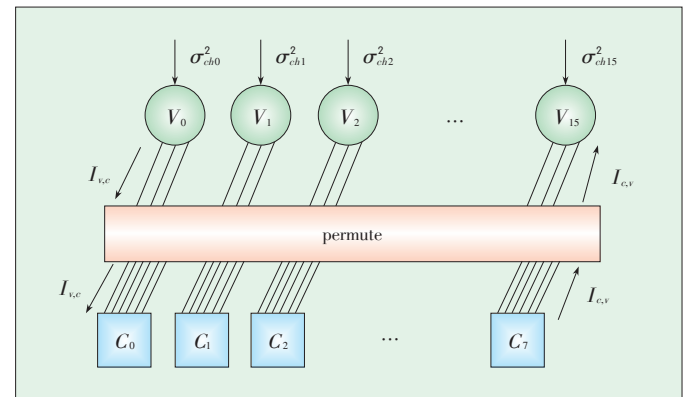
Protograph Extrinsic Information Transfer Chart (PEXIT) is a tool commonly used to evaluate the performance of a coding system. Here, PEXIT analysis [18] is used to investigate the impacts of shot noise on the performance of LDPC coded VLC systems. This method is utilized for accurate performance analysis in various scenarios such as fading channels [19] and half-duplex relay channels [20]. The calculation procedure in **Fig. 2** is similar to that in [18], except the initialization step. In this way, the convergence behavior of the LDPC decoding with different detection schemes can be evaluated by the fast numerical computation without extensive BER simulations. A lower threshold indicates that a better decoding performance can be achieved. Obviously, the gap between the decoding thresholds η_{opt} and η_{sub} varies depending on the parameters of SDGN channel.

4 Experimental and Numerical Results

In this section, we experimentally verify our proposed VLC SDGN channel model. Then, the BER performance of the SDGN channel is compared with that designed for the SIGN channel. The SDGN channel parameters, the modulation depth m and the power ratio f , are investigated from the perspective of decoding threshold with EXIT charts. The performance of the proposed modified MS algorithm is also evaluated.

4.1 The Experiment

To simulate the illuminance in the office, we adjust the bias current to keep the luminance at the receiver around 500 lux. Then a pilot sequence with length of 2047 at 10 Mbps symbol rate, which is much less than the channel bandwidth, is sent to estimate the shot noise variances at different OOK constella-



▲ Figure 2. PEXIT calculation procedure.

LDPC Decoding for Signal Dependent Visible Light Communication Channels

YUAN Ming, SHA Xiaoshi, LIANG Xiao, JIANG Ming, WANG Jiaheng, and ZHAO Chunming

tions. After a proper amplification, the received signals are sampled at the rate of 200 Mbps with Agilent T&M DSA91304A. The detailed verification setup is shown in Fig. 1 and the physical platform is in Fig. 3.

Fig. 4 shows the sampled alternating current (AC) waveform of received pilot sequences. According to the previous OOK mapping rules, symbol 0 is mapped to constellation $s = +1$, representing LED on state, and symbol 1 is mapped to constellation $s = -1$, representing LED off state. Known from (8), the induced shot noise for symbol 0 is larger than symbol 1. It is obvious that the amplitude fluctuations at $s = +1$ are much larger than those at $s = -1$, which is consistent with the SDGN channel model.

In Fig. 5, the corresponding conditional PDF of symbol 0 and symbol 1 are plotted, respectively. We also give the corresponding hard decision thresholds for the SIGN channel and SDGN channel. The well-known hard decision threshold for SIGN channel is 0. While the expression of hard decision threshold for SDGN channel is generally complicated, which depends on lots of parameters and can be evaluated with the

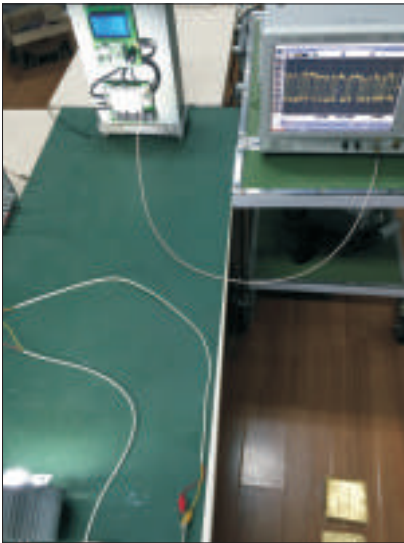


Figure 3. Platform for SDGN VLC channel model verification.

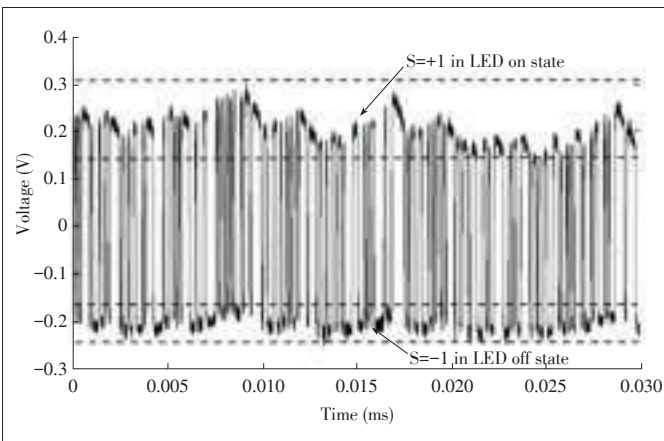


Figure 4. AC part of amplified received signals.

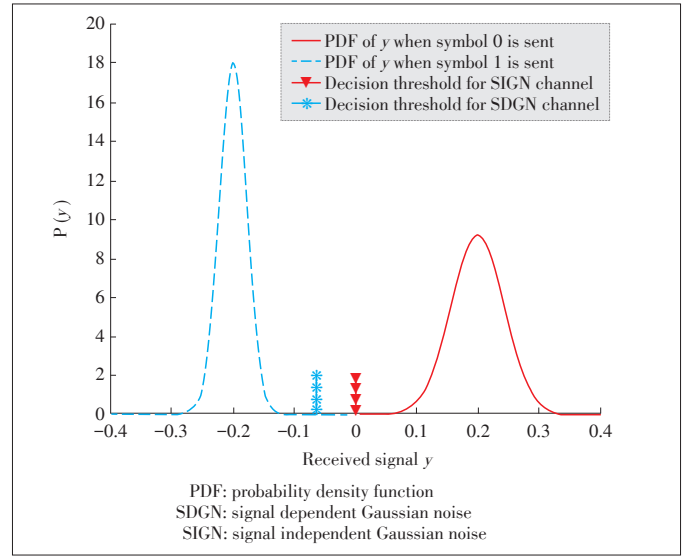


Figure 5. The corresponding conditional PDF of symbol 0 and symbol 1 over the SDGN channel.

MAP rule [21] if all the parameters have been known at the receiver.

Based on our evaluation, the power ratio $f \approx 1.4$ in our experimental system is under 500 lux luminance in presence of ambient lights, smaller than that in absence of ambient lights. These results will be applied in our next numerical decoding simulation for performance evaluations.

4.2 LDPC Decoding Performance Evaluations

Before starting our simulation, we would like to define SNR as:

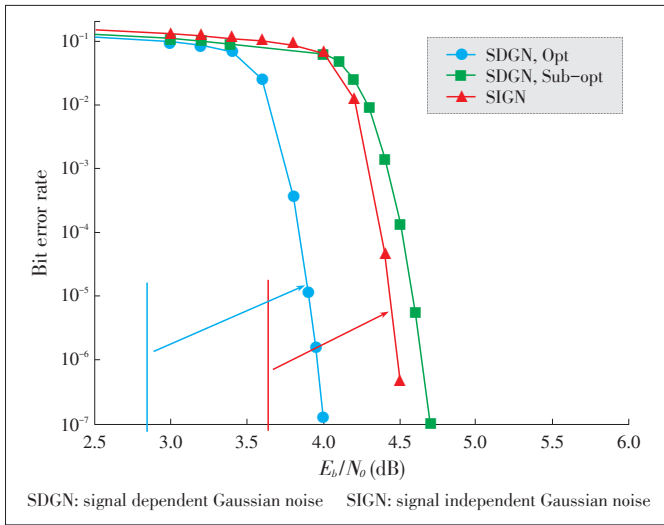
$$\frac{E_b}{N_0} = \frac{(\mu_0 + I_b)^2 + (\mu_1 + I_b)^2}{2R(\sigma_0^2 + \sigma_1^2)}, \quad (13)$$

where R is the LDPC code rate. This definition can be applied to both SDGN and SIGN channels. A regular (3, 6) LDPC code of block length 20 k is used in the decoding simulation. The maximum number of iterations for both the BP and MS algorithms is set to 100.

Fig. 6 shows the BER results of BP decoding using different detection schemes. The parameters m and f for SDGN channel are set to be 1 and 1.4 according to the previous measurements. The simulation results indicate that the iterative decoding with optimal detection for the SDGN channel achieves the best performance. The gain results from two factors. First, due to the shot noise, half of symbols are contaminated by noises with larger power, and the remaining symbols are with lower noise power. With the iterative channel decoding, these symbols help eliminate the errors by symbols with higher noise power. Second, the optimal detection scheme obtains the accurate LLR for the SDGN channel. Therefore, the shot noise component should be properly considered on the SDGN VLC chan-

LDPC Decoding for Signal Dependent Visible Light Communication Channels

YUAN Ming, SHA Xiaoshi, LIANG Xiao, JIANG Ming, WANG Jiaheng, and ZHAO Chunming

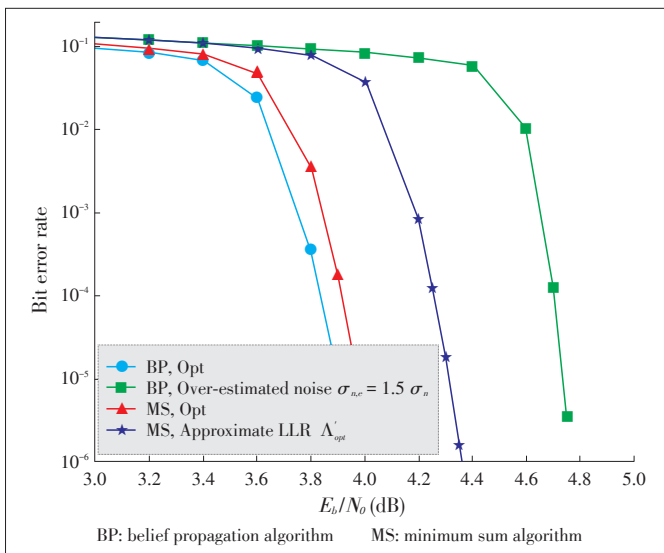


▲ Figure 6. Simulation results with SDGN channel and SIGN channel, where $m = 1$; $f = 1:4$.

nel.

The two vertical lines in Fig. 6 represent the numerical decoding thresholds with optimal and sub-optimal detection schemes on the SDGN channel, respectively. As mentioned before, the PEXIT chart is used to evaluate the performance alongside the decoding simulation. Clearly, the BER performances are quite consistent with the corresponding thresholds, indicating that the numerical thresholds calculated by PEXIT charts can reliably predict the decoding performance with different detection schemes.

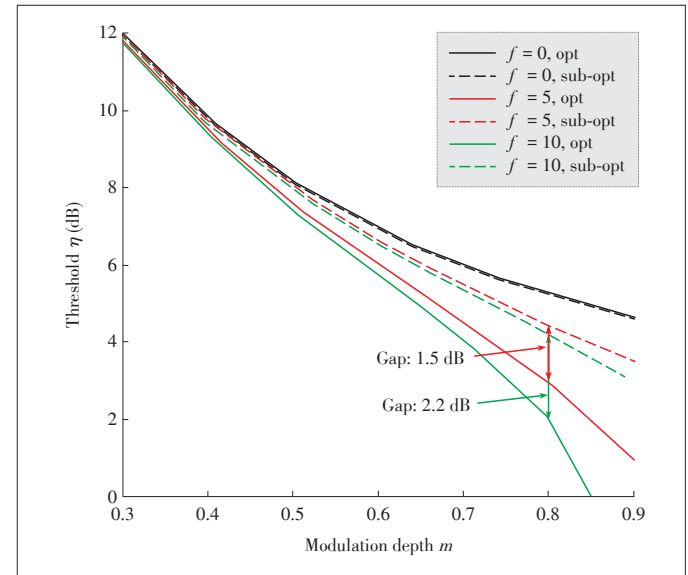
The MS algorithm has a little poorer performance than the BP algorithm (Fig. 7). Decoding with the approximated LLR from (12), the gap will be widened to about 0.4 dB. However, decoding performance with optimal detection is sensitive to the



▲ Figure 7. BP and MS decoding simulation results with SDGN channel, where $m = 1$; $f = 1:4$.

error of σ_n . The performance of the BP algorithm with an over-estimated $\sigma_{n,e} = 1.5\sigma_n$ is obviously worse than the MS algorithm using approximation LLR without the need of estimating σ_n . It is worthwhile to reduce the detection and decoding complexity and increase the robustness by sacrificing some performance.

Fig. 8 shows the effects of changing the noise power ratio f and the modulation depth m from the perspective of decoding thresholds. The decoding threshold decreases when the



▲ Figure 8. The decoding threshold of optimal and sub-optimal detection on the SDGN channel, where different channel parameters are specified.

channel parameter m or f increases. The difference between the thresholds is small at rather low modulation depth since the amplitudes of bit 0 and bit 1 tend to be equal when m goes to zero. In a specific VLC system, the modulation depth m is usually predetermined and fixed, in which case a large noise power ratio f contributes to better performance for the optimal detection scheme. This means higher performance gain can be achieved by the optimized detection scheme with lower thermal and background noise level at the APD receiver.

5 Conclusions

In this paper, we investigate the shot noise of VLC systems employing APD. A general signal dependent Gaussian noise channel is discussed. We present the accurate and approximated LLR evaluation on the SDGN channel for the decoding of LDPC code, respectively. The numerical results demonstrate that our proposed scheme achieves better performance than traditional schemes designed for the SIGN channel. 0.7 dB gain is achieved at the BER of 10^{-6} when the modulation depth equals 1 and the noise power ratio equals 1.4. The proposed system performance could be further improved by increasing

LDPC Decoding for Signal Dependent Visible Light Communication Channels

YUAN Ming, SHA Xiaoshi, LIANG Xiao, JIANG Ming, WANG Jiaheng, and ZHAO Chunming

the modulation depth of power amplifier circuit and decreasing the thermal noise in the TIA circuit.

References

- [1] G. Cossu, A. M. Khalid, P. Choudhury, R. Corsini, and E. Ciaramella, "3.4 Gbit/s visible optical wireless transmission based on RGB LED," *Optics Express*, vol. 20, no. 26, pp. B501–B506, 2012. doi: 10.1364/OE.20.00B501.
- [2] A. Khalid, G. Cossu, R. Corsini, P. Choudhury, and E. Ciaramella, "1-Gb/s transmission over a phosphorescent white LED by using rate-Adaptive discrete multi-tone modulation," *IEEE Photonics Journal*, vol. 4, no. 5, pp. 1465–1473, 2012. doi: 10.1109/JPHOT.2012.2210397.
- [3] J. Vücić, C. Kottke, S. Nerreter, K.-D. Langer, and J. W. Walewski, "513 Mbit/s visible light communications link based on DMT-modulation of a white LED," *Journal of Lightwave Technology*, vol. 28, no. 24, pp. 3512–3518, 2010. doi: 10.1109/JLT.2010.2089602.
- [4] S. Morris and H. S. Shin, "Optimal communication," *Journal of the European Economic Association*, vol. 5, no. 2–3, pp. 594–602, 2007. doi: 10.1162/jeea.2007.5.2-3.594.
- [5] R. Öktem, K. Egiazarian, V. V. Lukin, N. N. Ponomarenko, and O. V. Tsymbal, "Locally adaptive DCT filtering for signal-dependent noise removal," *EURASIP Journal on Advances in Signal Processing*, vol. 2007, no. 1, p. 042472, 2007. doi: 10.1155/2007/42472.
- [6] K. Hirakawa and T. W. Parks, "Image denoising for signal-dependent noise," in *Proc. IEEE International Conference on Acoustics, Speech, and Signal Processing*, Philadelphia, USA, 2005, pp. 29–32. doi: 10.1109/ICASSP.2005.1415333.
- [7] H. Arsenault, C. Gendron, and M. Denis, "Transformation of film-grain noise into signal-independent additive Gaussian noise," *Journal of the Optical Society of America*, vol. 71, no. 1, pp. 91–94, 1981. doi:10.1364/JOSA.71.000091.
- [8] G. K. Froehlich, J. F. Walkup, and R. B. Asher, "Optimal estimation in signal-dependent noise," *Journal of the Optical Society of America*, vol. 68, no. 12, pp. 1665–1672, 1978. doi:10.1364/JOSA.68.001665.
- [9] S. M. Moser, "Capacity results of an optical intensity channel with input-dependent Gaussian noise," *IEEE Transactions on Information Theory*, vol. 58, no. 1, pp. 207–223, 2012. doi:10.1109/TIT.2011.2169541.
- [10] T. J. Richardson and R. L. Urbanke, "The capacity of low-density parity-check codes under message-passing decoding," *IEEE Transactions on Information Theory*, vol. 47, no. 2, pp. 599–618, 2001. doi:10.1109/18.910577.
- [11] M. N. Khan and W. G. Cowley, "Signal dependent Gaussian noise model for FSO communications," in *Proc. IEEE AusCTW.*, Melbourne, Australia, 2011, pp. 142–147. doi:10.1109/AUSCTW.2011.5728752.
- [12] M. N. Khan, "Importance of noise models in FSO communications," *EURASIP Journal on Wireless Communications and Networking*, vol. 2014, no. 1, pp. 1–10, 2014. doi:10.1186/1687-1499-2014-102.
- [13] S. ten Brink, G. Kramer, and A. Ashikhmin, "Design of low-density parity-check codes for modulation and detection," *IEEE Transactions on Communications*, vol. 52, no. 4, pp. 670–678, 2004. doi:10.1109/TCOMM.2004.826370.
- [14] L. Zeng, D. O'Brien, H. Le-Minh, K. Lee, D. Jung, and Y. Oh, "Improvement of data rate by using equalization in an indoor visible light communication system," in *Proc. IEEE ICCSC*, Shanghai, China, May 2008, pp. 678–682. doi: 10.1109/ICCSC.2008.149.
- [15] J. Kahn and J. Barry, "Wireless infrared communications," *Proc. IEEE*, vol. 85, no. 2, pp. 265–298, 1997. doi:10.1007/978-1-4615-2700-8.
- [16] J. Chen and M. Fossorier, "Near optimum universal belief propagation based decoding of low-density parity check codes," *IEEE Transactions on Communications*, vol. 50, no. 3, pp. 406–414, 2002. doi:10.1109/26.990903.
- [17] J. Heo and K. Chugg, "Optimization of scaling soft information in iterative decoding via density evolution methods," *IEEE Transactions on Communications*, vol. 53, no. 6, pp. 957–961, 2005. doi:10.1109/TCOMM.2005.849782.
- [18] G. Liva and M. Chiani, "Protograph LDPC codes design based on EXIT analysis," in *Proc. IEEE GLOBECOM.*, Washington, USA, 2007, pp. 3250–3254. doi:10.1109/GLOCOM.2007.616.
- [19] T. V. Nguyen, A. Nosratinia, and D. Divsalar, "Threshold of protograph-based LDPC coded BICM for rayleigh fading," in *Proc. IEEE GLOBECOM.*, Houston, USA, 2011, pp. 1–5. doi:10.1109/GLOCOM.2011.6133952.
- [20] T. V. Nguyen, A. Nosratinia, and D. Divsalar, "Bilayer protograph codes for half-duplex relay channels," *IEEE Transactions on Wireless Communications*, vol. 12, no. 5, pp. 1969–1977, 2013. doi:10.1109/TWC.2013.040413.111745.
- [21] H. L. Van Trees, *Detection, estimation, and modulation theory*. Hoboken, USA: John Wiley & Sons, 2004. doi:10.1002/0471221082.

Manuscript received: 2015-11-17

Biographies

YUAN Ming (yuanming@seu.edu.cn) received his BE degree in electrical engineering from Southeast University, China in 2013. He is currently working toward an MS degree at the School of Information Science and Engineering, National Mobile Communications Research Laboratory (NCRL), Southeast University. His research interests include signal processing and visible light communications.

SHA Xiaoshi (xiaoshisha@seu.edu.cn) received his BSc degree in information science from Southeast University in 2014 and is currently working toward an MS degree at NCRL, Southeast University. His research interests include channel coding and high throughput LDPC encoder and decoder implementation.

LIANG Xiao (xiaoliang@seu.edu.cn) received his BSc, MS, and PhD degrees in communication and information engineering in 2000, 2005, and 2013, respectively, all from Southeast University. He is a lecturer with NCRL, Southeast University. His research interest is signal processing for communications and wireless network-ing.

JIANG Ming (jiang_ming@seu.edu.cn) received his BSc, MS, and PhD degrees in communication and information engineering in 1998, 2003, and 2007, respectively, all from Southeast University. He is an associate professor with NCRL, Southeast University. His research interest is channel coding for wireless communications.

WANG Jiaheng (jhwang@seu.edu.cn) received his BE and MS degrees from Southeast University in 2001 and 2006, respectively, and the PhD degree in electrical engineering from the Hong Kong University of Science and Technology, China in 2010. He is an associate professor with NCRL, Southeast University. From 2010 to 2011, he was with the Signal Processing Laboratory, ACCESS Linnaeus Center, KTH Royal Institute of Technology, Stockholm, Sweden. He also held visiting positions at the Friedrich-Alexander University Erlangen-Nürnberg, Nürnberg, Germany, and the University of Macau, China. His research interests mainly include optimization in signal processing, communication systems, and wireless networks. Dr. Wang serves as an associate editor for *IEEE Signal Processing Letters*. He is a recipient of the Humboldt Fellowship for Experienced Researchers, and a recipient of the Best Paper Award in WCSP 2014.

ZHAO Chunming (cmzhao@seu.edu.cn) received his BS and MS degrees from Nanjing Institute of Posts and Telecommunications, China in 1982 and 1984, respectively. In 1993, he received the PhD degree from the Department of Electrical and Electronic Engineering, University of Kaiserslautern, Germany. He is a professor and vice director at NCRL, Southeast University. He has managed several key projects of Chinese Communications High Tech. Program. His research interests include communication theory, coding/decoding, mobile communications, and VLSI design. Dr. Zhao won the First Prize of National Technique Invention of China in 2011. He was awarded "Excellent Researcher" from the Ministry of Science and Technology, China.

A Survey on Event Mining for ICT Network Infrastructure Management

LIU Zheng, LI Tao, and WANG Junchang

(Nanjing University of Posts and Telecommunications, Nanjing 210023, China)

1 Introduction

Nowadays in China, there are more than six hundred million netizens [1]. On April 11, 2015, the number of simultaneous online users of the Chinese instant message application QQ reached two hundred million [2]. The fast growth of the Internet pushes the rapid development of information technology (IT) and communication technology (CT). Many traditional IT service and CT equipment providers are facing the fusion of IT and CT in the age of digital transformation, and heading toward ICT enterprises. Large global ICT enterprises, such as Apple, Google, Microsoft, Amazon, Verizon, and AT&T, have been contributing to the performance improvement of IT service and CT equipment.

As a result, the performance of IT service and CT equipment has become increasing powerful. The speed of the world's top high-performance computing system, Chinese Tianhe-2 supercomputer, is 33.86 petaflop [3]. The data I/O of a modern Internet backbone router is more than tens of terabytes per seconds, while its routing table usually consists of millions of routes. The scale of modern networks becomes larger and larger. A global information grid [4] built by the US military is capable of collecting, processing, storing, disseminating and managing information from more than two million nodes.

These large-scale, high-performance ICT networks are supported by ICT network infrastructures. ICT network infrastructure refers to the combination of all computing and network hardware components, as well as software resources of an ICT network. Computing hardware components include computing servers, storage systems, etc. Network hardware components include routers, switches, LAN cards, etc. Software resources in-

Abstract

Managing large-scale complex network infrastructures is challenging due to the huge number of heterogeneous network elements. The goal of this survey is to provide an overview of event mining techniques applied in the network management domain. Event mining includes a series of techniques for automatically and effectively discovering valuable knowledge from historical event/log data. We present three research challenges (i.e., event generation, root cause analysis, and failure prediction) for event mining in network management and introduce the corresponding solutions. Event generation (i.e., converting messages in log files into structured events) is the first step in many event mining applications. Automatic root cause analysis can locate the faulty elements/components without the help of experienced domain experts. Failure prediction in proactive fault management improves network reliability. The representative studies to address the three aforementioned challenges are reviewed and their main ideas are summarized in the survey. In addition, our survey shows that using event mining techniques can improve the network management efficiency and reduce the management cost.

Keywords

event mining; failure prediction; log analysis; network infrastructure management; root cause analysis

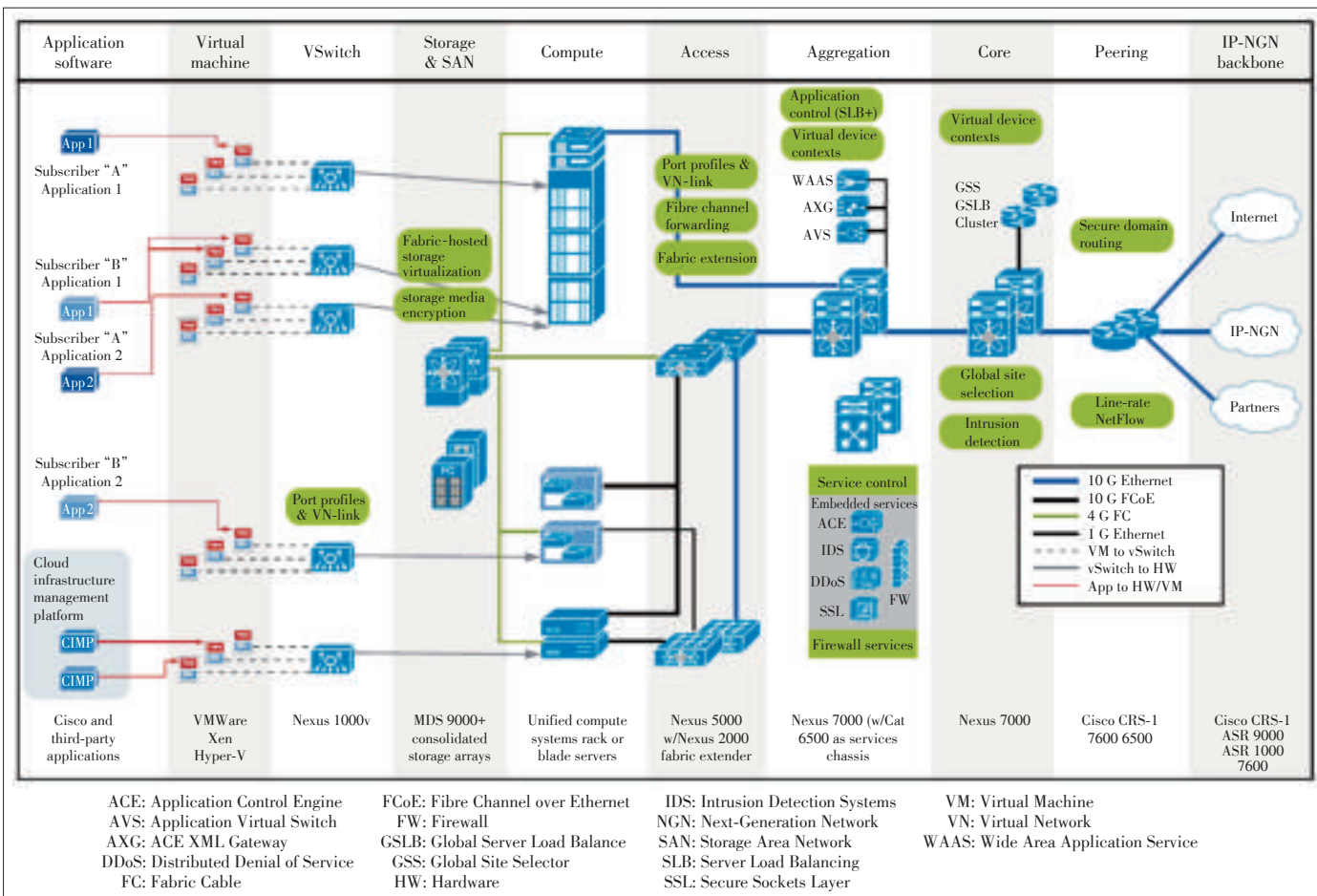
clude virtual machine platforms, operating systems, security applications, network operation and management platforms, etc. These resources facilitate the communications and services between users and service providers.

The network infrastructure of a large ICT enterprise, e.g., a world-wide online shopping company like Amazon, usually has several world-wide data centers. Each data center has tens of thousands of servers, switches, routers, firewalls, as well as other affiliated systems like power supply systems or cooling systems. A typical architecture of data centers is shown in **Fig. 1** [5]. The ICT network infrastructure for Carriers is even more complex. For example, besides data centers, there are nationwide communication networks in a 3G/4G network infrastructure (**Fig. 2**) [6]. Each communication network includes access network equipment, core network equipment, transport network equipment, and other application systems, containing tens of thousands of network elements that provide authentication, billing, data/voice communications, and multimedia services. These large-scale complex networks introduce many difficulties in designing, architecting, operating, and maintaining the corresponding network infrastructures, on which multiple

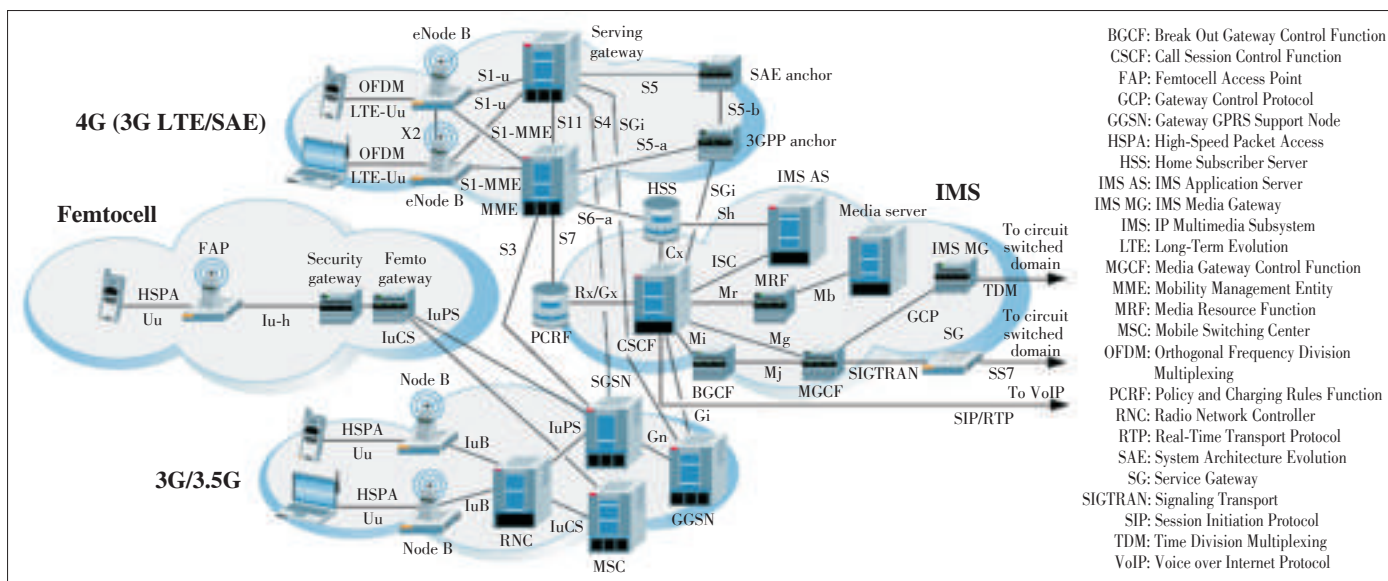
This work was supported in part by Ministry of Education / China Mobile joint research grant under Project No. 5-10, and Nanjing University of Posts and Telecommunications under Grants No. NY214135 and NY215045.

A Survey on Event Mining for ICT Network Infrastructure Management

LIU Zheng, LI Tao, and WANG Junchang



▲ Figure 1. The typical architecture of a data center [5].



▲ Figure 2. An example of 3G/4G network infrastructure [6].

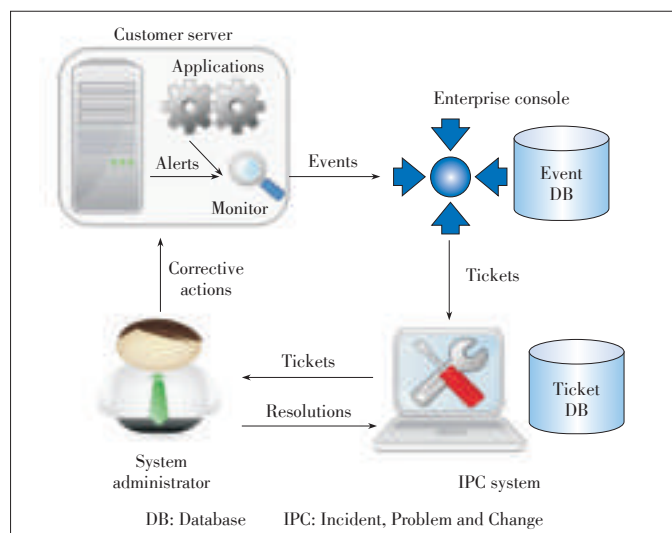
complex systems are coordinated to ensure that the computation and communication functions work smoothly. Cloud tech-

nology is widely used in modern ICT network infrastructures due to the development of virtualization technology and its low

cost. But cloud technology also brings hierarchy and heterogeneity to network infrastructures. During the operation and maintenance of network infrastructures, equipment failure, communication error and system misconfiguration have high impact on the reliability of the whole network [7]–[9], as a result of unstable upper-level service and business. Traditionally, system administrators resolve the aforementioned incidents according to the workflow consisting of detection, localization and repair, by using network tools such as ping, traceroute, and tcpdump, or network monitor toolkits such as Nagios [10], Zabbix [11], and OpsView [12]. This process has been well-known and experienced as a labor-intensive and error-prone process and may not be effective when the systems/networks become large and complex.

Fortunately, several industry organizations have already paid attention to these issues and put lots of efforts on making specifications related to best practices in operating and maintaining large-scale complex systems/networks. In the IT service area, Information Technology Infrastructure Library (ITIL) [13] is a collection of specifications for service management, with which the best practices are organized according to the full life cycle of IT services including incident management, failure management, problem management, configuration management, and knowledge management. In the carrier service area, international organizations, such as ITU-T [14] and TM Forum [15], also make recommended specifications for managing telecommunication network infrastructures, partial ideas of which are borrowed from ITIL.

Fig. 3 shows a general workflow of problem detection, determination and resolution for IT service providers prescribed by the ITIL specifications [16]. The workflow aims at resolving incidents and quickly restoring the provision of services while relying on monitoring or human intervention to detect the malfunction of a component [16]. For problem detection, there is



▲ **Figure 3.** A general workflow of problem detection, determination and resolution [16].

usually monitoring software running on servers or network elements, which continuously monitors the status of network elements and detects possible problems by computing metrics for the hardware and software performance at regular intervals. The monitoring software would issue an alert if those metrics are not acceptable according to predefined thresholds, known as monitoring situations, and emits an event if the alert does not disappear after a period. All events coming from the network infrastructure are consolidated in an enterprise console, where these events are analyzed and corresponding incident tickets are created, if necessary, in an Incident, Problem, and Change (IPC) system. System administrators are responsible for the problem determination and resolution based on the detailed information in these tickets. The efficiency of these resources is critical for the provisioning of the services [17].

However, the best practices in those specifications only provide the guidance on operating and maintaining network infrastructure, which is a standard workflow of consecutive procedures and definitions. Many key issues in these procedures are not answered in these specifications, especially in large-scale complex networks. The challenges in managing large-scale network infrastructures are listed as follows:

- 1) Large complex network infrastructures are heterogeneous and often consist of various network elements made by different equipment makers. There are different software components running on the various network elements and generating huge amount of messages and alerts in different types and formats. The heterogeneity complicates the management work [18], [19] and understanding these messages and alerts is not an easy task. In a small network, system administrators can analyze the messages and alerts one by one, and understand their corresponding event types. Apparently, it is not practical in large complex networks. Automatic event generation is important for reducing the maintenance cost with limited human resources.
- 2) The diagnosis and resolution depend on experienced system administrators who analyze performance metrics, alert logs, event information and other network characteristics. Unexpected behaviors are usually discovered in daily operation of large complex networks. Malfunction of certain network elements can cause alerts in both upper-level business applications and other connected network elements. The scale and complexity of root cause analysis [20] in such networks are often beyond the ability of human operators. Therefore, automatic root cause analysis is necessary in managing large complex network infrastructures.
- 3) Root cause analysis is to identify the actual network element that causes an alert, while failure prediction tries to avoid the situation where the expected services cannot be delivered [21], [22]. Proactive fault management can enhance the network reliability, which is usually done by system administrators based on predefined business rules. With failure prediction, proactive fault management can be more efficient.

Failure prediction based on historical incident tickets and server attributes plays an important role in managing large complex network infrastructures.

Mining valuable knowledge from events and tickets can efficiently improve the performance of system diagnosis. In this survey, we focus on recent research studies dealing with the above three challenges. The reminder of this survey is organized as follows. Section 2 reviews the event generation approaches. Root cause analysis and failure prediction are investigated in Section 3 and Section 4, respectively. Finally, Section 5 concludes the survey.

2 Event Generation

The monitoring software on network elements in large complex networks generates huge amount of alerts, alarms, and messages, indicating the equipment status at real time. These alerts, alarms, messages are usually collected in log files. Contents of the data in log files may include time, element name, the running states of software components (e.g., started, interrupted, connected, and stopped), and other performance parameter values. In this section, we mainly focus on the methodologies of event generation from log files.

The contents of log files in some systems are unstructured, that is, each event is stored as a short message in plain text files, such as server logs, Linux logs and Hadoop logs. In other systems, the logs may be semi-structured or structured, e.g., Window event logs, database management system logs. Such logs are often stored in a database. Each record in the database represents an event, often including time, server name, process name, error code and other related information. A lot of data mining algorithms are based on structured or semi-structured data, while unstructured textual logs cannot be handled by these algorithms. Event generation is to convert textual logs into structured events for later analysis.

A simple log example is shown in **Table 1** [23], in which messages from a Simple File Transfer Protocol (SFTP) log are collected from a FTP software called FileZilla. Each line in Table 1 is a short message describing a certain event. In order to analyze the behaviors of FTP visits, these raw log messages need to be translated into types of events. The generated events are usually organized by timeline so that people can understand the behaviors and discover event patterns [24]. In Table 1, Message 4 is the event of uploading a webpage to the FTP server, and Message 9 is an error alert that the operation of creating a new directory is not successful. By converting raw log messages into canonical events, these events are able to be correlated across logs from different elements.

It seems that obtaining events from the log files is not a difficult task. However, due to the heterogeneity of network infrastructures, each network element generates raw messages with its own format and contents. These messages may be disparate and inconsistent, which creates difficulty in deciphering

▼ **Table 1.** An example of messages in a simple file transfer protocol log [23]

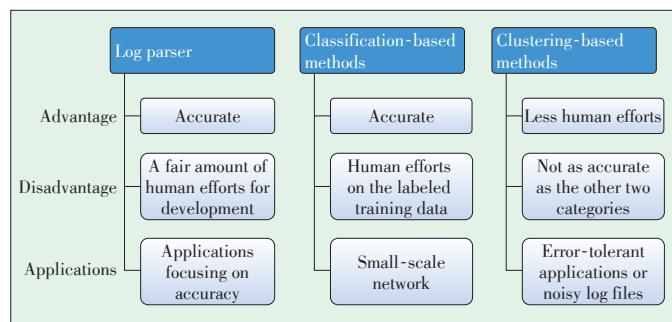
ID	Logs
1	2010-05-02 00:21:41 Command: cd "/disk/storage006/users/lt...
2	2010-05-02 00:21:42 Command: cd "/disk/storage006/users/lt...
3	2010-05-02 00:21:42 Command: put "E:/Tomcat/apps/record1.html" "/disk/...
4	2010-05-02 00:21:42 Status: Listing directory /disk/storage006/users/lt...
5	2010-05-02 00:21:42 Status: File transfer successful, transferred 1,232 bytes...
6	2010-05-02 00:21:42 Command: put "E:/Tomcat/apps/record2.html" "/disk/...
7	2010-05-02 00:21:42 Response: New directory is: "/disk/storage006/users/lt...
8	2010-05-02 00:21:42 Command: mkdir "libraries"
9	2010-05-02 00:21:42 Error: Directory /disk/storage006/users/lt...
10	2010-05-02 00:21:44 Status: Retrieving directory listing...
...	...

events reported by multiple network elements [24]. For example, it is supposed that we need to perform the following task: if any element stops, the system administrator is notified by email. Given the variability among different network elements, one element might record “The server has stopped” in the log file, while another one might record “The server has changed the state from running to stop.” The inconsistency in log files makes the above task difficult. All the messages indicating the stop status from all network elements must be collected, in order to write a program to automate this simple task. This is less possible in large complex networks with newly added network elements and many legacy network elements.

When one needs to analyze the historical event data across multiple elements, it is necessary to encode semantics in a system-independent manner. All raw log messages in log files should be consistent in semantics across similar fields, which allows the organization of common semantic events into categories. The converted canonical events provide the ability of describing the semantics of log data as well as the initial connection of syntax to semantics [24]. The research studies on event generation can be classified into three categories: log parser, classification, and clustering. The main characteristics of approaches in each category are summarized in **Fig 4**.

2.1 Log Parser

A straightforward solution is the log-parser-based approach, in which a log parser is built for log files in different formats. The system administrators must be familiar with the type and format of each raw message and understand its meaning, so that they can develop text parsers to extract the detailed semantic information from these messages accurately. Some messages might be easily parsed using simple regular expression. Clearly, the approach is not efficient for large complex network infrastructures, in which there are heterogeneous network elements having different log-generating mechanisms, and disparate formats and contents. In addition, the legacy systems with-



▲ Figure 4. Main characteristics of different event generation approaches.

out reliable log generation libraries make this problem even harder.

The approaches of building log parsers based on the analysis of source code have been investigated by many researchers. Xu et al. [25], [26] proposed that the source code can be viewed as the schema of logs and the structure of raw log messages can be inferred from the schema. The event type and event format are determined based on the schema, and the variable values are extracted from source code as the attributes of events.

IBM autonomic computing toolkit allows general data collection from heterogeneous data sources and uses the Generic Log Adapter (GLA) [27] to convert raw log messages into the Common Base Event (CBE) format. Modern software packages are likely to be open sources, e.g., Hadoop and Apache Tomcat, to which the above approaches can be naturally applied. The advantage of log-parse-based approaches is that they are accurate, but on the other hand they require a fair amount of human efforts to fully understand the log formats and to develop log parser software.

2.2 Classification-Based Methods

Not all applications in network management require extracting all possible field variable values from log messages. Some of them only need to know event types of raw messages and focus on discovering the unknown relationship between different event types [24]. For example, a network firewall system only need to know its current state, that is, whether the current log message is related to a certain security issue, a particular performance status, or an unexpected program exception. Here, event generation is to determine the event types of raw messages, which is a text classification problem.

A simple classifier can be built using regular expression patterns. For each event type, there is a corresponding regular expression pattern [28]. But similar to the issue in log-parser-based approaches, using regular expression for classification requires experienced domain experts to write the expression in advance, which is inefficient in large complex network infrastructures with heterogeneous network elements.

When labeled log messages are available for training, popular classification algorithms like support vector machine

(SVMs), can be applied to solve the text classification problem. A traditional approach for handling text information is the bag-of-words model [29], which splits the log messages into words or terms and uses binary vector representation. If a term exists in the message, the corresponding feature value is 1, otherwise, it is 0. Then, the classifier is built based on the joint distribution of the terms in log messages and corresponding event types. Pitakrat et al. [30] used supervised machine learning algorithms, e.g., decision trees and probabilistic representations, to classify log messages in order to conclude about computer system states, where log files are preprocessed and manually labeled for training the classifier.

Security log classification is an important research issue in log classification and has received a lot of research attention [31]–[34]. Network anomalies include DDoS attack, worm propagation, portscan activity, flash crowd, etc. One important task in security area is to categorize the anomalies into different types. Teufl et al. [32] built a classifier for combining different log messages into known event types based on relations between events or features. They proposed the concept of “Activation Patterns” which are generated from raw log messages for intrusion detection. Androulidakis et al. [31] focused on detection and classification of network anomalies in security application logs. They used an Entropy-base method to classify anomalies, where the entropy changes in each anomaly type. Kruegel et al. [33] analyzed the false alarm problem caused by incorrect classification of log messages, and proposed an event classification schema based on Bayesian network which improves the performance of model aggregation. Modi et al. [34] also used Bayesian classifier for network intrusion detection in Cloud platform by classifying alert messages from virtual machines.

The classification-based methods are accurate, but they need the labeled log messages for training. Obtaining the labeled data requires human efforts, which is often time consuming and costly. Classification-based methods are inappropriate for large complex networks due to the lack of experienced domain experts for labeling.

2.3 Clustering-Based Methods

Labeled training data is not required for clustering-based methods, because such the methods infer event types from raw log messages. Although clustering-based methods might not be very accurate, they are acceptable in certain event mining applications. Raw log messages are usually short but have a large vocabulary size, which leads to a vector space with very sparse high dimensional features. There are some recent studies [35], [36] on applying clustering techniques to partition log messages into separated groups, each of which represents an event type. The traditional clustering algorithms based on bag-of-words model cannot perform well due to the short message and large vocabulary, so these studies on clustering-based methods focus on the structured log messages.

Makanju et al. [36] proposed a log message clustering algorithm with the following four steps: 1) partitioning by the number of tokens; 2) partitioning by the word positions; 3) partitioning by the search for bijection; 4) discovering the descriptive words for each partition. Most frequent words are treated as template words. The log messages are partitioned based on these template words' positions. This method is quite efficient with linear time complexity. However, when the frequencies of these template words are flexible among different log files, the identification of template words is challenging.

Tang and Li [23] described an algorithm-independent framework for event generation from log messages named LogTree. LogTree utilizes the format and structural information in log messages and employs message segment table for effective and efficient event generation. LogTree builds tree patterns for log messages. The root of a tree pattern is the category of the log message, usually indicated by the message type, and the leaves are the field information in messages. The similarity between two tree patterns is defined based on the number of similar nodes and edges and nodes in higher levels are more discriminative.

Tang et al. [37] proposed to convert texture logs into events by clustering message signatures. Though log messages have various types, different log messages often have common subsequences. These common subsequences are treated as the signatures of event types. The most representative signatures are extracted from log messages, and based on these signatures, all messages are then partitioned into several segments by maximizing the total number of common pairs of signatures.

Makanju et al. [38] presented an approach for visualizing event log clusters, where log messages are partitioned into different groups for visualization using Simple Log File Clustering Tool (SLCT). SLCT can produce interpretable cluster results. Frequent attribute sets are found in an Apriori manner, and then the clusters based on their frequencies are built. Vaarandi and Pihelgas [39] presented the LogCluster algorithm for clustering textual log messages. LogCluster can discovery frequent occurring message patterns, as well as outliers. Sharma and Parvat [40] proposed to use k-mean clustering algorithm to partition network alert logs generated during network attacks. The generated clusters are used for further security alert analysis.

The advantage of clustering-based methods is that they do not require lots of human efforts, but they are not as accurate as log-parser-based or classification-based approaches. So clustering-based approaches should be applied when the applications are error-tolerant or the log files are noisy.

3 Root Cause Analysis

Network infrastructures usually include systems at multiple levels and these systems consist of computer servers, routers, and other network elements. For example, the system architec-

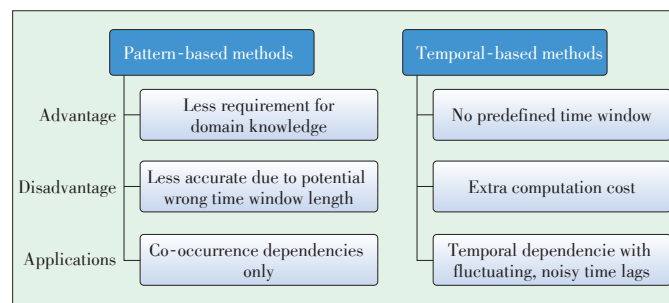
ture of an enterprise portal website may contain Web servers, application servers, database servers and storage servers. When a system error occurs at a lower-level server, it might propagate to upper-level servers and cause system errors at different levels. If a storage server stops working, the database server may report I/O errors due to inaccessible files, resulting in malfunctioning application servers and Web servers. The alert messages from the Web server might be caused by any of these lower-level servers. To find the root cause of the fault, it is not possible to check the servers one by one to verify whether there is a hardware failure or a software exception. Therefore, automatic root cause analysis is needed. Event mining is a solution to highly efficient root cause analysis and cost reduction as well.

Most root cause analysis methods are based on the dependency graph of network elements [41], [42]. Dependency graphs could be built by experts if the network architecture is simple. For large complex networks, dependency graphs are built by finding the dependencies of network elements using event mining techniques. Root cause analysis can be done by locating the deepest element with alert messages on dependency graphs. Dependency might be bi-directional in practice, in which case we need to build a Bayesian network to calculate the probability of an element's status. Then the key step in root cause analysis is to discover the dependencies between events from log messages. Some of these approaches do not consider the time lag between events while others do. The research studies along this direction are divided into two categories: pattern-based methods and temporal-based methods. **Fig. 5** shows an overview of these two categories.

3.1 Pattern-Based Methods

Lou et al. [43] proposed an approach to find the hidden dependencies between components from unstructured logs. The raw log messages are parsed into keys and parameters first. Then, the dependent log pairs are found by co-occurrence analysis. Bayesian decision theory is adopted to estimate the dependency direction for each pair. The log pairs are further filtered by removing pairs with inconsistent time lags.

Nagaraj et al. [44] described an automated tool to help system administrators diagnose and correct performance issues in modern large-scale distributed systems. The tool leverages log



▲ Figure 5. Main characteristics of two root cause analysis approaches.

data to reduce the required knowledge for administrators. Both the state and event information are extracted from log messages, and behavior patterns are discovered from the extracted states and events. During root cause analysis, the tool infers the most possible system components which might cause the performance issue using machine learning techniques.

Khan et al. [45] presented a tool for uncovering bugs in wireless sensor networks. Bugs in wireless sensor networks usually do not caused by a particular component but the unexpected interactions between multiple working components. The tool performs root cause analysis by discovering event sequences that are responsible for the faulty behavior. All log messages are divided into two categories, good and bad. Then all frequent event sequences up to a predefined length are generated. The good and bad frequent event sequences are used to perform discriminative analysis and these discriminative subsequences are used for bug analysis by matching.

3.2 Temporal-Based Methods

Zeng et al. [46] proposed to mine time lags of hidden temporal dependencies from sequential data for root cause analysis. Unlike traditional methods using a predefined time window, this method is used to find fluctuating, noisy, interleaved time lags. The randomness of time lags and the temporal dependencies between events are formalized as a parametric model. The parameters of the maximal likelihood model are inferred using an EM-based approach.

Tang et al. [47] presented a non-parametric method for finding the hidden temporal dependencies. By investigating the correlations between temporal dependency and other temporal patterns, both the pattern frequency and the time lag between events are considered in their proposed model. Two algorithms utilizing the sorted table in representing time lags are proposed to efficiently discover the appropriate lag intervals.

Yan et al. [48] described a generic root cause analysis platform for large IP networks. The Platform collects all kinds of network information including configurations, alarm logs, router logs, command logs, and performance measurements. With additional help from the spatial model of IP route, the platform supports tasks such as temporal/spatial correlation and Bayesian inference.

4 Failure Prediction

Failure prediction is a key step in proactive fault management of large complex networks. As mentioned, failure prediction tries to avoid service interrupt by applying resolution before fault happens. Most failure prediction approaches are similar in general. The main steps of failure prediction are summarized as follows:

- 1) extracting features from labeled training data based on historical failure log messages
- 2) building a prediction model using popular classifiers in ma-

chine learning techniques

- 3) monitoring continuously the current status of network elements to find whether a potential failure will happen in the near future based on classification results.

Salfner and Malek [49] presented an approach for online failure prediction in telecommunication systems using event-driven data sources. Hidden Semi-Markov Models (HSMMs) are used to model the failure event flow. The historical event sequence for failure and non-failure are collected for building two HSMMs. The failure likelihood of current event sequence is calculated using the two HSMMs.

Sipos et al. [50] presented a data-driven approach based on multiple-instance learning for failure prediction using equipment events. The log files contain both the daily operation records and the service details. Predictive features include event keywords, event codes, variations, sequence of event codes, etc. Keywords, event codes and variations are generated by parsers. Sequences of event codes are generated by applying sequential pattern mining techniques. A sparse linear classifier is trained with selected stable features for failure prediction.

Fronza et al. [51] introduced a method for predicting failures of a running system using log files. First, event sequences are extracted from log files. Supported Vector Machines (SVMs) are used to classify these event sequences into two categories: fail and non-fail. The process of extracting the event sequences is done in an incremental way. Each word in log files is assigned to a unique high dimensional index vector. When the log message is scanned, a context vector is calculated by summarizing index vectors in the sliding window.

Liang et al. [52] applied several classification methods on event logs collected from supercomputer IBM BlueGene/L and tried to predict the fatal event in the near future based on events in current window and historical observation period. There are six different types of events in the log files and for each event type. The following features are extracted from log files for training the classifiers: event number, accumulated event number, event distribution, interval between failures, and entry keywords in log messages.

Sahoo et al. [53] described a framework of a proactive prediction and control system for large clusters. Event logs and system activity reports are collected from a 350-node cluster for one year. A filtering technique is applied to remove the redundant and misaligned event data. They evaluated three different failure prediction approaches: linear time series models, rule-based classification algorithms, and Bayesian network models.

Fu and Xu [54] developed a spherical covariance model and a stochastic model to qualify the temporal correlation and the temporal correlation between events, respectively. The failure events are clustered into groups based on the correlations. Each group is represented by a failure signature which contains various attributes of computer nodes including type, I/O request, user information, system utilities, etc. Failure predic-

A Survey on Event Mining for ICT Network Infrastructure Management

LIU Zheng, LI Tao, and WANG Junchang

tion is done by predicting the future occurrences of each group.

Mohammed et al. [55] developed an approach for predicting failure and in categorical event sequences. Sequential data mining techniques are applied on the historical plan failure information for generating predictive rules. Normative, redundant, and dominated patterns are removed in order to select the most predictive rules for failure prediction.

5 Conclusions

In this paper, we present a comprehensive survey of event mining techniques applied in the domain of large-scale complex network management. Based on the general workflow of problem detection, determination and resolution, we present three challenges in modern network infrastructure management, which are related to event generation, root cause analysis, and failure prediction. For each challenge, we present the corresponding event mining techniques by reviewing the representative studies and summarizing their main ideas. In summary, mining valuable knowledge from events and logs greatly improves the reliability of large-scale complex network infrastructures.

References

- [1] China Internet Information Center, "The 36th statistical report on the Internet development in China," China, 2015.
- [2] C. Liang. (2014, Apr. 12). Tencent technology news [Online]. Available: <http://tech.qq.com/a/20140412/000129.htm>
- [3] TOP500.org. (2015, Jun.). TOP500 supercomputer sites [Online]. Available: <http://www.top500.org/lists/2015/06>
- [4] National Security Agency. (2012, Apr. 23). Global information grid—NSA/CSS [Online]. Available: https://www.nsa.gov/ia/programs/global_information_grid/index.shtml
- [5] K. Bakshi. (2009, Aug. 25). Cisco cloud computing—data center strategy, architecture [Online]. Available: http://www.cisco.com/c/dam/en_us/solutions/industries/docs/gov/CiscoCloudComputing_WP.pdf
- [6] RCR Wireless News. (2014, May 13). Diagram, LTE network architecture [Online]. Available: <http://www.rcrwireless.com/20140513/network-infrastructure/lte-network-architecture-diagram>
- [7] D. Turner, K. Levchenko, A. C. Snoeren, and S. Savage, "California fault lines: understanding the causes and impact of network failures," *ACM SIGCOMM Computer Communication Review*, vol. 40, no. 4, pp. 315–326, Oct. 2010. doi: 10.1145/1851275.1851220.
- [8] D. Ford, F. Labelle, F. Popovici, et al., "Availability in globally distributed storage systems," in *the 9th USENIX Symposium on Operating Systems Design and Implementation*, Vancouver, Canada, Oct. 2010.
- [9] P. Gill, N. Jain, and N. Nagappan, "Understanding network failures in data centers: measurement, analysis, and implications," *ACM SIGCOMM Computer Communication Review*, vol. 41, no. 4, pp. 350–361, Aug. 2011. doi: 10.1145/2043164.2018477
- [10] Nagios Enterprises, LLC. (2015). Nagios: the industry standard in IT infrastructure monitoring [Online]. Available: <http://www.nagios.org>
- [11] Zabbix LLC. (2015). Zabbix—an enterprise-class open source monitoring solution [Online]. Available: <http://www.zabbix.com>
- [12] Opsview Ltd. (2015) Opsview: IT monitoring for networks, applications, virtual servers and the cloud [Online]. Available: <http://www.opsview.com>
- [13] AXELOS. (2015). ITIL—information technology infrastructure library [Online]. Available: <https://www.axelos.com/best-practice-solutions/itil>
- [14] ITU. (2015). ITU-T Recommendations [Online]. Available: <http://www.itu.int/en/ITU-T/publications/Pages/recs.aspx>
- [15] TM Forum. (2015). Forum, framework—TM [Online]. Available: <https://www.tmforum.org/tm-forum-framework>
- [16] L. Tang, T. Li, L. Shwartz, F. Pinel, and G. Y. Grabarnik, "An integrated framework for optimizing automatic monitoring systems in large IT infrastructures," in *ACM International Conference on Knowledge Discovery and Data Mining*, San Francisco, USA, Aug. 2013, pp. 1249–1257. doi: 10.1145/2487575.2488209.
- [17] Y. Jiang, C.-S. Perng, T. Li, and R. Chang, "Intelligent cloud capacity management," in *IEEE Network Operations and Management Symposium*, Maui, USA, Apr. 2012, pp. 502–505. doi: 10.1109/NOMS.2012.6211941.
- [18] A. Y. Halevy, N. Ashish, D. Bitton, et al., "Enterprise information integration: successes, challenges and controversies," in *ACM SIGMOD International Conference on Management of Data*, Baltimore, USA, Jun. 2005, pp. 778–787. doi: 10.1145/1066157.1066246.
- [19] P. A. Bernstein and L. M. Haas, "Information integration in the enterprise," *ACM Communication*, vol. 51, no. 9, pp. 72–79, Sep. 2008. doi: 10.1145/1378727.1378745.
- [20] C. Zeng, L. Tang, T. Li, L. Shwartz, and G. Ya, "Mining temporal lag from fluctuating events for correlation and root cause analysis," in *IEEE International Conference on Network and Service Management*, Rio de Janeiro, Brazil, Nov. 2014.
- [21] J. Bogojeska, I. Giurgiu, D. Lanyi, G. Stark, and D. Wiesmann, "Impact of HW and OS type and currency on server availability derived from problem ticket analysis," in *IEEE Network Operations and Management Symposium*, Krakow, Poland, May. 2014, pp. 1–9. doi: 10.1109/NOMS.2014.6838347.
- [22] J. Bogojeska, D. Lanyi, I. Giurgiu, G. Stark, and D. Wiesmann, "Classifying server behavior and predicting impact of modernization actions," in *the 9th International Conference on Network and Service Management*, Zurich, Switzerland, Oct. 2013, pp. 59–66. doi: 10.1109/CNSM.2013.6727810.
- [23] L. Tang and T. Li, "LogTree: a framework for generating system events from raw textual logs," in *IEEE International Conference on Data Mining*, Sydney, Australia, Dec. 2010, pp. 1550–1558. doi: 10.1109/ICDM.2010.76.
- [24] T. Li, *Event Mining: Algorithms and Applications*. USA: Chapman and Hall/CRC, 2015.
- [25] W. Xu, L. Huang, A. Fox, D. A. Patterson, and M. I. Jordan, "Mining console logs for large-scale system problem detection," in *the 3rd Workshop on Tackling System Problems with Machine Learning Techniques*, San Diego, USA, Dec. 2008, pp. 4–4.
- [26] W. Xu, L. Huang, A. Fox, D. Patterson, and M. I. Jordan, "Detecting large-scale system problems by mining console logs," in *ACM 22nd symposium on Operating Systems Principles*, Big Sky, USA, Oct. 2010, pp. 117–132. doi: 10.1145/1629575.1629587.
- [27] G. Grabarnik, A. Salahshour, B. Subramanian, and S. Ma, "Generic adapter logging toolkit," in *IEEE International Conference on Autonomic Computing*, May, 2004, pp. 308–309. doi: 10.1109/ICAC.2004.1301391.
- [28] BalaBit IT Security. (2015). Pattern DB™—real-time syslog message classification [Online]. Available: <http://www.balabit.com/network-security/syslog-ng/opensource-logging-system/features/pattern-db>
- [29] C. D. Manning, P. Raghavan, and H. Schütze, *Introduction to information retrieval*. Cambridge, UK: Cambridge University Press, 2008.
- [30] T. Pitakra, J. Grunert, O. Kabierschke, F. Keller, and A. v. Hoorn, "A framework for system event classification and prediction by means of machine learning," in *the 8th International Conference on Performance Evaluation Methodologies and Tools*, Bratislava, Slovakia, Dec. 2014, pp. 173–180. doi: 10.4108/icst.valuetools.2014.258197.
- [31] G. Androulidakis, N. Tech, V. Chatzigiannakis, and S. Papavassiliou, "Network anomaly detection and classification via opportunistic sampling," *IEEE Network*, vol. 23, no. 1, pp. 6–12, Jan./Feb. 2009. doi: 10.1109/MNET.2009.4804318.
- [32] P. Teufl, U. Payer, and R. Fellner, "Event correlation on the basis of activation patterns," in *the 18th Euromicro International Conference on Parallel, Distributed and Network-Based Processing*, Pisa, Italy, Feb. 2010, pp. 631–640. doi: 10.1109/PDP.2010.80.
- [33] C. Kruegel, D. Mutz, W. Robertson, and F. Valeur, "Bayesian event classification for intrusion detection," in *the 19th Annual Computer Security Applications Conference*, Las Vegas, USA, Dec. 2003, pp. 14–23. doi: 10.1109/CSAC.2003.1254306.
- [34] C. Modi, D. Patel, A. Patel, and R. Muttukrishnan, "Bayesian classifier and snort based network intrusion detection system in cloud computing," in *International Conference on Computing Communication & Networking Technologies*,

A Survey on Event Mining for ICT Network Infrastructure Management

LIU Zheng, LI Tao, and WANG Junchang

- Coimbatore, India, Jul. 2012, pp. 1–7. doi: 10.1109/ICCCNT.2012.6396086.
- [35] M. Aharon, G. Barash, I. Cohen, and E. Mordechai, "One graph is worth a thousand logs: uncovering hidden structures in massive system event logs," in *European Conference on Machine Learning and Knowledge Discovery in Databases*, Bled, Slovenia, Sep. 2009, pp. 227–243. doi: 10.1007/978-3-642-04180-8_32.
- [36] A. Makanju, A. N. Zincir-Heywood, and E. E. Milios, "Clustering event logs using iterative partitioning," in *ACM International Conference on Knowledge Discovery and Data Mining*, Paris, France, Jun. 2009, pp. 1255–1264. doi: 10.1145/1557019.1557154.
- [37] L. Tang, T. Li, and C.-S. Perng, "LogSig: generating system events from raw textual logs," in *ACM International Conference on Information and Knowledge Management*, Glasgow, UK, Oct. 2011, pp. 785–794. doi: 10.1145/2063576.2063690.
- [38] A. Makanju, S. Brooks, A. N. Zincir-Heywood, and E. E. Milios, "LogView: visualizing event log clusters," in *Annual Conference on Privacy, Security and Trust*, Frederickton, USA, Oct. 2008, pp. 99–108. doi: 10.1109/PST.2008.17.
- [39] R. V. a. M. Pihelgas, "LogCluster—a data clustering and pattern mining algorithm for event logs," in *the 11th International Conference on Network and Service Management*, Barcelona, Spain, Nov. 2015, pp. 1–7. doi: 10.1109/CNSM.2015.7367331.
- [40] P. Sharma and T. J. Parvat, "Network log clustering using k-means algorithm," in *International Conference on Recent Trends in Information, Telecommunication and Computing*, Kochi, India, Aug. 2012, pp. 115–124. doi: 10.1007/978-1-4614-3363-7_14.
- [41] M. Brodie, I. Rish, and S. Ma, "Intelligent probing: a cost-effective approach to fault diagnosis in computer networks," *IBM System Journal*, vol. 41, no. 3, pp. 372–385, Apr. 2002. doi: 10.1147/sj.413.0372.
- [42] E. Kiciman and A. Fox, "Detecting application-level failures in component-based internet services," *IEEE Transactions on Neural Networks*, vol. 16, no. 5, pp. 1027–1041, Sep. 2005. doi: 10.1109/TNN.2005.853411.
- [43] J.-G. Lou, Q. Fu, Y. Wang, and J. Li, "Mining dependency in distributed systems through unstructured logs analysis," *ACM SIGOPS Operating Systems Review*, vol. 44, no. 1, pp. 91–96, Jan. 2010. doi: 10.1145/1740390.1740411.
- [44] K. Nagaraj, C. Killian, and J. Neville, "Structured comparative analysis of systems logs to diagnose performance problems," in *the 9th USENIX conference on Networked Systems Design and Implementation*, San Jose, USA, Apr. 2012, pp. 26–26.
- [45] M. M. H. Khan, H. K. Le, H. Ahmadi, T. F. Abdelzaher and J. Han, "Troubleshooting interactive complexity bugs in wireless sensor networks using data mining techniques," *ACM Transactions on Sensor Networks*, vol. 10, no. 2, Jan. 2014. doi: 10.1145/2530290.
- [46] C. Z. Tang, T. Li, L. Schwartz, and G. Grabarnik, "Mining temporal lag from fluctuating events for correlation and root cause analysis," in *the 10th International Conference on Network and Service Management*, Rio de Janeiro, Brazil, Nov. 2014.
- [47] L. Tang, T. Li, and L. Schwartz, "Discovering lag intervals for temporal dependencies," in *ACM International Conference on Knowledge Discovery and Data Mining*, Beijing, China, Aug. 2012, pp. 633–641. doi: 10.1145/2339530.2339633.
- [48] H. Yan, L. Breslau, Z. Ge, et al., "G-RCA: a generic root cause analysis platform for service quality management in large IP networks," *IEEE/ACM Transactions on Networking*, vol. 20, no. 6, pp. 1734–1747, Mar. 2012. doi: 10.1109/TNET.2012.2188837.
- [49] F. Salfner and M. Malek, "Using hidden semi-Markov models for effective online failure prediction," in *the 26th IEEE International Symposium on Reliable Distributed Systems*, Beijing, China, Oct. 2007, pp. 161–174. doi: 10.1109/SRDS.2007.35.
- [50] R. Sipos, D. Fradkin, F. Moerchen, and Z. Wang, "Log-based predictive maintenance," in *ACM International Conference on Knowledge Discovery and Data Mining*, New York, USA, Aug. 2014, pp. 1867–1876. doi: 10.1145/2623330.2623340.
- [51] I. Fronza, A. Sillitti, G. Succia, M. Terhob, and J. Vlasenko, "Failure prediction based on log files using random indexing and support vector machines," *Journal of Systems and Software*, vol. 86, no. 1, pp. 2–11, Jan. 2013. doi: 10.1016/j.jss.2012.06.025.
- [52] Y. Zhang and A. Sivasubramaniam, "Failure prediction in IBM BlueGene/L event logs," in *IEEE International Symposium on Parallel and Distributed Processing*, Miami, USA, Apr. 2008, pp. 1–5. doi: 10.1109/IPDPS.2008.4536397.
- [53] R. K. Sahoo, A. J. Oliner, I. Rish, et al., "Critical event prediction for proactive management in large-scale computer clusters," in *the ninth ACM SIGKDD International Conference on Knowledge Discovery and Data Mining*, Washington, USA, Aug. 2003, pp. 426–235. doi: 10.1145/956750.956799.
- [54] S. Fu and C.-Z. Xu, "Exploring event correlation for failure prediction in coalitions of clusters," in *ACM/IEEE Conference on Supercomputing*, Reno, USA, Nov. 2007, pp. 1–12. doi: 10.1145/1362622.1362678.
- [55] M. J. Zaki, N. Lesh, and M. Ogihara, "Predicting failures in event sequences," in *Data Mining for Scientific and Engineering Applications*. US: Springer, 2001. doi: 10.1007/978-1-4615-1733-7_27, pp. 515–539.

Manuscript received: 2016-01-15

Biographies

LIU Zheng (zliu@njupt.edu.cn) is an assistant professor at the school of computer science and technology, the Nanjing University of Posts and Telecommunications, China. He obtained his PhD from the Chinese University of Hong Kong, China in 2011. He was a research engineer with Huawei Technologies from 2011 to 2015. His research interests include mining and querying large graph data, mining multimedia data and mining event logs in network management. He has published research papers in major conferences including ICDE, ICDM, DASFAA, and PAKDD. He is an IEEE member.

LI Tao (taoli@cs.fiu.edu) is dean and professor at the school of computer science and technology, the Nanjing University of Posts and Telecommunications, China. He received his PhD in computer science from the University of Rochester, USA in 2004. His research interests are in data mining, information retrieval, and computing system management. He was a recipient of an NSF CAREER Award and multiple IBM Faculty Research Awards. He is on the editorial boards of *ACM Transactions on Knowledge Discovery from Data*, *IEEE Transactions on Knowledge and Data Engineering*, and *Knowledge and Information System Journal*.

WANG Junchang (wangjc@njupt.edu.cn) is a lecturer at Nanjing University of Posts and Telecommunications, China. He received a Ph.D. degree in computer science from University of Science and Technology of China. His research focuses on software defined networking (SDN), network management, and high-performance computing (HPC).

Review of AVS Audio Coding Standard

ZHANG Tao, ZHANG Caixia, and ZHAO Xin

(School of Electronic Information Engineering, Tianjin University, Tianjin 300072, China)



Abstract

Audio Video Coding Standard (AVS) is a second-generation source coding standard and the first standard for audio and video coding in China with independent intellectual property rights. Its performance has reached the international standard. Its coding efficiency is 2 to 3 times greater than that of MPEG-2. This technical solution is more simple, and it can greatly save channel resource. After more than ten years' development, AVS has achieved great success. The latest version of the AVS audio coding standard is ongoing and mainly aims at the increasing demand for low bitrate and high quality audio services. The paper reviews the history and recent development of AVS audio coding standard in terms of basic features, key techniques and performance. Finally, the future development of AVS audio coding standard is discussed.



Keywords

Audio Video Coding Standard (AVS); audio coding; AVS1 audio; AVS2 audio

1 Introduction

The Audio Video Coding Standard (AVS) workgroup of China was approved by the Science and Technology Department under the former Ministry of Industry and Information Technology of People's Republic of China in June, 2002 [1]. The goal of the AVS workgroup is to establish the generic technical standards for high-quality compression, decompression, processing and representation of digital audio and video. The AVS workgroup also aims to provide the digital audio-video equipment and systems with high-efficient and economical coding/decoding technologies [2]. The formal name of AVS is "Information Technology-Advanced Audio and Video Coding", including four main technical standards: system, video, audio, digital rights management and the supporting standards, such as conformance testing. The members of AVS workgroup are domestic and international institu-

tions and enterprises that focus on the research of digital audio and video coding technology and the development of related products.

Since 2002, the AVS audio subgroup has drafted a series of audio coding standards, including AVS1-P3, AVS1-P10 and AVS-Lossless. Since 2009, the AVS audio subgroup started drafting the next generation audio coding standards. To identify the difference between these two series, the former serial is called AVS1 audio coding standards and the later one is called AVS2 audio coding standards. The AVS1 audio coding standards has been finished and widely used in various applications so far. The AVS2 audio coding standards is still under development and will be released soon.

This paper reviews AVS audio coding standards. It is organized as follows. In section 2, the series standards of AVS1 audio including AVS1-P3, AVS1-P10 and AVS-Lossless will be introduced. AVS2 audio coding scheme are presented in section 3. At last, the conclusion is given in section 4.

2 The Development of AVS1 Audio Coding Standards

The AVS audio subgroup started drafting the first generation AVS audio standard in 2003. The prime goal of the AVS audio subgroup is to establish an advanced audio codec standard with general performance equivalent or superior to MPEG AAC, on the premise of developing our own intellect property [2]. The first generation of AVS audio codec standard includes three parts: Information Technology—Advanced Audio Video Coding Part 3: Audio (AVS1-P3), Information Technology—Advanced Audio Video Coding Part 10: Mobile Voice and Audio (AVS1-P10 or AVS1-P10 audio), and AVS Lossless Audio Coding Standard (AVS-LS). **Tables 1** and **2** show the development of AVS1 audio coding standards [3].

2.1 AVS1-P3

After three years of effort, in 2005 the AVS working group finished the first AVS audio standard. The audio codec supports the scalable audio coding and is applied in mass information industries such as digital broadcasting of high resolution, intense laser digital storage media, wireless wideband multimedia communication, wideband stream media on the Internet and other related applications [1].

The AVS1-P3 encoder supports mono, dual and multichannel PCM audio signal. One frame audio signal includes 1024 samples. It is separated into 16 blocks, every 128-point block with 50% overlap is hanning windowed. The transform length is determined by the long/short window switching module: 2048 for long and 256 for short in order to accommodate both stationary and transient signals. The sampling rate ranges from 8 kHz to 96 kHz for the input signal. The output bitrate ranges from 16 kbps to 96 kbps per channel. The transparent audio quality could be provided at 64 kbps per channel. The com-

▼Table 1. History of AVS1 audio

Project	Project No. (national standard)	Working Draft (WD)	Committee Draft (CD)	Final Committee Draft (FCD)	Publicity	Final Draft (FD)	Final Draft for Standard (FDS)	Standard (GB)
AVS1-P3 (Dual Track)	20051305-T-339	2004.12	2005.3	2005.12		2006.4	2009.3	
AVS1-P3 (5.1)	20051305-T-339	2005.9	2005.12	2005.12		2006.4	2009.3	
AVS1-P3 (lossless)		2010.6	2010.7	2011.9				
AVS1-P10 (Mobile speech and audio coding)	20080548-T-469	2007.3	2008.9	2009.12	2010.6	2010.9	2011.6	2013.12

▼Table 2. Review of AVS1 audio

Time	Standard	Application and major coding tools
Dec. 2003	AVS1-P3	High quality application; multi-resolution analysis linear prediction, vector quantization, fine granularity scalable coding (FGSC)
Aug. 2005	AVS1-P10	Wireless network and mobile equipment; sampling rate conversion filter, ACELP/TVC mixed encoding, ISF vector quantization, Mono-signal High-Band Encoding (BWE), parametric stereo coding
Dec. 2009	AVS-Lossless	Reconstruction of original digital audio, data archive; lifting wavelet analysis, linear prediction

pression ratio is 10–16 [2].

2.1.1 Basic Encoding Process

Fig. 1 shows the framework of the AVS1-P3 audio codec [2]. Audio input PCM signals are analyzed by a psychoacoustic model. Then long/short window switch module determines the length of the analysis block depending on the transients. The signals are transformed to frequency domain by integer Modified Discrete Cosine Transform (intMDCT). For stereo signals, Square Polar Stereo Coding (SPSC) may be applied to the encoder if there are strong correlations between the channel pair. After that, frequency domain signals undergo nonlinear quantization. Context-Dependent Bitplane Coding (CBC) is used for entropy coding of quantized spectrum data. Finally the coded bits are written to the output bitstream based on the format defined in AVS1-P3 standard.

2.1.2 Key Technologies in AVS1-P3

The structure of the encoder in the AVS1-P3 standard is similar to that in Advanced Audio Coding - Low Complexity (AAC-LC). It has higher coding efficiency and better sound quality as a result of the use of new coding technologies, such as multi-resolution analysis, linear prediction in frequency domain, vector quantization and fine granularity scalable coding (FGSC).

Window switching is applied to reduce pre-echoes. A two-stage window switch decision is recommended in the AVS audio coding standard, which is called Energy and Unpredictability Measure Based Window Switching Decision (ENUPM - WSD) [2]. In the first stage, one frame audio signal is separated into 16 blocks, and then the energy variation of every sub-block is analyzed. If the maximum energy variation of a sub-block meets a given condition, the second stage based on unpredictability measurement in the frequency domain is ap-

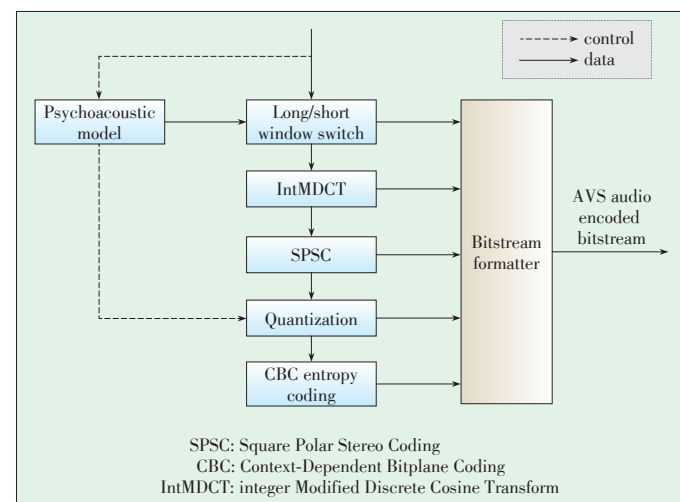
plied. Otherwise, it judges the window type by analyzing signal characteristics in the time domain and frequency domain. ENUPM - WSD has the merits of low complexity and high accuracy.

Considering the extension of lossless compression for the future, AVS audio subgroup adopted Integer MDCT as the time-frequency mapping module instead of traditional DCT [2]. IntMDCT can be used in lossless audio coding or combined perceptual and lossless audio coding. The advantages of MDCT, such as a good spectral representation of the audio signal, critical sampling and overlapping of

blocks are all reserved.

SPSC is applied as an efficient stereo coding scheme in AVS. Compared with Mid/Side stereo coding in AAC, its coding efficiency is higher. When SPSC is applied, one channel transmits the bigger value of the channel pair, and the other transmits the difference. In terms of quantization noise, the final decoded audio noise is smaller in SPSC than in M/S. Because in SPSC, noise superposition happens at only one channel at decoder end, while in Mid/Side, noise disperses to both channels.

In entropy coding, AVS adopts Context-dependent Bit-plane Coding (CBC). It is more efficient compared with Huffman coding. CBC entropy coding technology gets an improvement of 6% of bitrate in comparison with Huffman coding at 64 kbps/channel. The most striking characteristic of CBC is its Fine



▲Figure 1. AVS1-P3 audio encoder block diagram.

Review of AVS Audio Coding Standard

ZHANG Tao, ZHANG Caixia, and ZHAO Xin

Grain Scalability (FGS). CBC coded bitstream are evenly layered (16 to 96 layers, each layer 1 kbps), and as it changes from higher layer to lower layer, the audio quality downgrades from high to low, but still audible [1].

2.1.3. Performance

Figs 2, 3 and 4 show the informal subjective listening tests between AVS1-P3 and other three most popular audio compression formats, MP3 (lame 3.96), AAC (FAAC 1.24) and WMA (WMA 10) [1]. The tests use ITU-T P.800/P.830 test basic model. Four sequences, es02, sc02, si02, and sm02 were used in this test. These are speech, complex mixage audio, single instrument sound and simple mixage audio, respectively. Bitstreams were coded at 128 kbps.

The following conclusion could be obtained from Figs 2–4: at 128 kbps, AVS1-P3 is superior to MP3 (lame 3.93), the same as AAC (FAAC 1.24), but slightly worse than WMA

(WMA 10.0) [1].

2.2 AVS1-P10

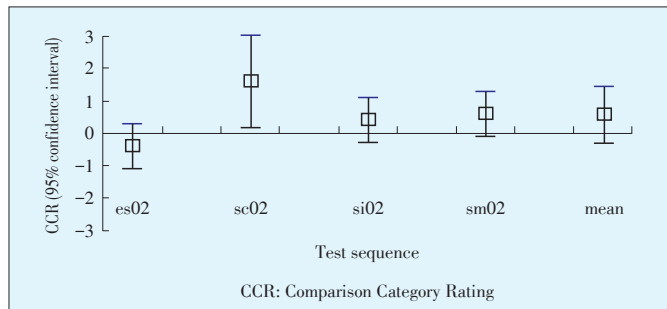
With the development of third-generation mobile communication, many challenges have arisen. There is a growing demand for low bitrate and high fidelity quality audio codec. At present, there have been many international audio standards for mobile applications such as G.7XX series standard (ITU-T) and AMR series standard (3GPP).

In order to provide a mobile audio standard with independent intellectual property rights for the quickly developing mobile communication system, the AVS Audio Subgroup started drafting the AVS1-P10 in August 2005. The AVS1-P10 Final Committee Draft (FCD) was completed in December 2009. It is approved as the national standard in December 2013 and has wide applications in 3G communication, wireless broad-band multimedia communications, broadband Internet streaming service and more. The advantages of AVS1-P10 include high efficiency, flexible compression quality, low complexity and strong error prevention mechanism [4].

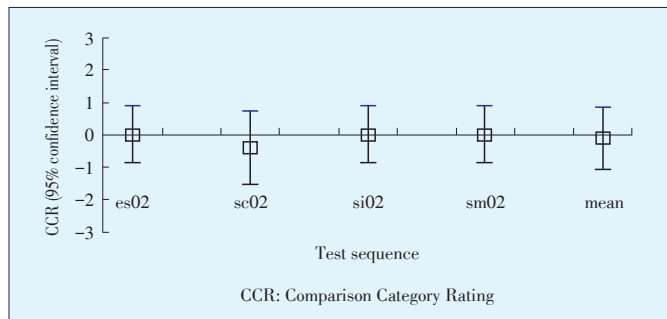
The encoder supports mono and stereo Pulse Code Modulation (PCM) signals with sampling rate of 8 kHz, 16 kHz, 24 kHz, 32 kHz, 48 kHz, 11 kHz, 22 kHz and 44.1 kHz. The output bitrate for mono ranges from 10.4 kbit/s to 24.0 kbit/s, and for stereo, ranges from 12.4 kbit/s to 32.0 kbit/s.

2.2.1 Basic Encoding Process

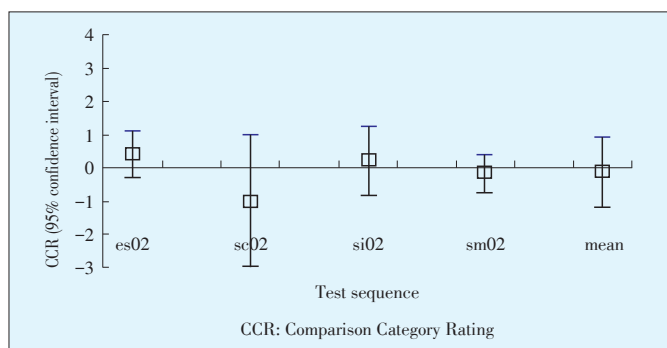
AVS1-P10 adopts the basic framework of AMR-WB+ (Fig. 5). It firstly convert the sampling frequency of the input signal into an internal sampling frequency F_s . For mono mode, the low frequency (LF) signal adopts Algebraic Code Excited Linear Prediction/Transform Vector Coding (ACELP/TVC) codec mode, while the high-frequency signal is encoded using a bandwidth extension (BWE) approach. For stereo mode, the same band decomposition as in the mono case is used. The HF part of the left channel and right channel is encoded by using parametric BWE on the two stereo channels. The LF part of the left channel and right channel is down mixed to main channel and



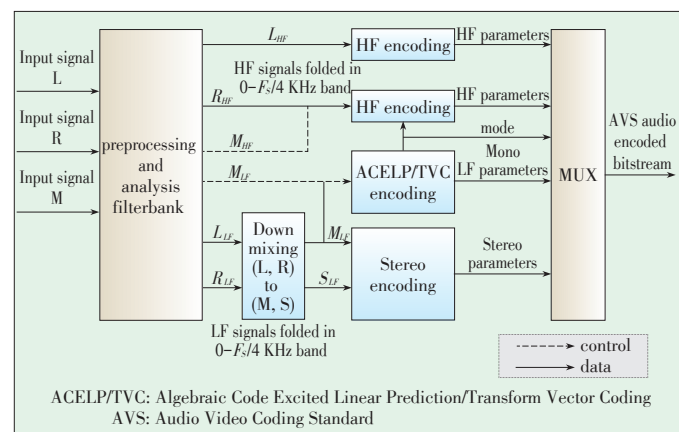
▲ Figure 2. AVS1-P3 128 kbps vs. MP3 128 kbps.



▲ Figure 3. AVS1-P3 128 kbps vs. FAAC 128 kbps.



▲ Figure 4. AVS1-P3 128 kbps vs. WMA 128 kbps.



▲ Figure 5. AVS1-P10 encoder block diagram.

side channel (M/S). The main channel is encoded by ACELP/TVC module. The stereo encoding module processes the M/S channel and produces the stereo parameters [5].

2.2.2 Key Technologies in AVS1-P10

1) ACELP/TVC Mixed Encoding Module

The core codec module in AVS1-P10 is ACELP/TVC mixed encoding module. AVS1-P10 codec integrates ACELP coding and the Transform Vector Coding (TVC) into a mixed orthogonal encoder. It can choose the best encoding mode between two coding modes according to the signal type. ACELP mode is based on time-domain linear prediction, so it is suitable for encoding speech signals and transient signals [6]. On the other hand, TVC mode is based on transform domain coding, so it is suitable for encoding music signals. Thus it can encode a variety of complex audio signals.

Several coding methods, such as ACELP256, TVC256, TVC512, and TVC1024, can be applied to one superframe. There are 26 mode combinations of ACELP/TVC for each superframe [7]. The mode can be selected by adopting the closed-loop search algorithm or the open-loop search algorithm. The latter is relatively simple, but the mode selected may be not optimum.

2) High-Band Encoding

AVS1-P10 adopts BWE approach to code HF signal with the frequency components above $F_s/4$ kHz of the input signal. In BWE, energy information is sent to the decoder in the form of spectral envelop and gain [5]. However, the fine structure of the signal is extrapolated at the decoder from the decoded excitation signal in the LF signal. Besides, in order to keep the continuity of the signal spectrum at the $F_s/4$, the HF gain needs to be adjusted according to the correlation between the HF and LF gain in each frame.

3) Stereo Signal Encoding

In order to support stereo signal encoding, AVS1-P10 adopts a high effective configurable parametric stereo coding scheme in the frequency domain. This scheme provides a flexible and extensible codec structure with coding efficiency, which is similar to that of AMR-WB+. Because it avoids the resampling in the time domain, it reduces the complexity of encoder and decoder. The ability to flexibly configure the low frequency bandwidth determined by the coding bit rate is also available, which makes it a high-effective stereo coding approach [6].

2.2.3 Complexity Analysis

In order to analyze the complexity of the AVS1-P10 Codec, the AVS1-P10 Fixed-point Codec is developed, and the functions of complexity analysis are integrated into it. The Weighted Million Operation per Second (WMOPS) method approved by ITU is used to analyze the complexity of the AVS1-P10 Codec. The basic operation's weighting is given in **Table 3** [8]. The complexity of the AVS1-P10 Codec is shown in **Tables 4**

and **5** [8].

2.2.4 Performance

In order to evaluate the performance of AVS1-P10 codec, objective test - perceptual evaluation of speech quality (PESQ) and subjective test-complementary metal-oxide-semiconductor (CMOS) methods are applied to the 20 test sequences selected from AVS workgroup at the bit rate of 12 kbps and 24 kbps, including pure speech, pure music, noisy speech, speech over music and speech between music. Each of these contained two mono audio and two stereo audio.

1) Objective Performance Evaluation of AVS1-P10 Audio

PESQ result between AVS1-P10 (AVS1-P10) and AMR-

▼ **Table 3. Operation's weighting**

Operation	Weight
16bit add	1
16bit sub	1
16bit abs	1
16bit shift	1
16bit multiply	1
16bit divide	18
32bit add	2
32bit sub	2
32bit abs	3
32bit shift	2

▼ **Table 4. AVS1-P10 encoder complexity**

Condition	Command	Complexity (WMOPS)
12 kbps, mono	-rate 12 -mono	Average=56.318 Worst=58.009
24 kbps, mono	-rate 24 -mono	Average=79.998 Worst=80.055
12.4 kbps, stereo	-rate 12.4	Average=72.389 Worst=73.118
24 kbps, stereo	-rate 24	Average=83.138 Worst=83.183
WMOPS: Weighted Million Operation per Second		

▼ **Table 5. AVS1-P10 decoder complexity**

Condition	Command	Complexity (WMOPS)
12 kbps, mono	-mono	Average=9.316 Worst=9.896
24 kbps, mono	-mono	Average=13.368 Worst=13.981
12.4 kbps, stereo	None	Average=16.996 Worst=17.603
24 kbps, stereo	None	Average=18.698 Worst=19.103
WMOPS: Weighted Million Operation per Second		

Review of AVS Audio Coding Standard

ZHANG Tao, ZHANG Caixia, and ZHAO Xin

WB+ are given respectively in **Figs 6** and **7** [8].

2) Subjective Performance Evaluation of AVS1-P10 Audio

CMOS result between AVS1-P10 and AMR-WB+ are given respectively in **Figs 8** and **9** [8].

It can be concluded from these figures that the performance of AVS1-P10 is no worse than AMR-WB+ on average.

2.3 AVS Lossless Audio Coding

Nowadays, the ever-decreasing price of storage and ever-increasing Internet bandwidth make storing and distributing lossless coded audio possible. Lossless audio coding technology is designed to perfectly reconstruct original digital audio. After decoding, its output sequence is same as the original audio sequence. There are many lossless audio coding standards, such

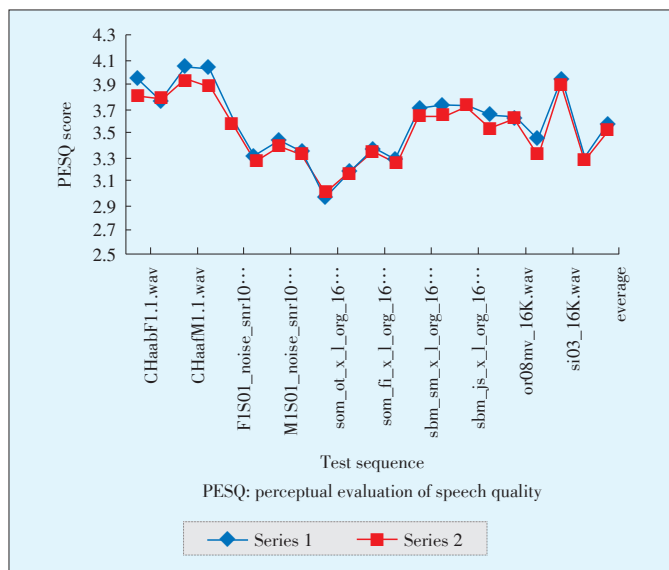
as MPEG-4 Audio Lossless Coding (MPEG-4 ALS), MPEG-4 Scalable to lossless standard (MPEG-4 SLS), Free Lossless Audio Codec (FLAC) and so on [9]. In order to make a lossless audio coding standard with independent intellectual property rights, AVS audio subgroup started to draft lossless audio coding standard in early 2010, and the FCD and reference software were finished in September 2010 [10].

2.3.1 Basic Encoding Process

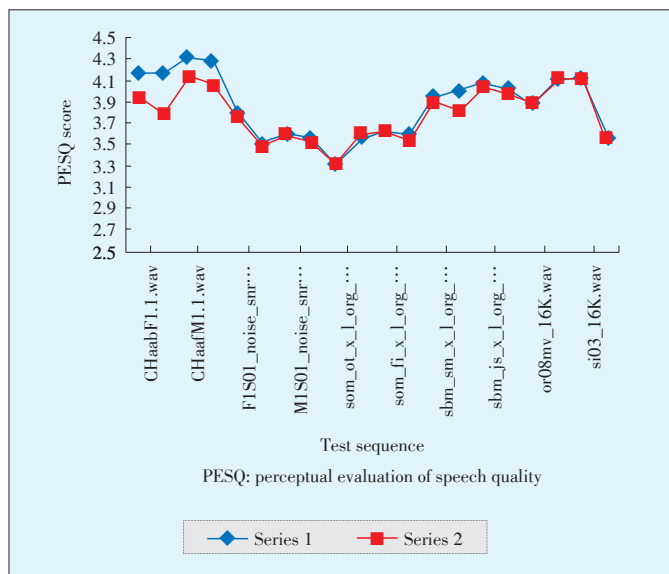
Fig. 10 shows the the AVS lossless encoder [9]. The input audio signal is decorrelated to remove the correlation between different channels. Then, the de-correlated signal is filtered into a high-frequency band and a low-frequency band by a lifting the wavelet filter. After that, subband signals go through the linear predictor to generate prediction residual signals. Then, the residual signal is sent to the preprocessor, where it is normalized. Finally, the normalized signal goes through the entropy codec and a bitstream is generated.

2.3.2 Key Technologies in AVS-Lossless

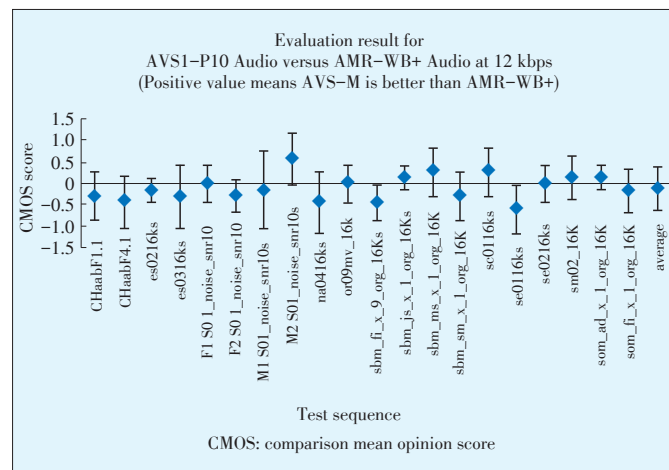
1) De-correlation



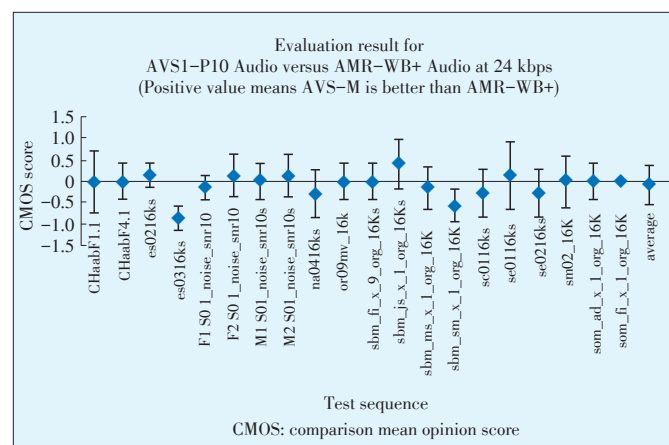
▲ Figure 6. PESQ test result at 12 kbps.



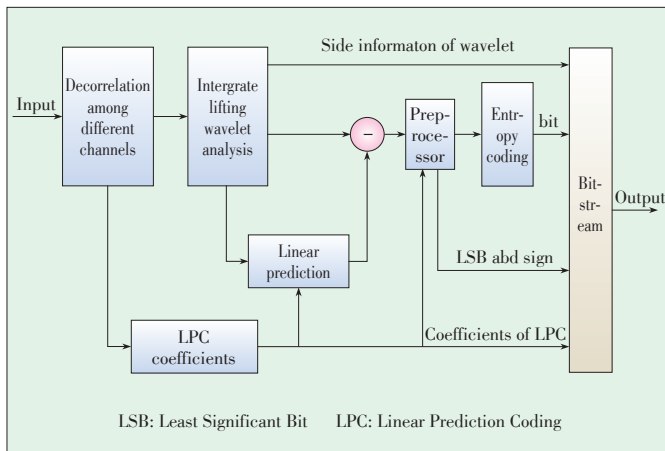
▲ Figure 7. PESQ test result at 24 kbps.



▲ Figure 8. CMOS test result at 12 kbps.



▲ Figure 9. CMOS test result at 24 kbps.



▲ Figure 10. Framework of AVS lossless audio encoder.

In an AVS lossless audio encoder, a sum and subtraction coding method is used to de-correlate multichannel signals sounds.

2) Integer Lifting Wavelet Transform

The coder of the lifting wavelet transform has two steps. First, an input signal is processed by the lifting wavelet transform to generate a high-frequency signal and a low-frequency signal. Then, the two subband signals are processed by the LPC algorithm. In the first step, the integer lifting wavelet is used to avoid the rounding error [9].

3) Entropy Coding

Before entropy coding, the residual signal is normalized because there is often a few large-valued samples in the first part of residual signal. The residual signal is coded according to the probability distribution. The entropy coder first segregates the input sequence, calculates the mean of each subsequence, and then quantifies the mean value. The MSB of mean index and residual signal is coded according to the probability table, which is generated by the probability model [9]. Gaussian-like probability distribution is used to fit the probability distribution of predicted residuals.

2.3.3 Performance

Table 6 shows the average compression rate of AVS-LS and

▼ Table 6. Average compress rate of AVS1-lossless coder (%)

Coder	32 kHz/16 bit	44.1 kHz/16 bit	96 kHz/22 bit	192 kHz/22 bit
AVS-LS	51.44	47.98	46.37	35.22
Monkey EH	50.77	47.02	47.19	35.57
Monkey normal	52.23	48.32	49.08	36.31
TAK	52.29	47.95	47.97	35.01
MPEG4 ALS (RICE)	52.49	48.6	47.89	35.91
MPEG4 ALS (BGMC)	51.95	48.09	47.57	35.54
FLAC	53.31	49.38	51.68	40.33
WavPack	54.39	50.64	51.38	46.03

other popular lossless coding methods, including Monkey's Audio (extra high/normal), TAK (normal), ALS RM21 (RICE/BGMC 1024 sample), FLAC (normal), and WavPack (default) [9]. The table shows that the average compression rates of AVS-LS are equivalent or superior to others.

3 Progress of AVS2 Audio Coding Standard

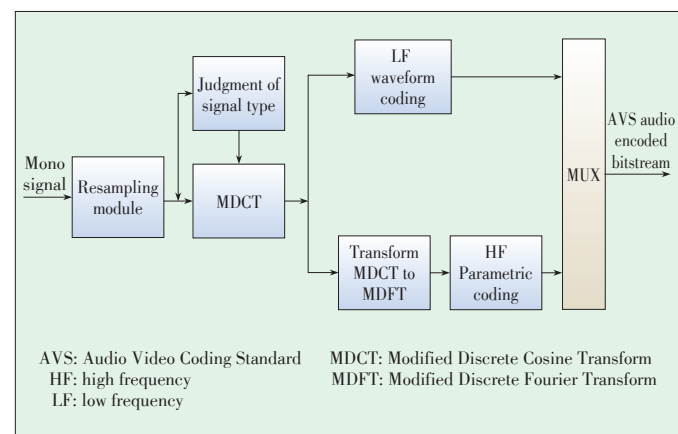
At the end of 2008, the AVS workgroup declared the project plan about the second generation of AVS standard, called "Information Technology - New Multimedia Coding Technology". AVS2 is an ongoing standardization effort for efficient coding performance compared to the previous standard (AVS1). It includes two compatible compression schemes, lossless audio coding and lossy audio coding. The later completely contains the first generation of AVS lossless audio coding. If the bit-stream is decoded completely the audio signals could be restored nearly transparent. Now the workgroup focuses more on surround sound encoding for super-high-definition television.

AVS1-P3 has good quality under high and medium bitrate but is not suitable for low bit rate coding. To solve this problem, the AVS Audio Subgroup has set up the project of AVS2-P3 in July 2013. The following three requirements are formally proposed for the AVS2 audio coding standard in the AVS M2845 in September 2011:

- 1) It is suitable for high, medium and low bit rate coding;
- 2) It can achieve hierarchical coding, or it can achieve the coarse scalable coding ability to meet different network application and the incremental download ability;
- 3) It has high scalability, low complexity and low decoding delay.

AVS2 audio called for proposals in December 2011. A hybrid audio coding technology of waveform coding and parameter coding proposed in the AVSM2977. AVSM2983 is adopted as the basic structure and reference model output (RM0) of the AVS2 audio coding (Fig. 11 [11]).

This scheme is based on the waveform coding in AVS1-P3 and uses frequency band extension technology, parameter ste-



▲ Figure 11. AVS2 encoder block diagram.

Review of AVS Audio Coding Standard

ZHANG Tao, ZHANG Caixia, and ZHAO Xin

reo coding technique and surround sound coding technique. The goal is to guarantee the quality of the medium and high bit rate coding and, at the same time, greatly increase the quality of the low bit rate audio coding. AVS2 codec is an initial reference release, so it will be improved for audio quality at the final release after more optimization.

At present, the AVS workgroup is collecting and evaluating the parametric stereo coding technology. In order to realize the low bit rate stereo and surround sound audio coding, AVS make full use of the inter-aural phase difference and intensity time difference (IPD/ITD), inter - aural intensity differences (IID), the binaural correlation, the binaural masking effect and other psychological mechanism.

4 Conclusions

AVS standardization is an indigenous innovation of China and has finished the transition from the development of technology to a maturing industry chain. The highly efficient and simple implementation of the AVS standard ensures its successful applications [12]. It fills up the current empty space in the development of our information industry and greatly promotes the development of audio-video industry in our nation. AVS2 audio coding standardization is ongoing. Although it is far from being a fully-fledged standard, it is moving forward steadily. With the continuous development and improvement of AVS standardization, it will serve better for our audio-video industry.

References

- [1] R. Hu, S. Chen, H. Ai, and N. Xiong, "AVS generic audio coding," in *Sixth International Conference on Parallel and Distributed Computing, Applications and Technologies*, Dalian, China, Dec. 2005, pp.679–683. doi: 10.1109/PD-CAT.2005.97.
- [2] R. Hu, Y. Zhang, and H. Ai, "Digital audio compression technology and AVS audio standard research," in *Intelligent Signal Processing and Communication Systems*, Hong Kong, China, Dec. 2005, pp. 757–759. doi:10.1109/ISPACS.2005.1595520.
- [3] AVS Working Group. (2015, November 11). The Development of AVS [Online]. Available: <http://www.avs.org.cn/avsStandard.asp>
- [4] R. Hu and Y. Zhang, "Research and application on AVS-P10 audio standard," *Audio Engineering*, vol. 31, no. 7, pp. 65–70, Aug. 2007. doi: 10.3969/j.issn.1002-8684.2007.07.023.
- [5] T. Zhang, C.-T. Liu, and H.-J. Quan, "AVS1-M audio: algorithm and implementation," *EURASIP Journal on Advances in Signal Processing*, vol. 2011, no.4, pp. 307–323, Jan. 2011. doi:10.1155/2011/567304.
- [6] L. Jiang, R. Hu, X. Wang, *et al.*, "AVS2 speech and audio coding scheme for high quality at low bitrates," in *IEEE International Conference on Multimedia and Expo Workshops (ICMEW)*, Chengdu, China, Jul. 2014, pp.1–6. doi: 10.1109/ICMEW.2014.6890693.
- [7] H. Zhang, "Research of AVS-P10 audio codec and implementation on DSP," M. S. Thesis, School of Electronic Information Engineering, Tianjin University, Tianjin, China, 2008.
- [8] W. Zhang, T. Zhang, L. Zhao, *et al.*, "Performance analysis and evaluation of AVS-M audio coding," in *2010 International Conference on Audio Language and Image Processing (ICALIP)*, Shanghai, China, Nov. 2010, pp. 31–36. doi: 10.1109/ICALIP.2010.5685024.
- [9] W. He, Y. Gao, and T. Qu, "Introduction to AVS audio lossless coding/decoding standard," *IEEE COMSOC MMT E-Letter*, vol. 7, no. 2, pp. 21–29, Feb. 2012.
- [10] H. Huang, H. Shu, R. Yu, *et al.*, "Introduction to AVS lossless audio coding standard: entropy coding," *Audio Engineering*, vol. 34, no. 12, pp. 69–71, 2010.
- [11] X. Pan, "Progress review and planning of AVS2 audio coding technology," in *Academic Forum and Academic Exchange Conference of Audio Engineering*, Ningbo, China, 2014.
- [12] W. Gao, Q. Wang, and S. Ma, "Digital audio video coding standard of AVS," *ZTE Communications*, vol. 12, no. 3, pp. 6–13, Aug. 2006.

Manuscript received: 2015-11-15

Biographies

ZHANG Tao (Zhangtao@tju.edu.cn) received his master's degree and PhD from Tianjin University, China in 2001 and 2004. He is an associate professor in the Texas Instruments DSP Collaboration Lab, Tianjin University. His principal interests are in acoustic signal processing, auditory model, and speech enhancement.

ZHANG Caixia (zhangcaixia@tju.edu.cn) is currently pursuing the master's degree at the School of Electronic Information Engineering, Tianjin University, China. Her research interests include audio coding and audio information hiding.

ZHAO Xin (zhaoxin_tju@126.com) is currently pursuing the master's degree at the School of Electronic Information Engineering, Tianjin University, China. His research interests include audio processing and DSP application.

ZTE Communications Guidelines for Authors

• Remit of Journal

ZTE Communications publishes original theoretical papers, research findings, and surveys on a broad range of communications topics, including communications and information system design, optical fiber and electro-optical engineering, microwave technology, radio wave propagation, antenna engineering, electromagnetics, signal and image processing, and power engineering. The journal is designed to be an integrated forum for university academics and industry researchers from around the world.

• Manuscript Preparation

Manuscripts must be typed in English and submitted electronically in MS Word (or compatible) format. The word length is approximately 3000 to 8000, and no more than 8 figures or tables should be included. Authors are requested to submit mathematical material and graphics in an editable format.

• Abstract and Keywords

Each manuscript must include an abstract of approximately 150 words written as a single paragraph. The abstract should not include mathematics or references and should not be repeated verbatim in the introduction. The abstract should be a self-contained overview of the aims, methods, experimental results, and significance of research outlined in the paper. Five carefully chosen keywords must be provided with the abstract.

• References

Manuscripts must be referenced at a level that conforms to international academic standards. All references must be numbered sequentially in-text and listed in corresponding order at the end of the paper. References that are not cited in-text should not be included in the reference list. References must be complete and formatted according to *ZTE Communications* Editorial Style. A minimum of 10 references should be provided. Footnotes should be avoided or kept to a minimum.

• Copyright and Declaration

Authors are responsible for obtaining permission to reproduce any material for which they do not hold copyright. Permission to reproduce any part of this publication for commercial use must be obtained in advance from the editorial office of *ZTE Communications*. Authors agree that a) the manuscript is a product of research conducted by themselves and the stated co-authors, b) the manuscript has not been published elsewhere in its submitted form, c) the manuscript is not currently being considered for publication elsewhere. If the paper is an adaptation of a speech or presentation, acknowledgement of this is required within the paper. The number of co-authors should not exceed five.

• Content and Structure

ZTE Communications seeks to publish original content that may build on existing literature in any field of communications. Authors should not dedicate a disproportionate amount of a paper to fundamental background, historical overviews, or chronologies that may be sufficiently dealt with by references. Authors are also requested to avoid the overuse of bullet points when structuring papers. The conclusion should include a commentary on the significance/future implications of the research as well as an overview of the material presented.

• Peer Review and Editing

All manuscripts will be subject to a two-stage anonymous peer review as well as copyediting, and formatting. Authors may be asked to revise parts of a manuscript prior to publication.

• Biographical Information

All authors are requested to provide a brief biography (approx. 100 words) that includes email address, educational background, career experience, research interests, awards, and publications.

• Acknowledgements and Funding

A manuscript based on funded research must clearly state the program name, funding body, and grant number. Individuals who contributed to the manuscript should be acknowledged in a brief statement.

• Address for Submission

magazine@zte.com.cn
12F Kaixuan Building, 329 Jinzhai Rd, Hefei 230061, P. R. China

ZTE COMMUNICATIONS



ZTE Communications has been indexed in the following databases:

- Cambridge Scientific Abstracts (CSA)
- China Science and Technology Journal Database
- Chinese Journal Fulltext Databases
- Inspec
- Ulrich's Periodicals Directory
- Wanfang Data—Digital Periodicals